Discovering Ocean Dynamics from Space:Sensor synergies in studies of mesoscale and submesoscale dynamics

An Earth Observation Challenge: 3D dynamics of the upper ocean

What can we measure and infer from Space ?

Ocean remote sensing: a privileged view

- Spatially detailed
  - Spatial resolution from meters to Kms
  - A synoptic picture that is 100 km - 10 000 km wide
- Regularly repeated
  - Revisit intervals between 30 min. and 35 days
  - Continuously repeated over years to decades
- Global coverage
  - Satellites see the parts where ships rarely go
  - Single-sensor consistency - no intercalibration uncertainties
- Measures parameters that cannot be observed in situ
  - Surface roughness at short length scales (2-50 cm)
  - Surface slope (a few cm over 100s of kilometres)

Satellite orbits

•Geostationary sensors typically offer a revisit interval of less than 30 min and spatial resolution of 3 to 5 km.

•The polar orbiting sensor cover the whole Earth in a single day if it is the swath at least 2700 km.

• Each point on the Earth surface is viewed once from descending track and once from ascending track.

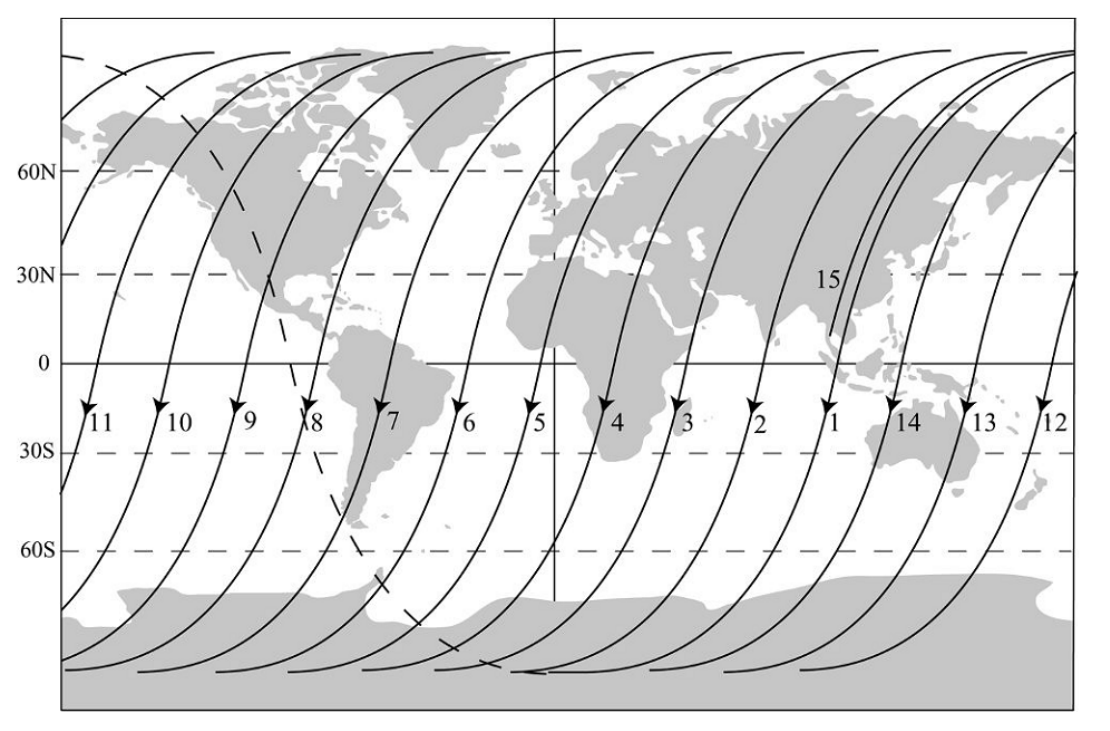

Ground track of a typical near-polar, low-Earth orbit, showing all the descending passes for one day and one ascending pass (dashed).

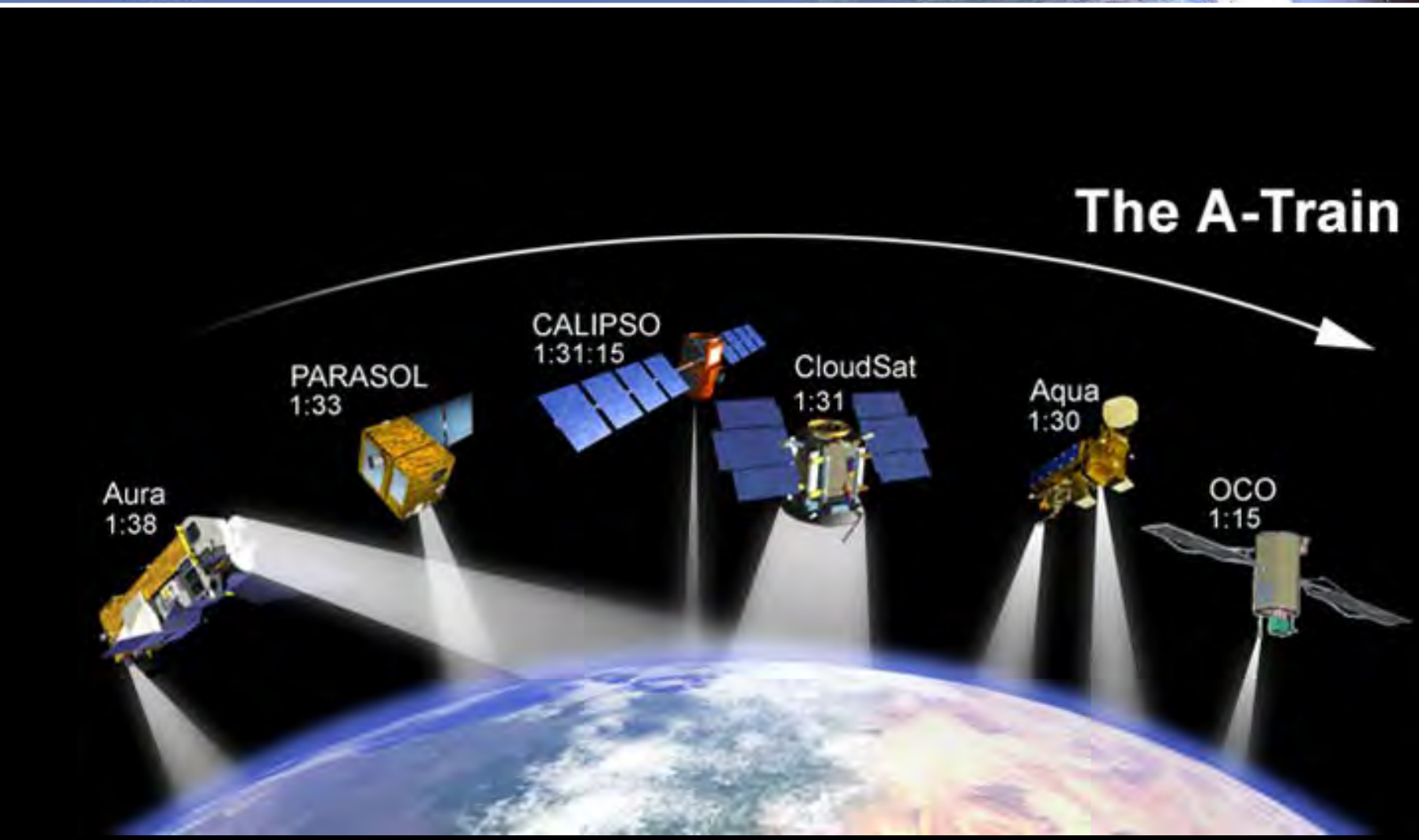
The A-Train
Aura
1:38
PARASOL
1:33
CALIPSO
1:31:15
CloudSat
1:31
Aqua
1:30
OCO
1:15

Global Environmental Satellite Observation Network

The COMET Program / EUMETSAT / NASA / NOAA / WMO

Satellites currently in space

New Era - Nanosatellites - CubeSat

A **CubeSat** is a type of miniaturized satellite for space research that usually has a volume of exactly one liter (10 cm cube) mass of no more than 1.33 kilograms.

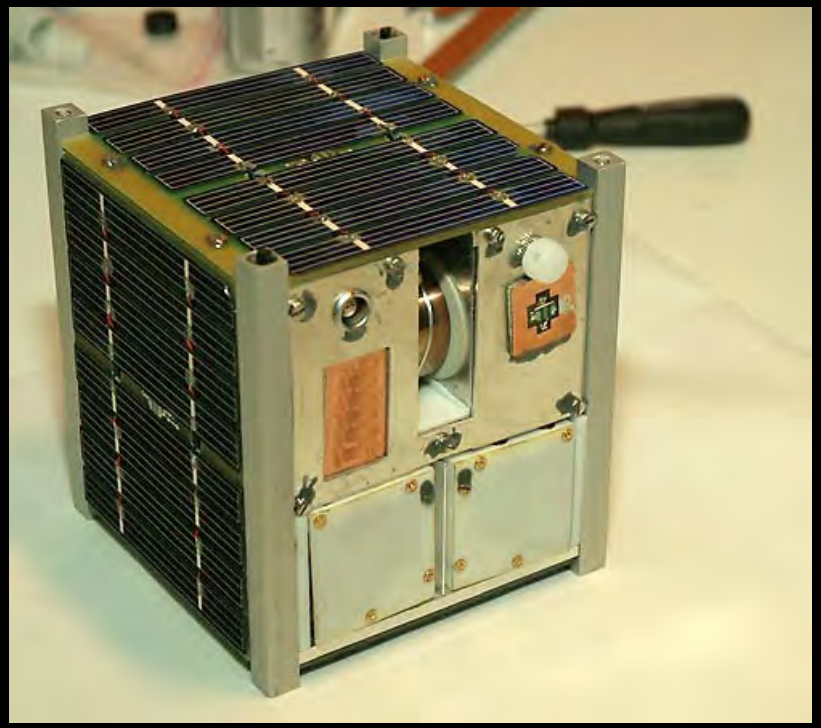

Opening the Pandora's box ?

Archiving data leads to very large heterogeneous and multimodal databases

Data assimilation is growing in response to the growth of data collected, but (personal opinion) tremendous amounts of information still remain hidden in data archives.

Knowledge trees and complex algorithms are essential to avoid the Google's principle, i.e. pertinence = popularity

Research efforts to be concerned with the definition of adequate exploratory processes to detect relevant patterns in large, heterogeneous, multidimensional observation data sets with different resolutions to better approach complex spatial and/or temporal dynamics of the ocean system.

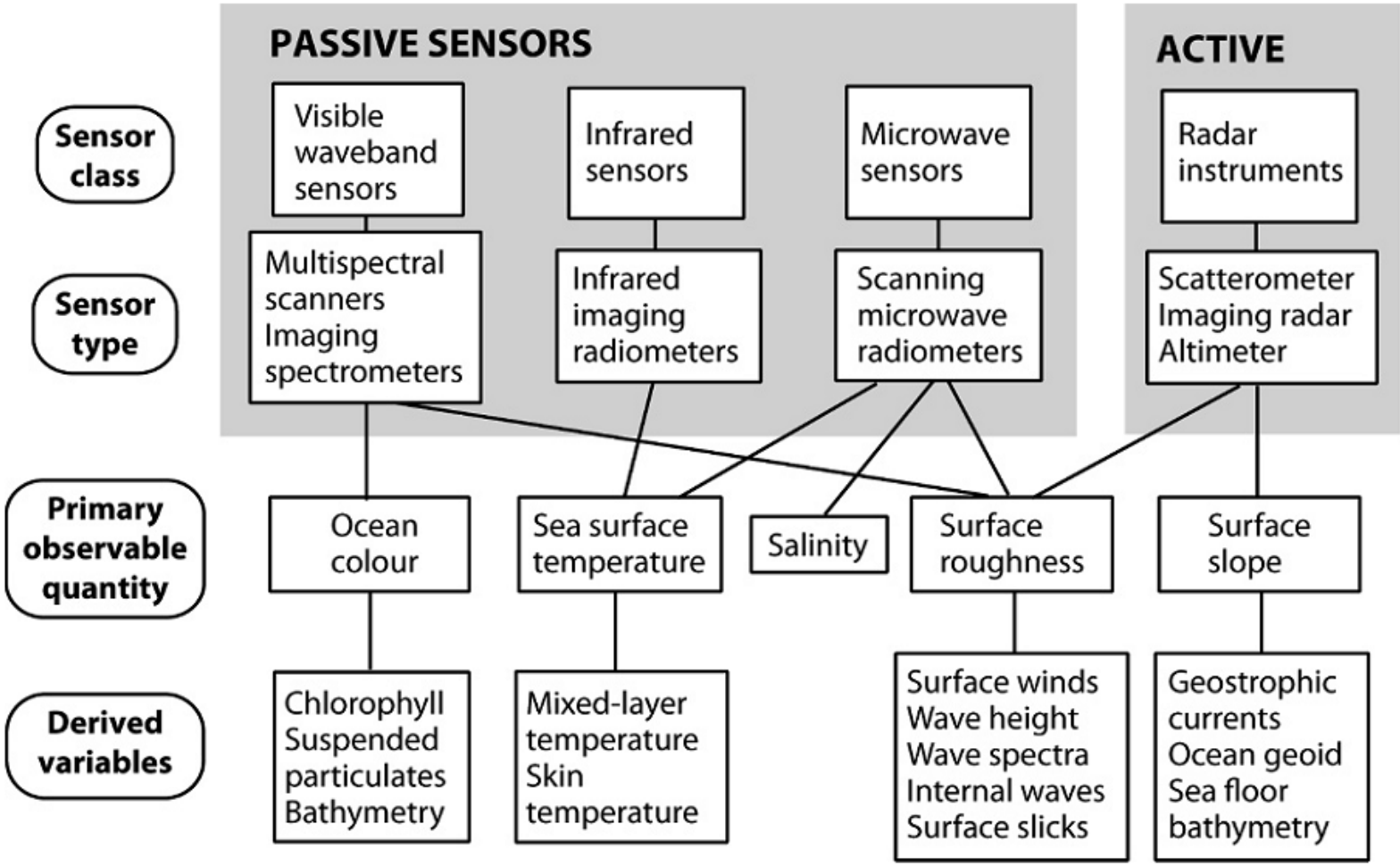

Schematic illustrating the different remote-sensing methods and classes of sensors used in satellite oceanography, along with their applications (from Robinson, 2004).

Discovering Ocean Dynamics from Space:Sensor synergies in studies of mesoscale and submesoscale dynamics

- Numerous Remote sensing measurements
  - Very high resolution (100 m – 1 km) SST, Ocean Colour, radar roughness images
  - Low resolution Altimetry (80 km)
  - Mesoscale Ocean Wind Vector Scatterometry and Microwave SST and SSS (25 km)

- Increased In Situ measurements
  - Fixed networks
  - ARGO floats
  - Drifters

- Dynamical frameworks
  - Operational models
  - Quasi-geostrophy, Surface Quasi-geostropy, Ekman

Sub-mesoscale (10 km eddies) and high resolution radar sea surface roughness variations

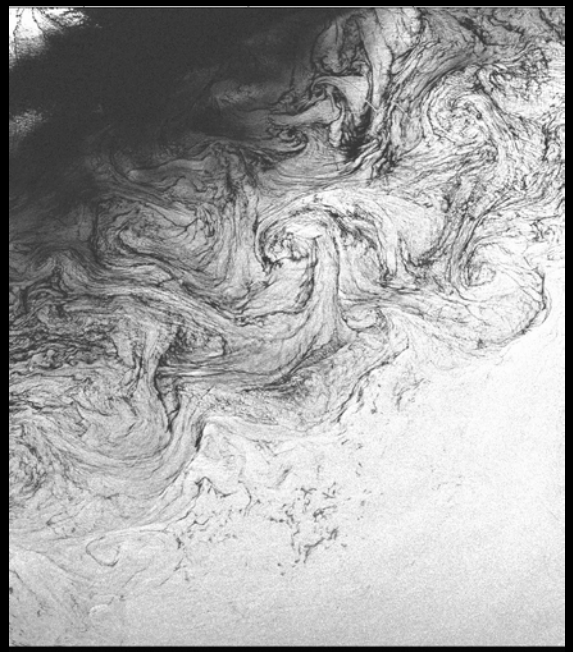

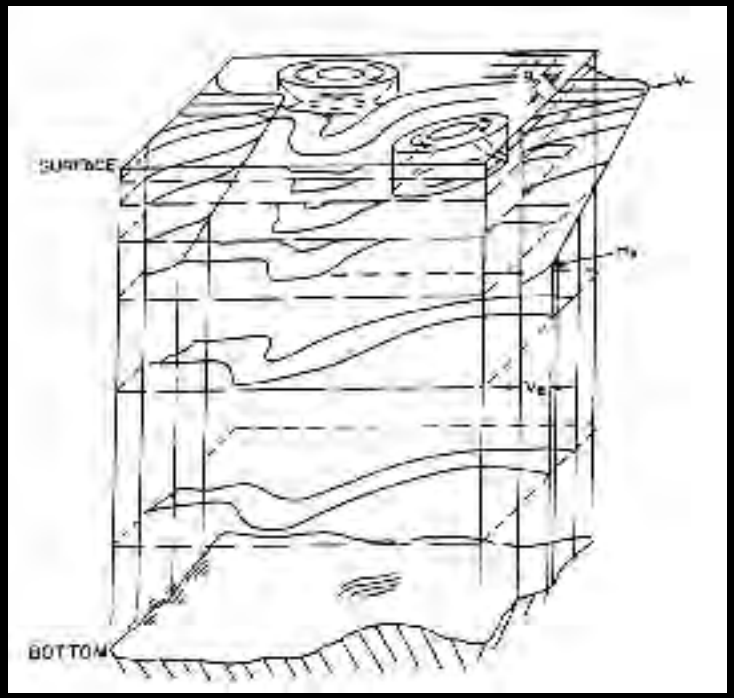

LETTRE XX.

De M. JEAN SPOONER,
A. B. S.t JOHN'S CAMBRIDGE.

Gênes 1.er Mai 1822.

Vous m'avez fait l'honneur, M. le Baron, de me demander un extrait du mémoire que j'ai pris la liberté de vous communiquer relativement à un phénomène lumineux qui se montre sur la mer lorsque le soleil ou la lune y donnent dessus (*), et que vous voulez avoir la bonté d'insérer dans votre *Correspondance*

L'équation en question est:

$$\frac{a^2}{a^2+x^2+y^2}+\frac{2\cos.Z\,a}{\sqrt{a^2+x^2+y^2}}+\cos.^2Z=\frac{2.\cos.^2J+2\cos.^2J.a.\cos.Z}{\sqrt{a^2+x^2+y^2}}$$
$$-\frac{2\cos.J\sin.Z.x}{\sqrt{a^2+x^2+y^2}}.$$

Par la quatrième observation.

$$A^2=\frac{.0000013+.000593+.0585262}{2+.000593-1.9281164}=\frac{.0590868}{.0724429}$$

De-là, log. A = 1.95574725 = log. cosin. de 25° 26'.

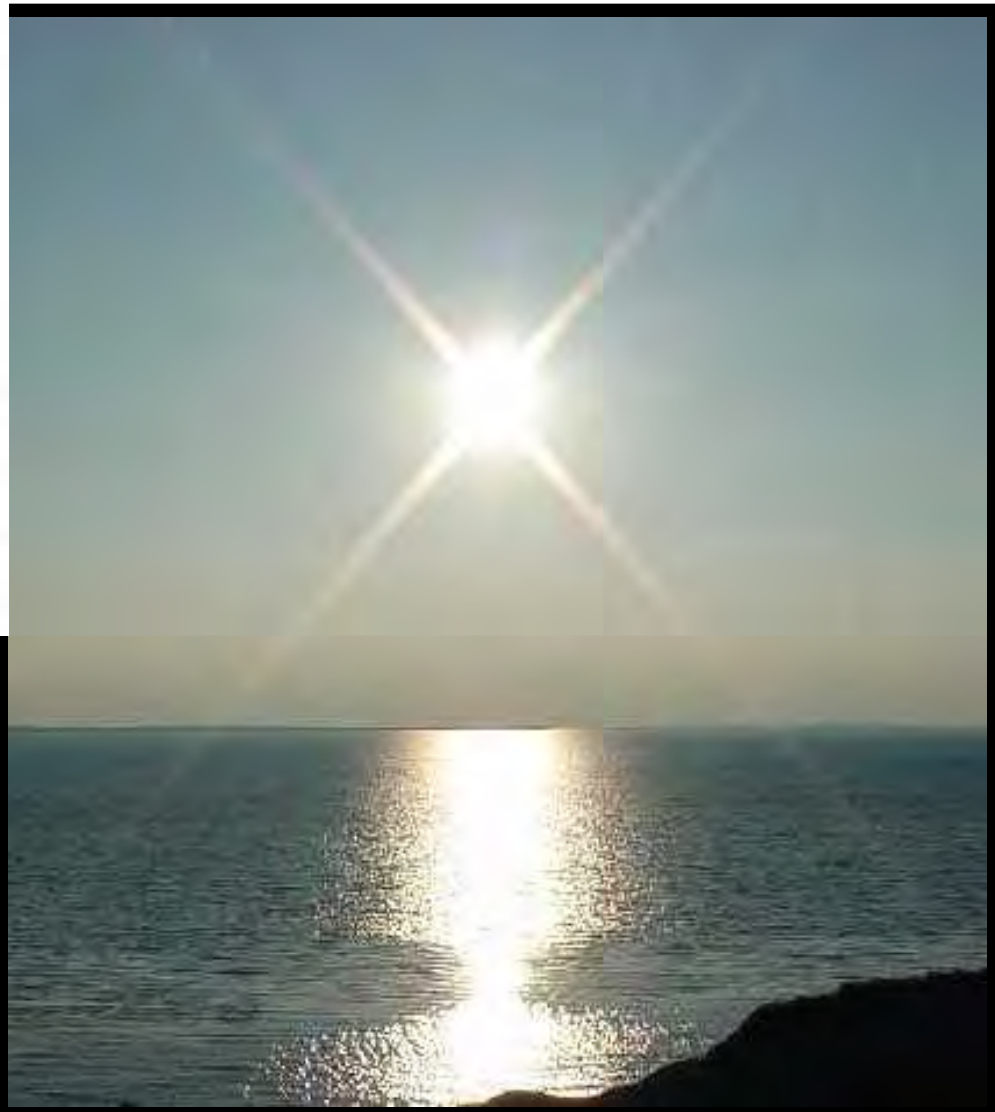

JOURNAL OF THE OPTICAL SOCIETY OF AMERICA VOLUME 44, NUMBER 11 NOVEMBER, 1954

Measurement of the Roughness of the Sea Surface from Photographs of the Sun's Glitter

CHARLES COX AND WALTER MUNK
Scripps Institution of Oceanography, La Jolla, California*
(Received April 28, 1954)

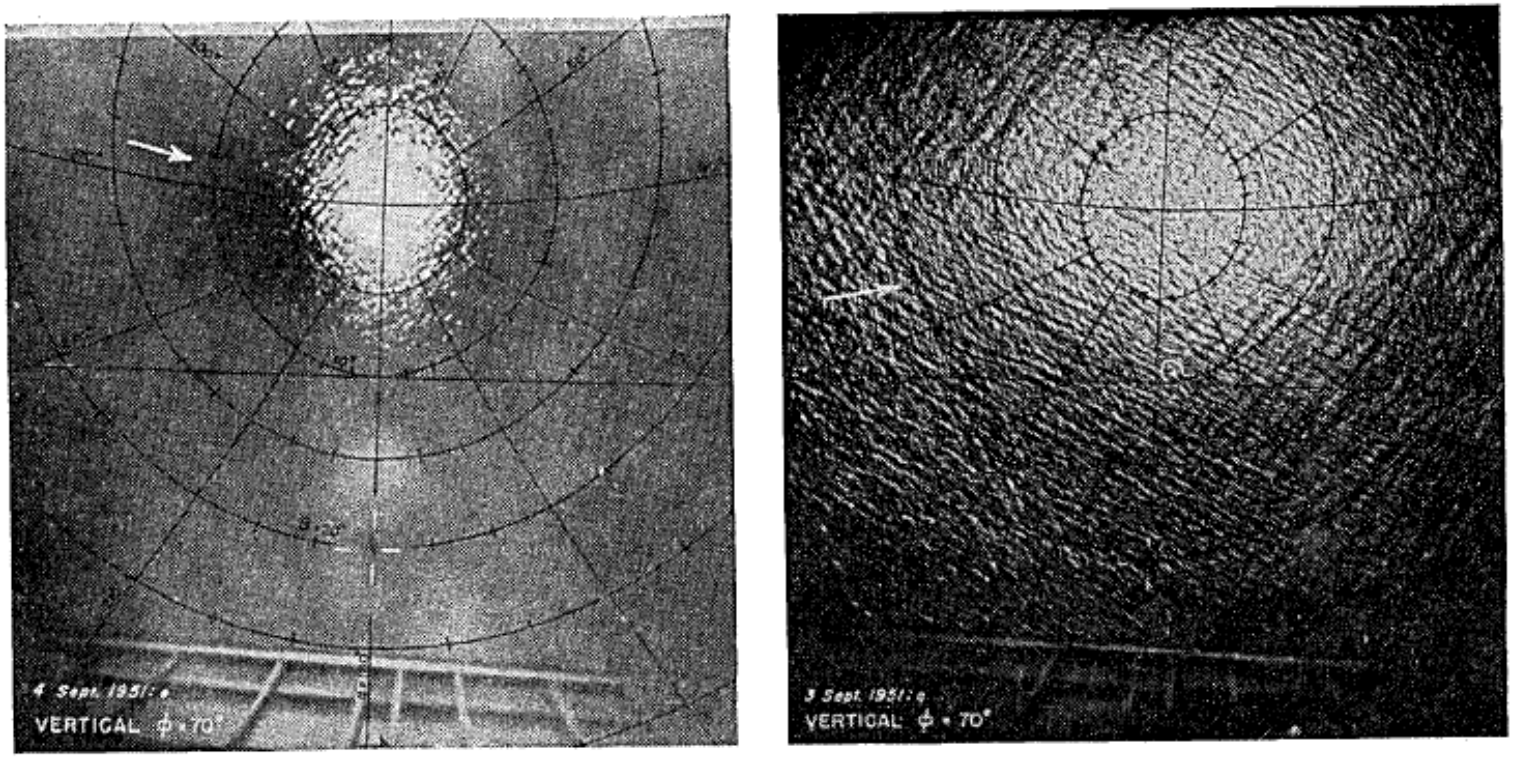

FIG. 1. Glitter patterns photographed by aerial camera pointing vertically downward at solar elevation of $\phi=70°$. The superimposed grids consist of lines of constant slope azimuth α (radial) drawn for every 30°, and of constant tilt β (closed) for every 5°. Grids have been translated and rotated to allow for roll, pitch, and yaw of plane. Shadow of plane can barely be seen along $\alpha=180°$ within white cross. White arrow shows wind direction. *Left:* water surface covered by natural slick, wind 1.8 m sec^{-1}, rms tilt $\sigma=0.0022$. *Right:* clean surface, wind 8.6 m sec^{-1}, $\sigma=0.045$. The vessel *Reverie* is within white circle.

Cox and Munk (1956)

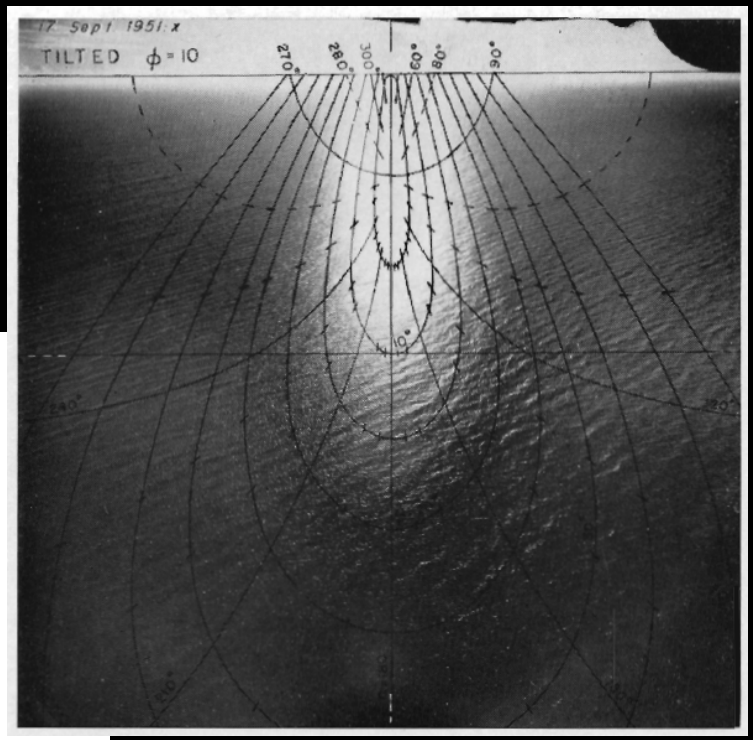

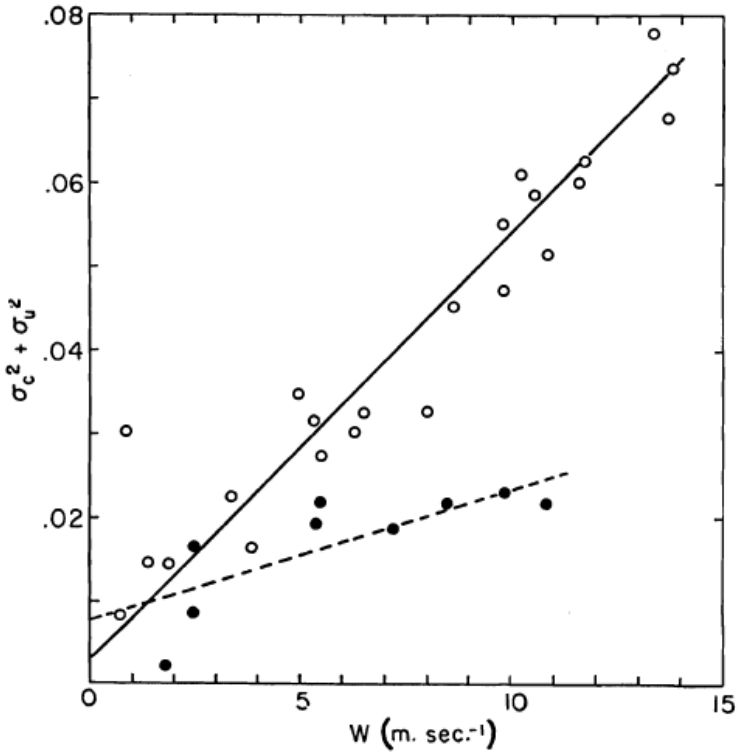

Fig. 13. Mean square slope components and their sum as functions of the wind speed W measured 41 ft. above sea level. The plot includes all analyzed data for clean sea surfaces (open circles) and slick surfaces (solid circles). Continuous lines are regression lines for clean surfaces; dashed lines for slick surfaces.

Paul Desmond Scully-Power
NASA's astronaut

Application to Oil Spills Detection

Deepwater Horizon
May 24, 2010
Terra/MODIS

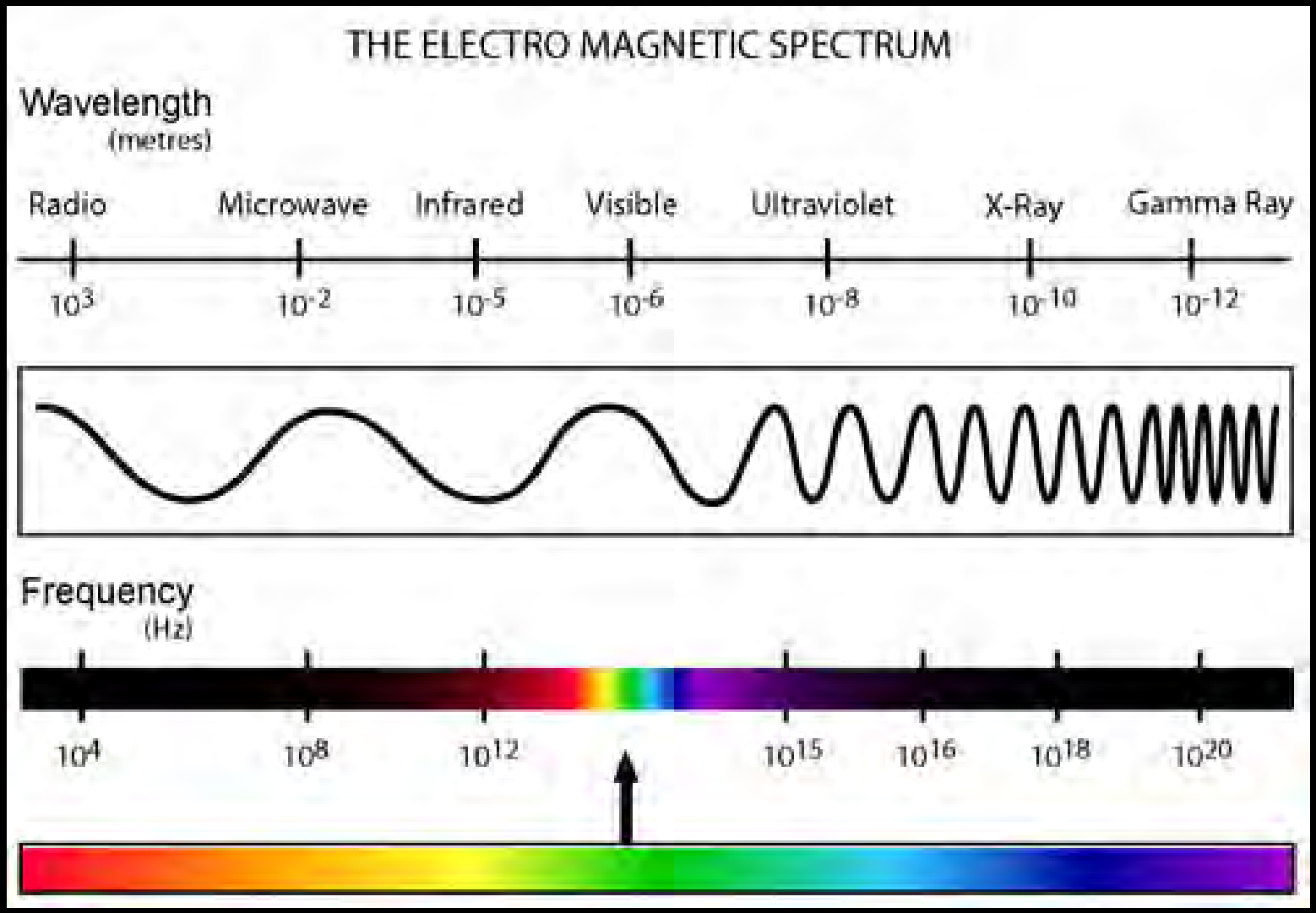
THE ELECTRO MAGNETIC SPECTRUM
Wavelength
(metres)
Radio
Microwave
Infrared
Visible
Ultraviolet
X-Ray
Gamma Ray
10^{3}
10^{-2}
10^{-5}
10^{-6}
10^{-8}
10^{-10}
10^{-12}
Frequency
(Hz)
10^{4}
10^{8}
10^{12}
10^{15}
10^{16}
10^{18}
10^{20}

Constrains of cloud cover

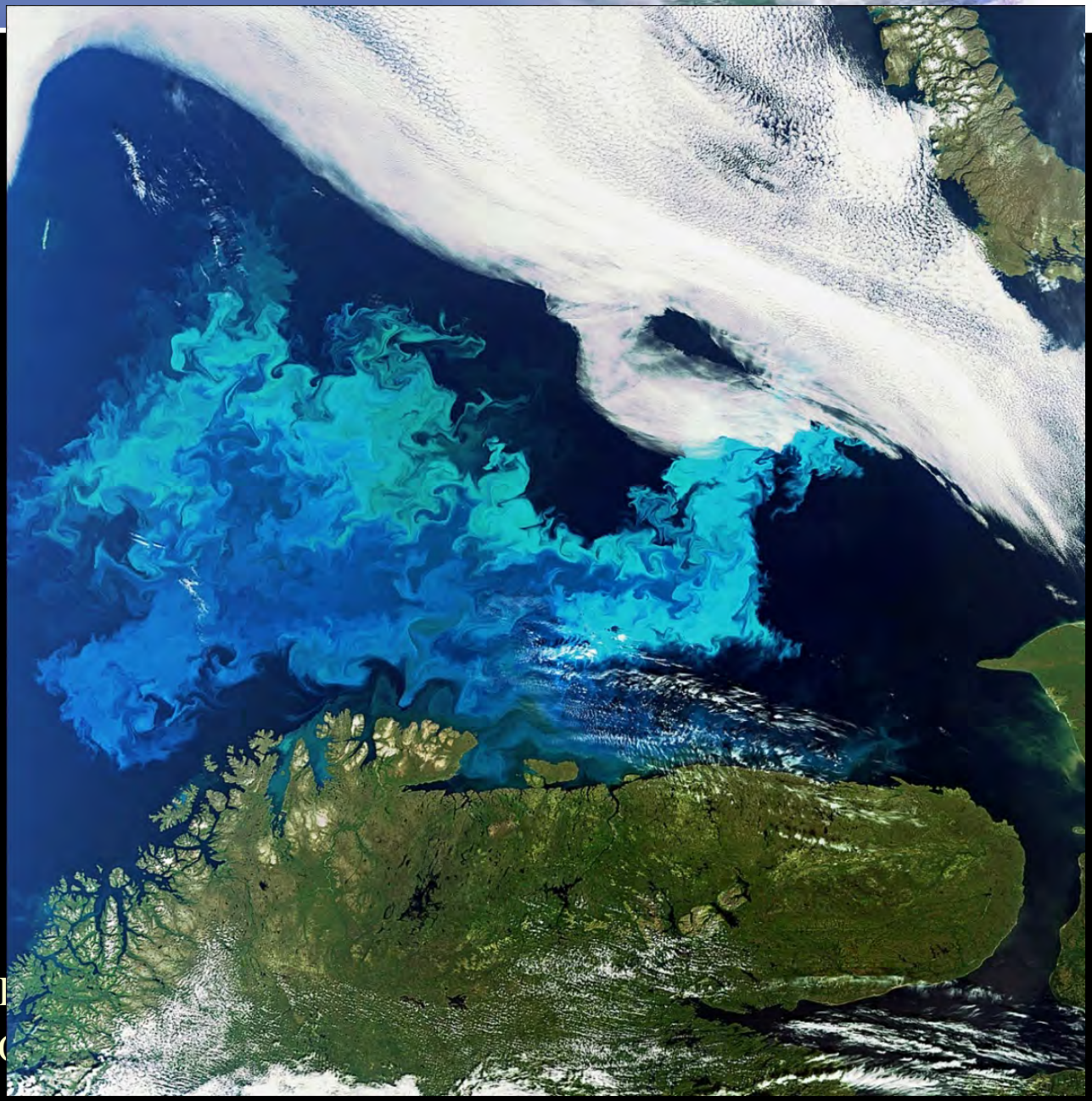

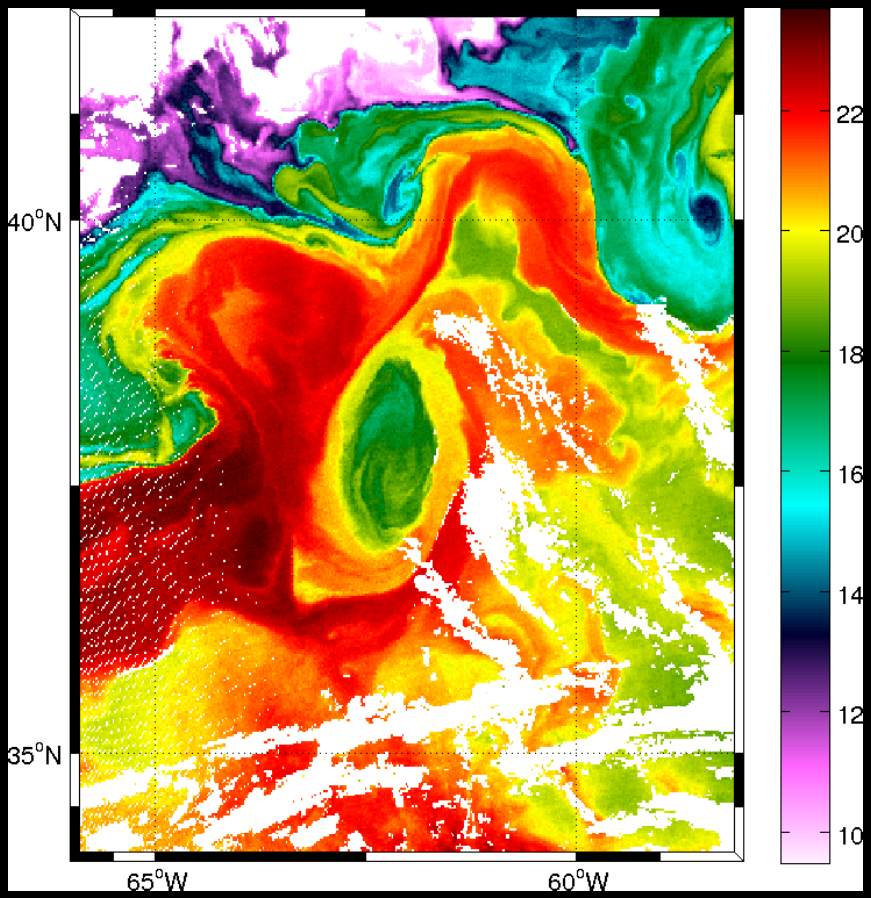
40°N
35°N
65°W
60°W
22
20
18
16
14
12
10

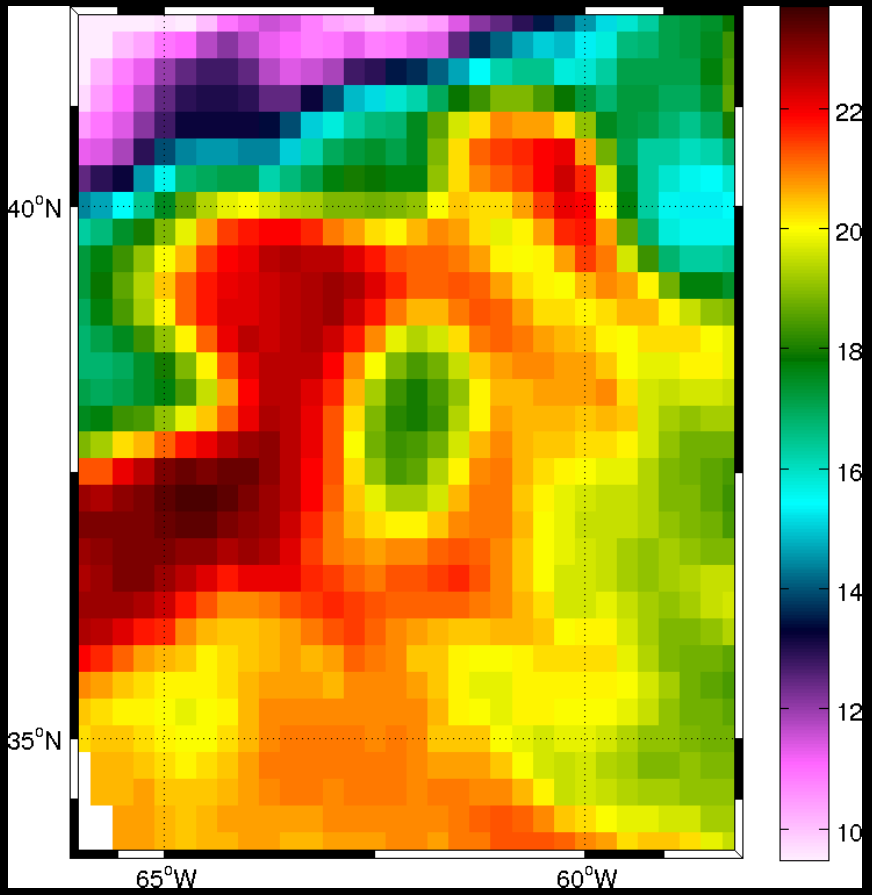
40°N
35°N
65°W
60°W
22
20
18
16
14
12
10

SST

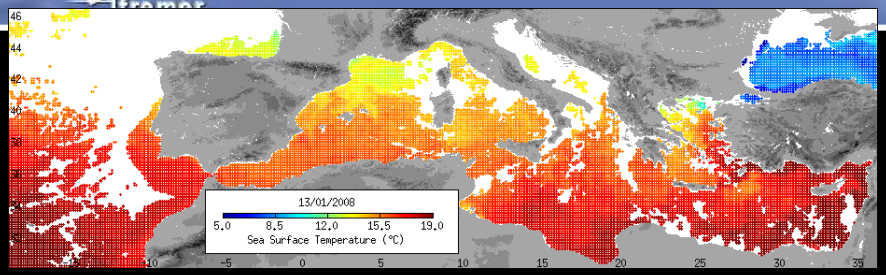

MSG/SEVIRI (10km, 3 heures)

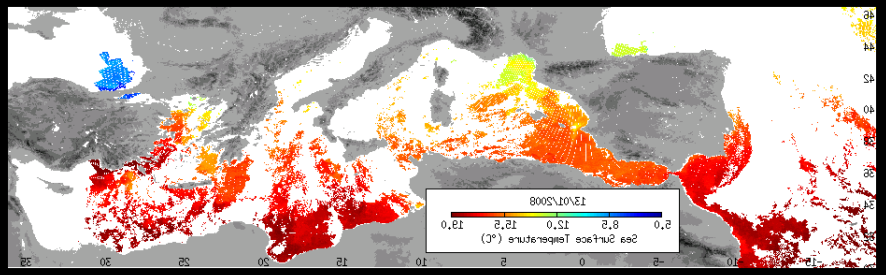

SAF O&SI NAR pour AVHRR17 (2km, 2 passes/jour)

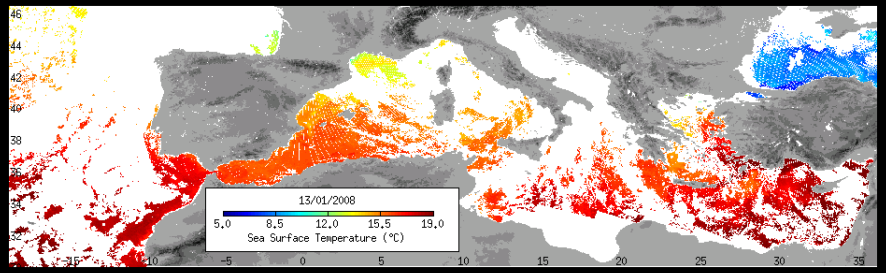

SAF O&SI NAR18 pour AVHRR17 (2km, 2 passes/jour)

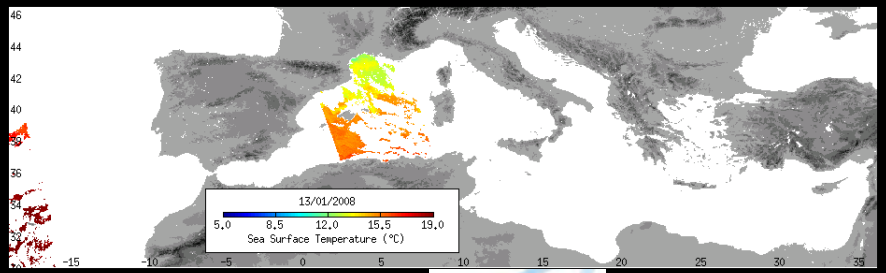

AT

1 jour

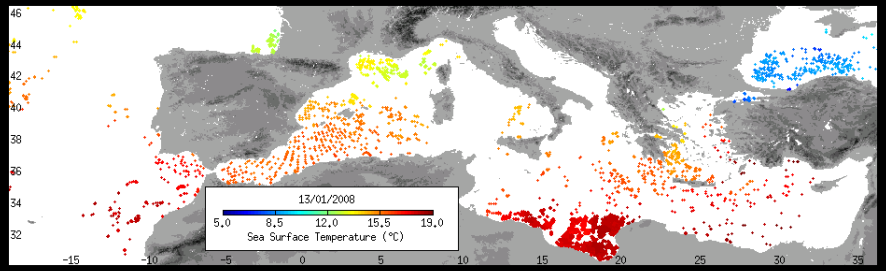

Avhrr 18

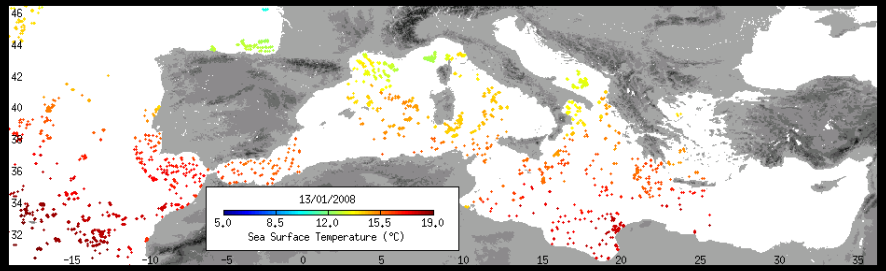

Avhrr 17

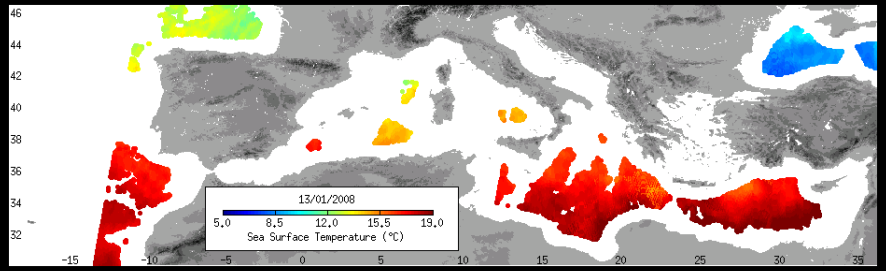

ENVISAT/AATSR (1 km, 14-15 orbites/jour)

Multi-satellite product

medspiration

esa

Sea surface temperature

High resolution daily product 2006-present, 2 km resol

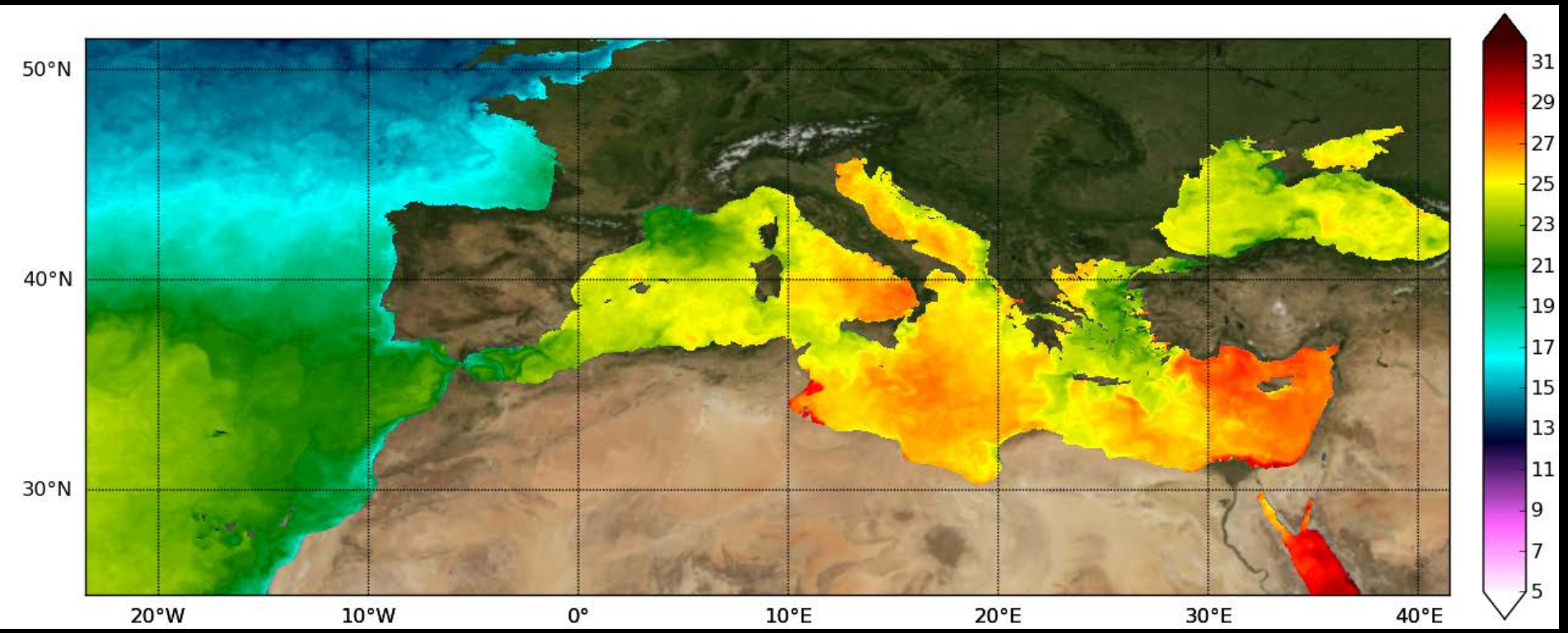

projet ESA Medspiration

Global SST

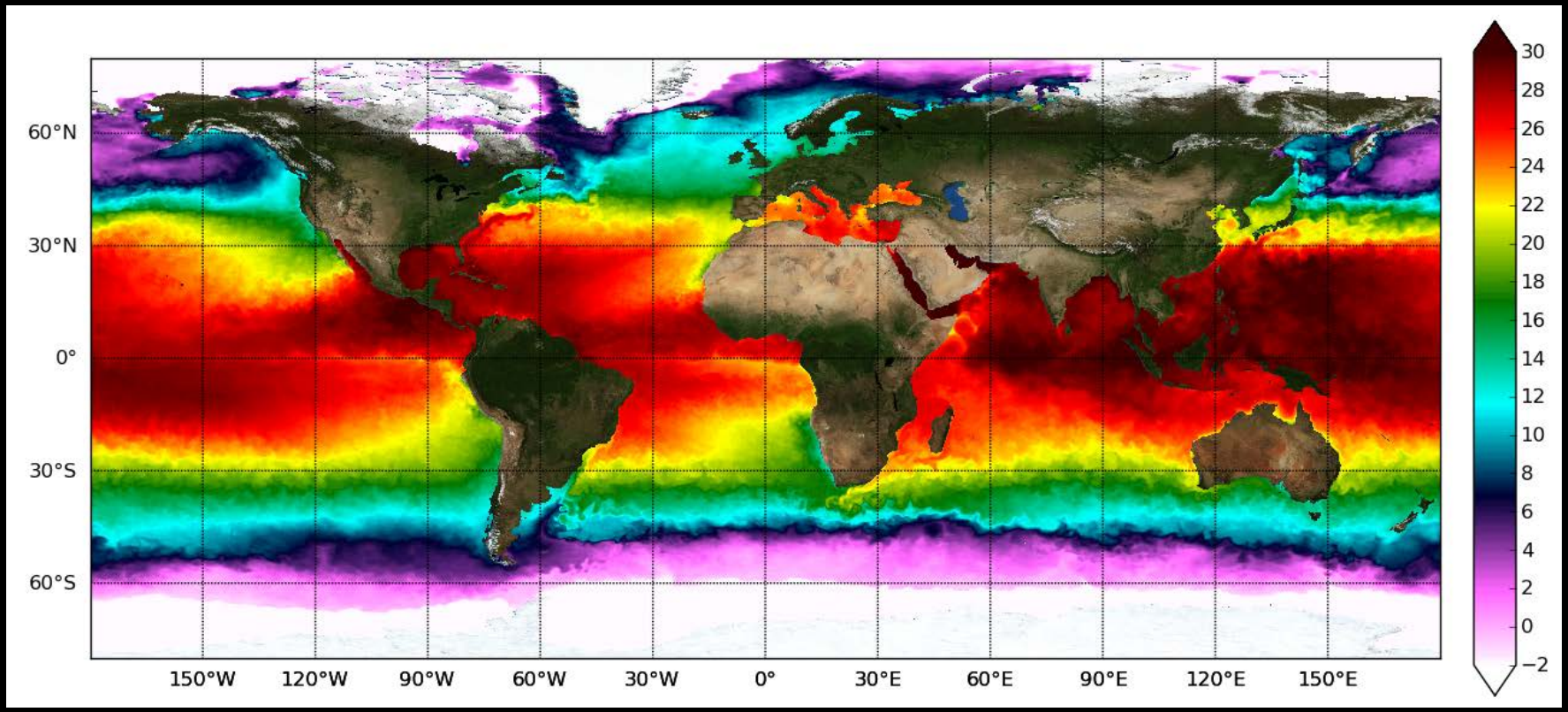

Global reanalysis 2006-present
at 10 km resolution

Synergy SSS (SMOS+AMSR-E)+Altimeter-derived surface currents +SST (GHRSST)+ Ocean Colour (CDOM MERIS/MODIS)

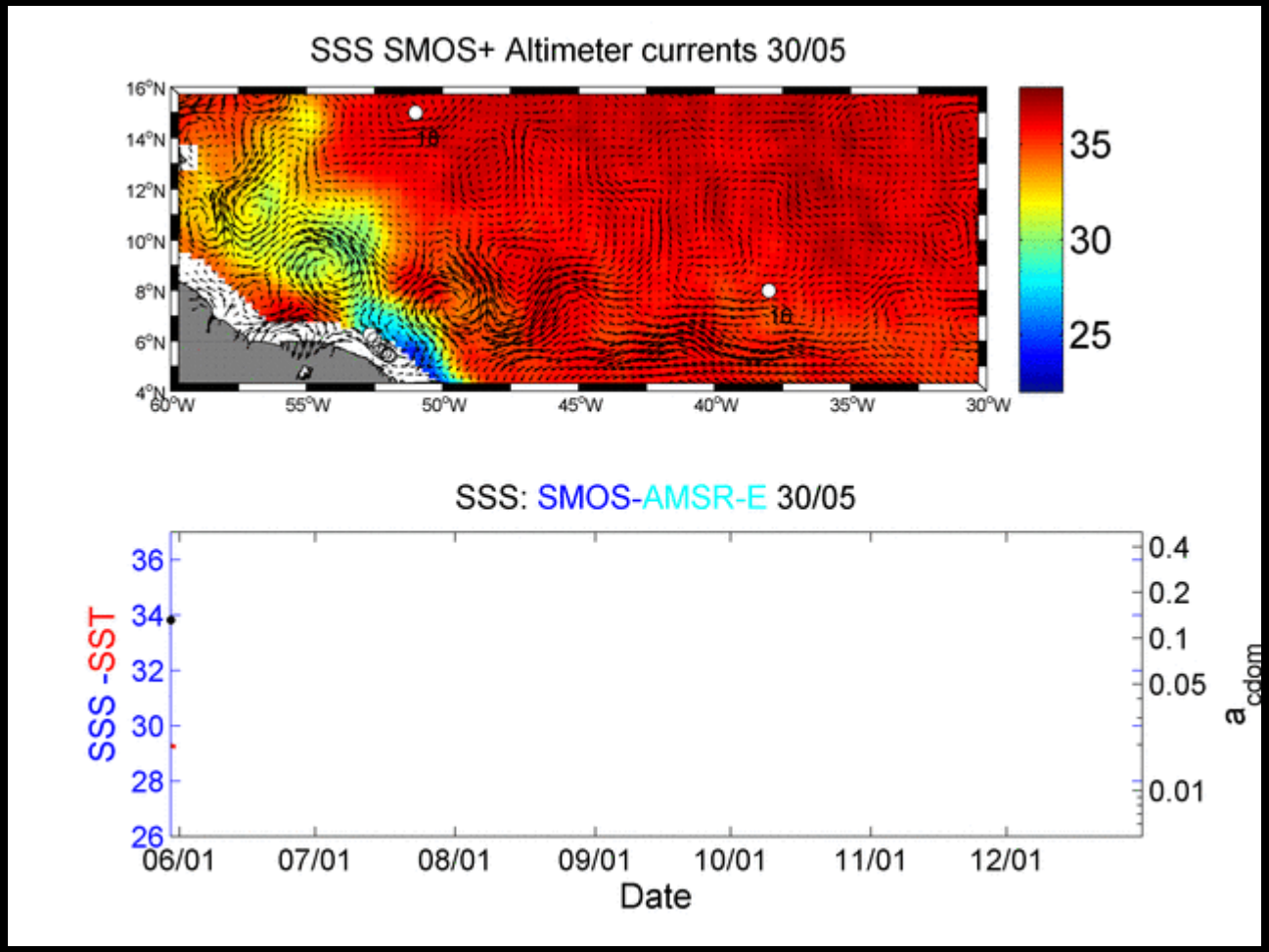

Lagangian Optical-Physical properties

Numerous questions and challenges

Some of the Living Planet Challenges to better assess the existing pressures on the marine environment (e.g. overfishing, pollution, habitat destruction, ...) potentially leading to increased risks to global food security, economic prosperity, …

Evolution of coastal ocean systems including the interactions with land in response to natural and human-induced environmental perturbations

Mesoscale and submesoscale circulation and the role of the vertical ocean pump and its impact on energy transport and biogeochemical cycles

Response of the marine ecosystem and associated ecosystem services to natural and anthropogenic changes,

Physical and biogeochemical air/sea interaction processes on different spatio-temporal scales and their fundamental role in weather and climate

Sea level changes from global to coastal scales and from days (e.g. storm surges) to centuries (e.g. climate change)

Essential Challenges

P. Niiler (2009) Oceanography in 2025

Oceanography of 2025 will require observations and realistic modeling of the circulation patterns that contain the vertical motion of the upper 200 m. Models will be compared not by how well they assimilate or replicate the sea level or reproduce the geostrophic velocity, but rather by how their internal vorticity and thermal energy and fresh water balances maintain ageostrophic velocity structures and the associated vertical circulations. This task calls for development and implementation of continued new methods and instruments for direct velocity observations of the oceans.

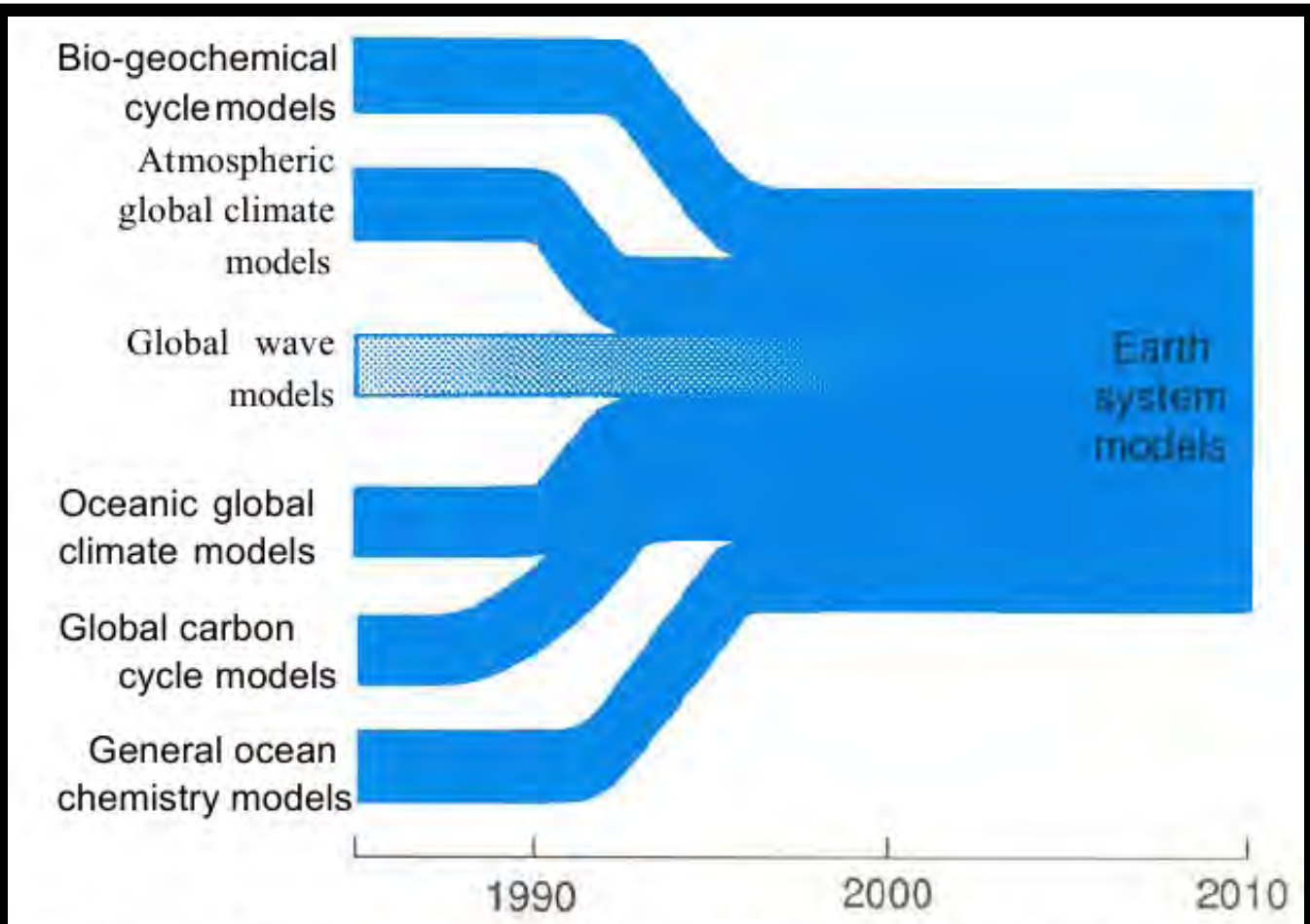

Figure 1. Future role of wave models as an essential coupling component for ocean-atmosphere-carbon-cycle modets developed in the context ot the World Climate and Global Change programs.

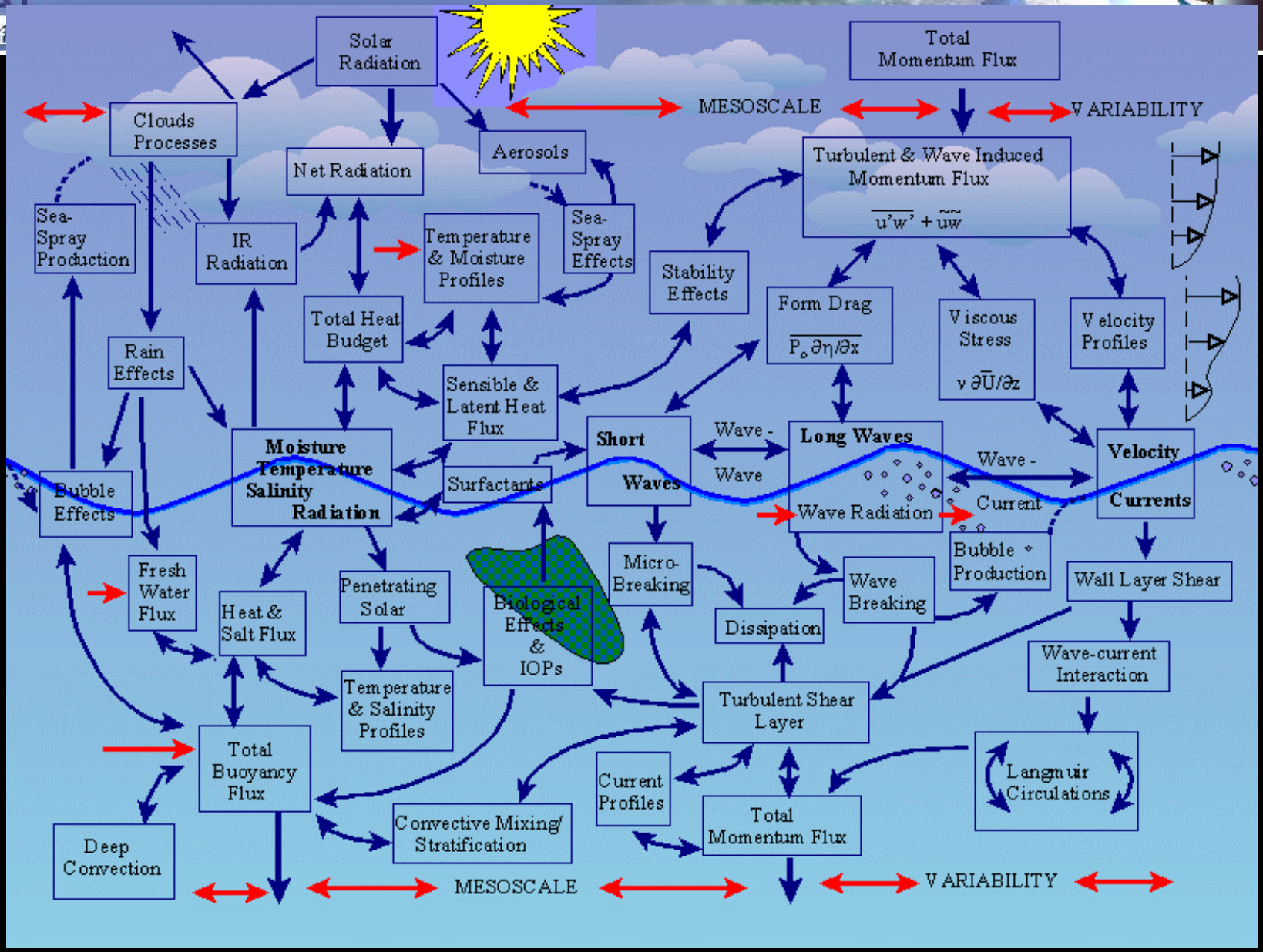
Solar Radiation
Total Momentum Flux
MESOSCALE
VARIABILITY
Clouds Processes
Aerosols
Net Radiation
Turbulent & Wave Induced Momentum Flux
$\overline{u'w'} + \widetilde{uw}$
Sea-Spray Production
IR Radiation
Temperature & Moisture Profiles
Sea-Spray Effects
Stability Effects
Form Drag
$\overline{P_o \partial\eta/\partial x}$
Viscous Stress
$\nu \partial\bar{U}/\partial z$
Velocity Profiles
Total Heat Budget
Rain Effects
Sensible & Latent Heat Flux
Moisture
Temperature
Salinity
Radiation
Short Waves
Wave - Wave
Long Waves
Wave - Current
Velocity Currents
Bubble Effects
Surfactants
Wave Radiation
Bubble Production
Fresh Water Flux
Heat & Salt Flux
Penetrating Solar
Biological Effects & IOPs
Micro-Breaking
Wave Breaking
Wall Layer Shear
Dissipation
Wave-current Interaction
Temperature & Salinity Profiles
Turbulent Shear Layer
Total Buoyancy Flux
Current Profiles
Langmuir Circulations
Convective Mixing/ Stratification
Total Momentum Flux
Deep Convection
MESOSCALE
VARIABILITY

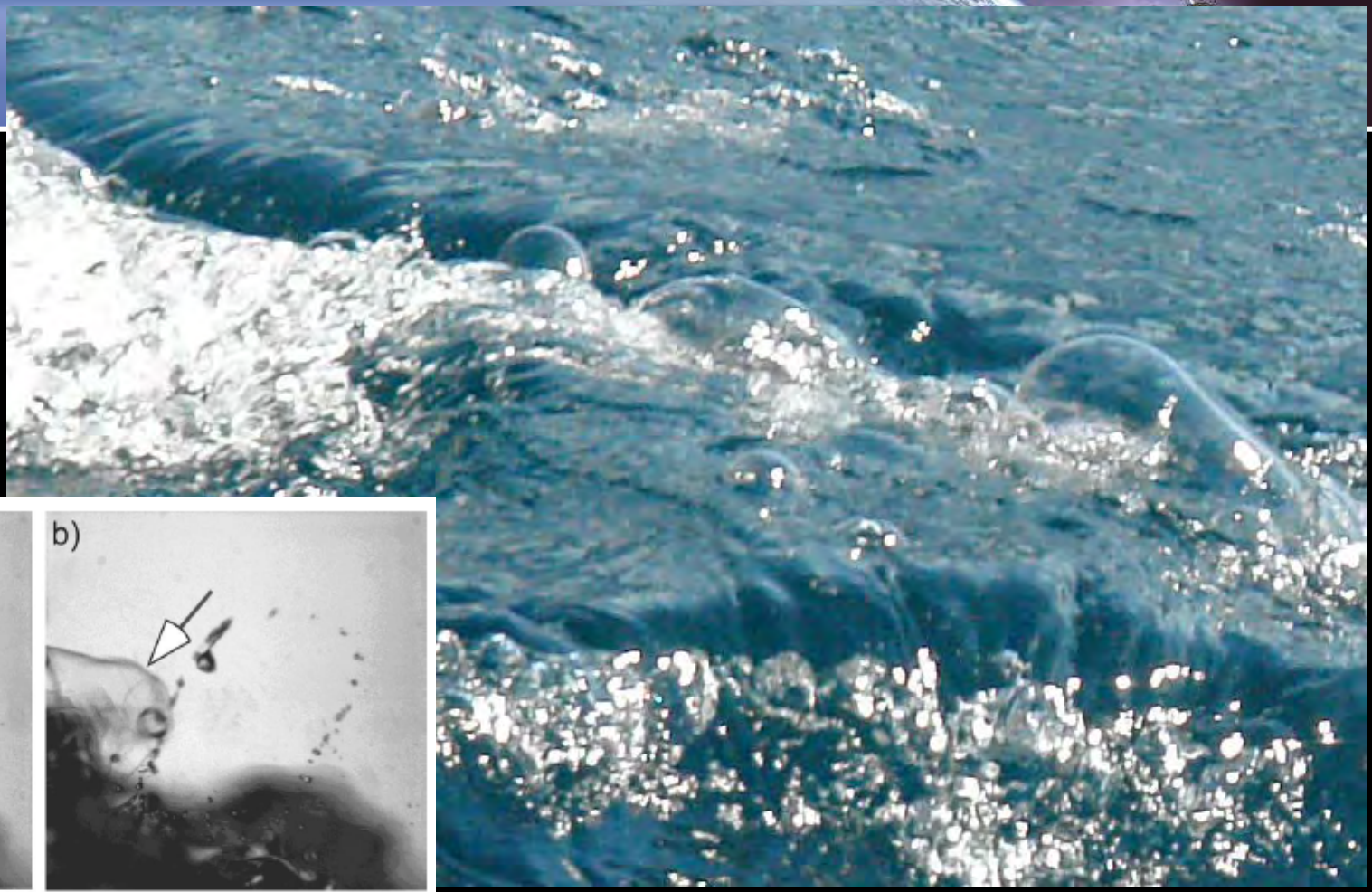

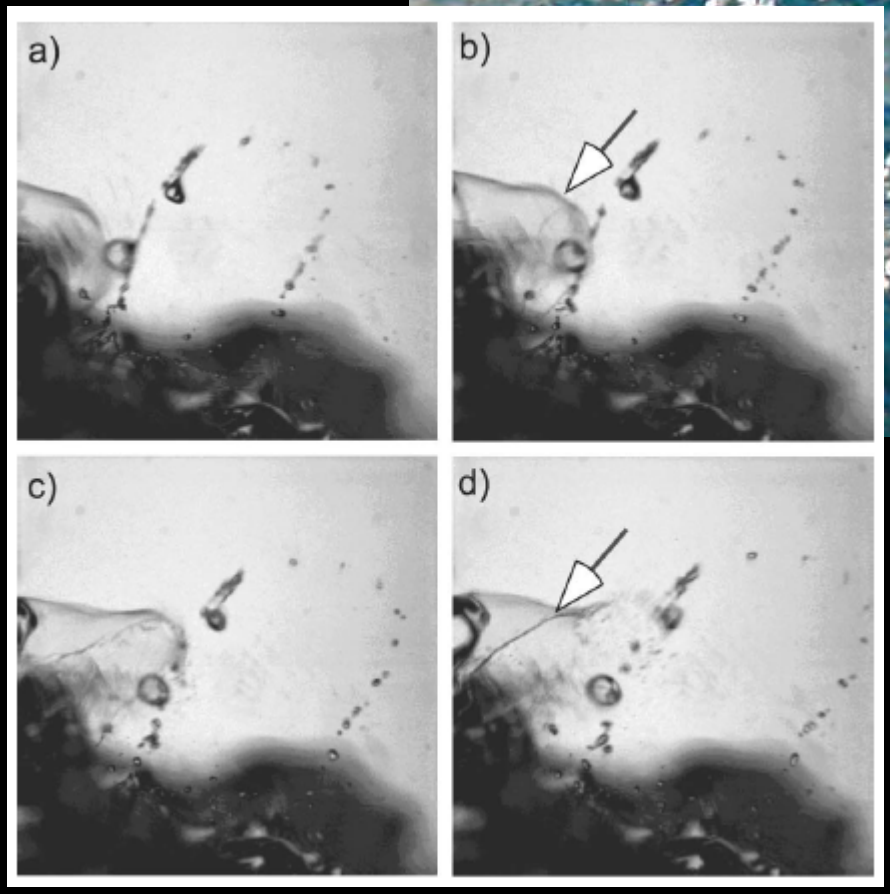
a)
b)
c)
d)

Coupled Ocean-Atmosphere system: Eddy/wind interactions , i.e. the nonlinear Ekman effects

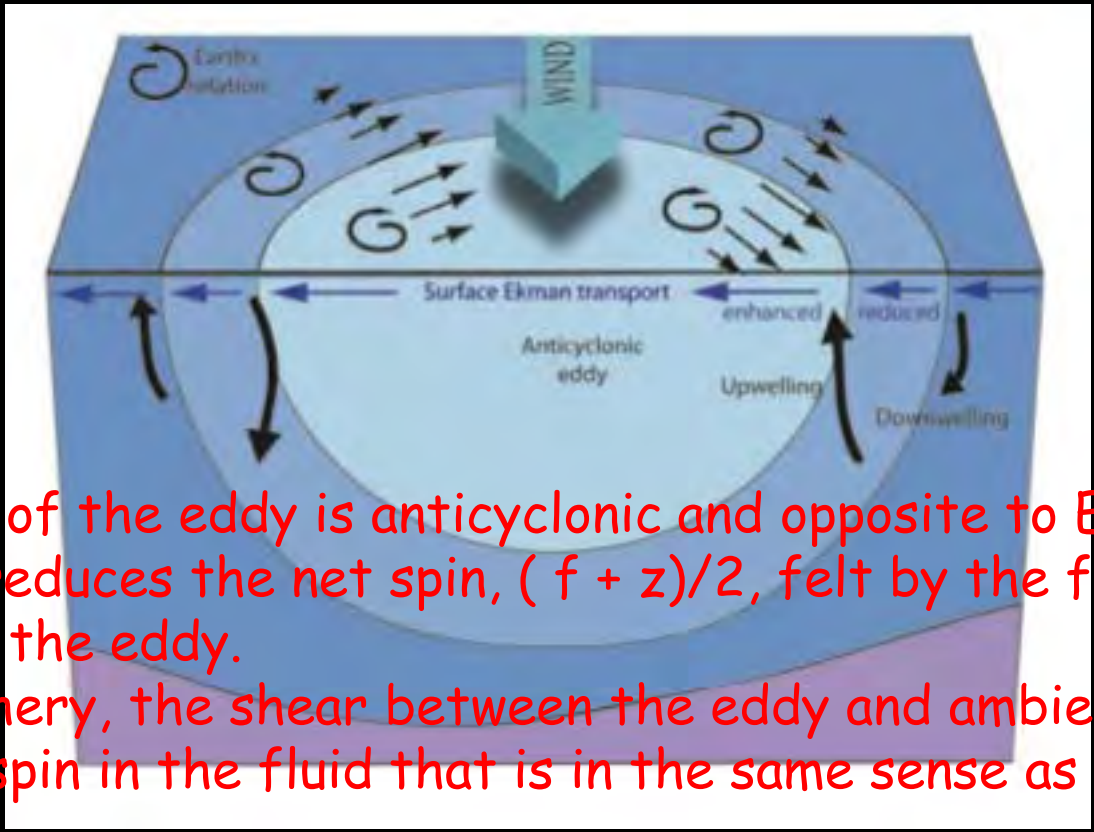

The rotation of the eddy is anticyclonic and opposite to Earth's rotation. It reduces the net spin, (f + z)/2, felt by the fluid toward the inside of the eddy.

At the periphery, the shear between the eddy and ambient fluid generates a spin in the fluid that is in the same sense as Earth's rotation

The divergence/convergence of the Ekman transport can then drive alternate up/down motions

- … most observations are not yet sufficiently explored and used

  Synergy between high resolution observations to reveal mean states and trends, near-surface ocean-atmosphere dynamics, local and non-local interactions, convergence/divergence surface fronts and numerous roughness contrasts

Far from the coasts, Extreme Events are opportunities of high scientific values to investigate how natural processes at their peaks can transfer energy and matter within and across boundaries, and to identify the mechanisms involved and their rates, jointly with their local and/or long term impacts

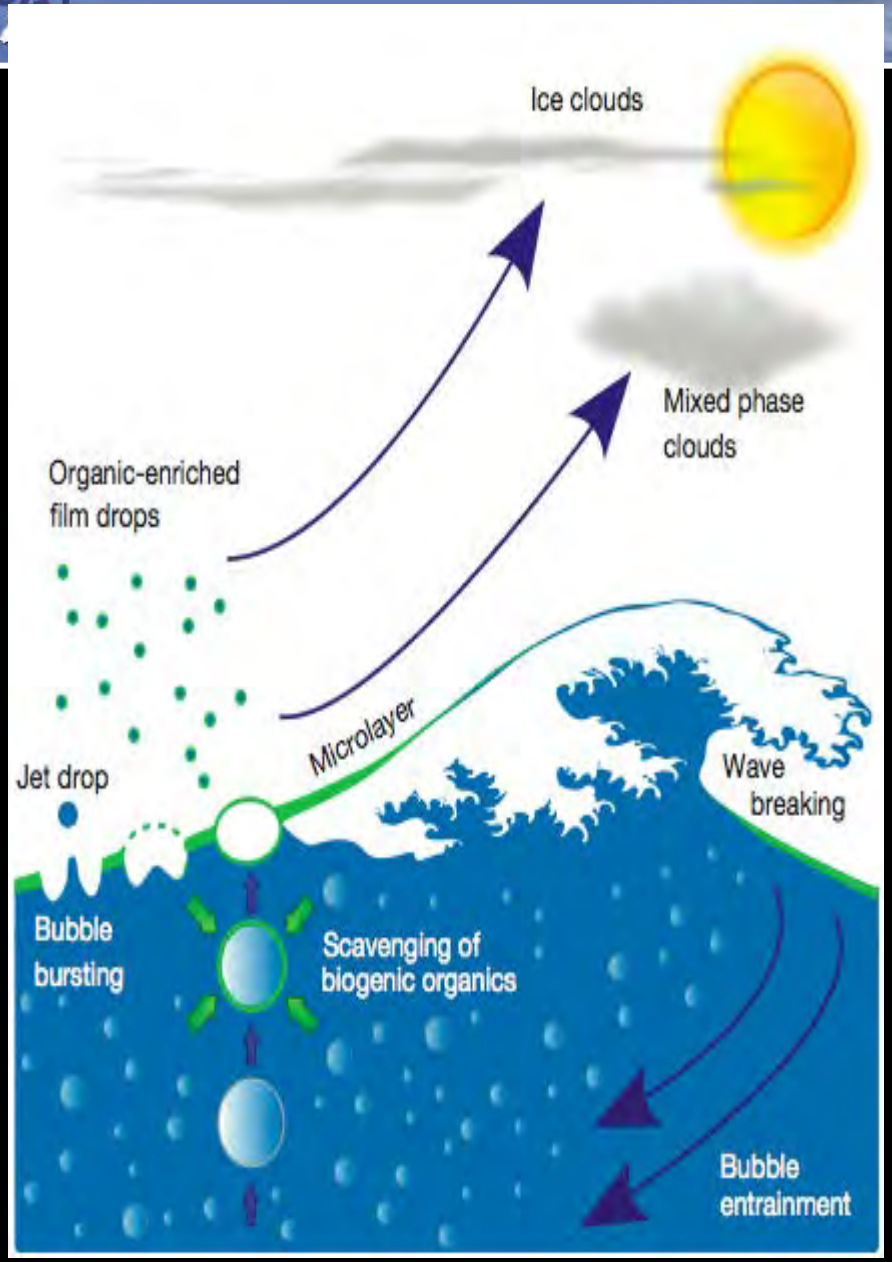

Sea-spray aerosol particles enriched in organic material are possibly generated when the air-sea interface is bursting

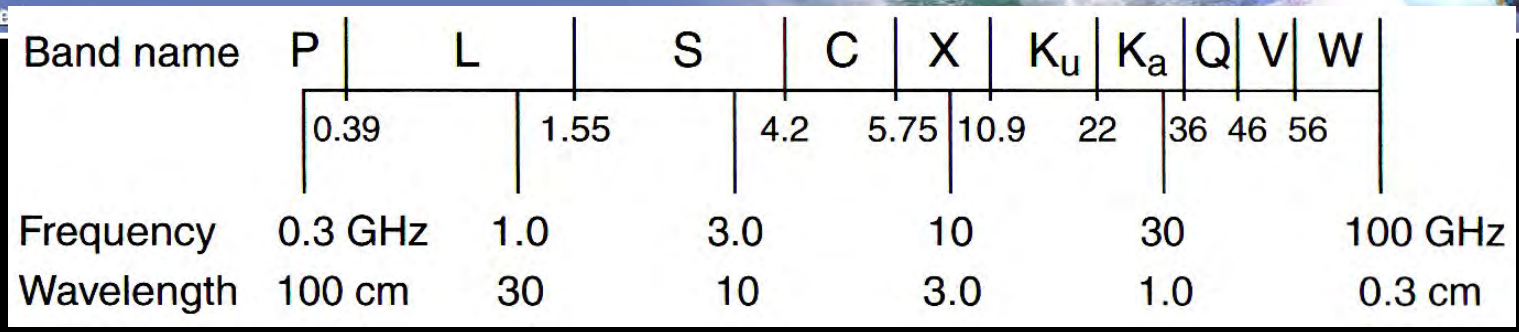

Table 2.1. Band letter designations used in microwave remote sensing.

Band	Frequency (GHz)	Wavelength
P	0.225–0.390	76.9–133 cm
L	0.390–1.55	19.35–76.9 cm
S	1.55–4.20	7.14–19.35 cm
C	4.20–5.75	5.22–7.14 cm
X	5.75–10.9	2.75–5.22 cm
K_u	10.9–22.0	1.36–2.75 cm
K_a	22.0–36.0	8.33–13.6 mm
Q	36.0–46.0	6.52–8.33 mm
V	46.0–56.0	5.36–6.52 mm
W	56.0–100	3.0–5.36 mm

With remote sensing we measure all these

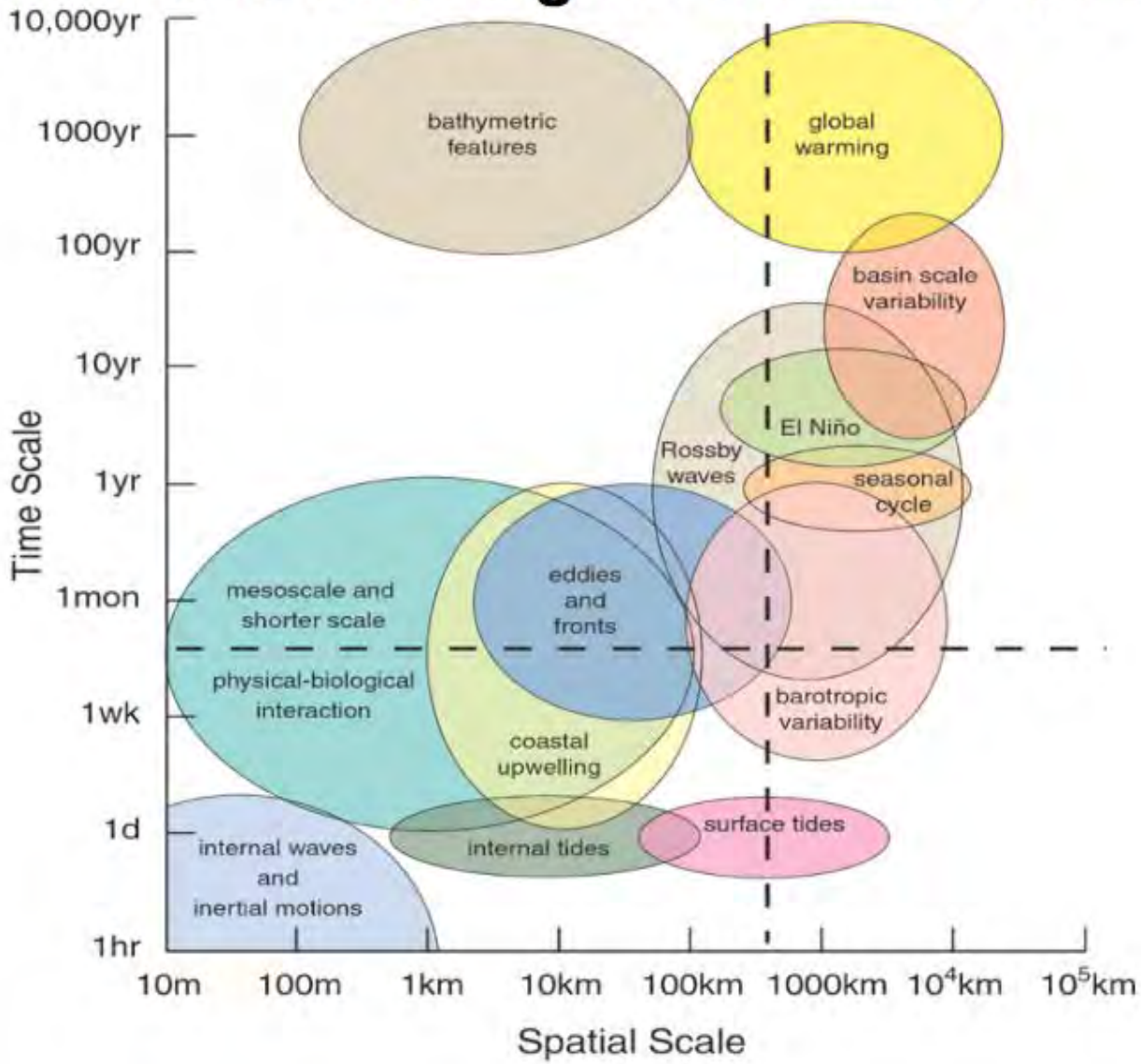

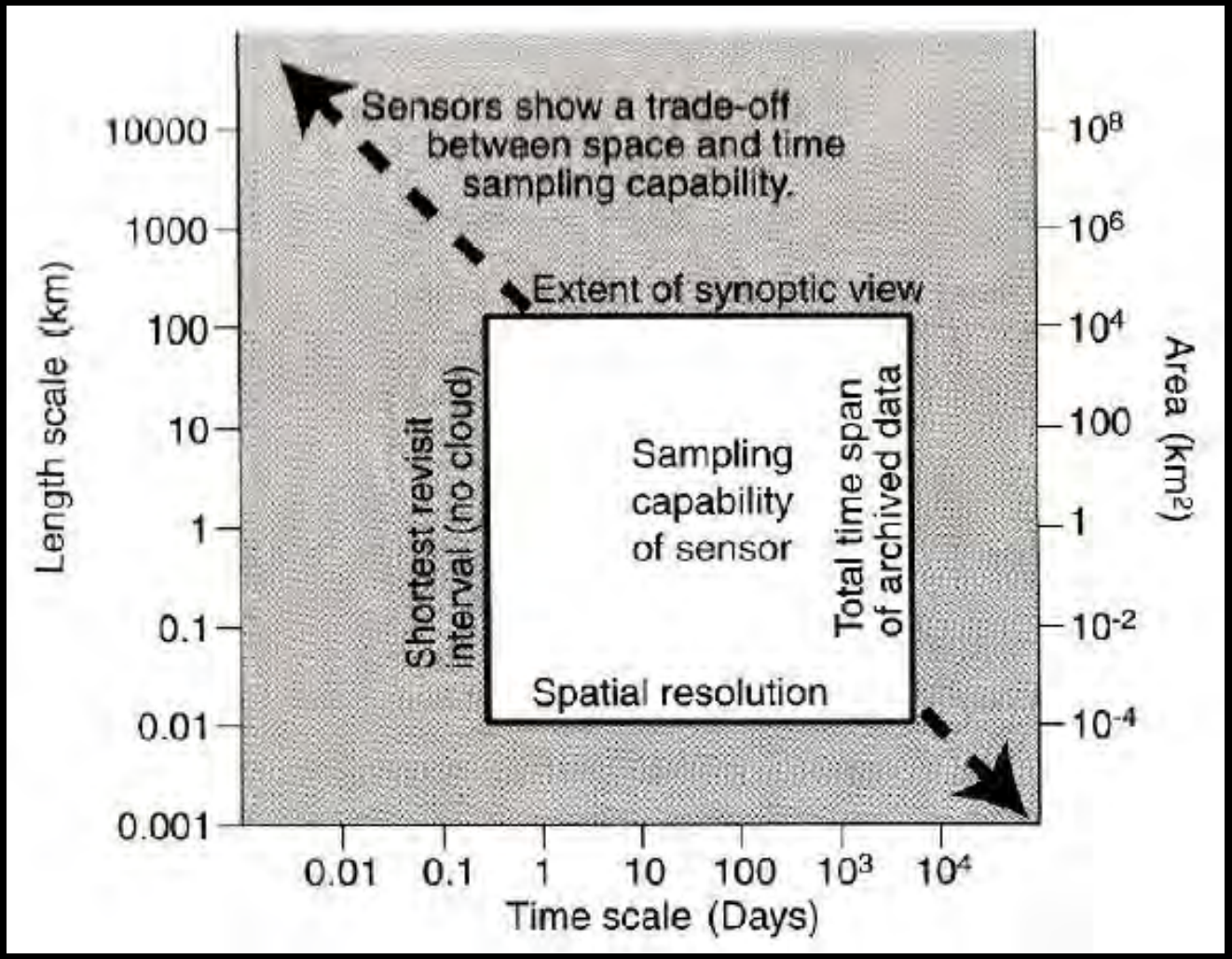

Figure 4.12. Guide to interpreting boundaries of the sensor boxes on the space–time sampling diagrams.

Typical Atmosphere Space-Time scales

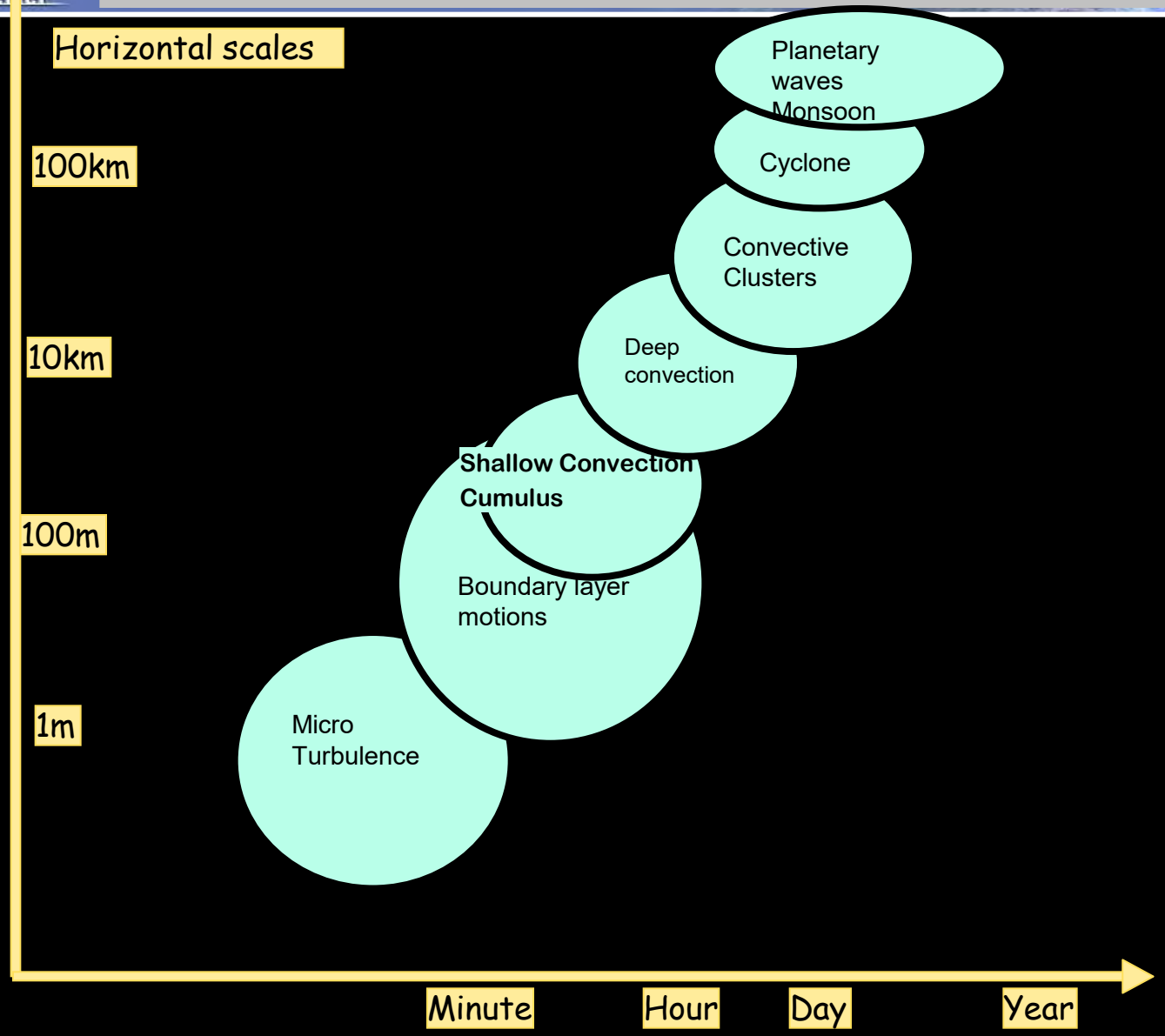

Typical Ocean Space-Time Scales

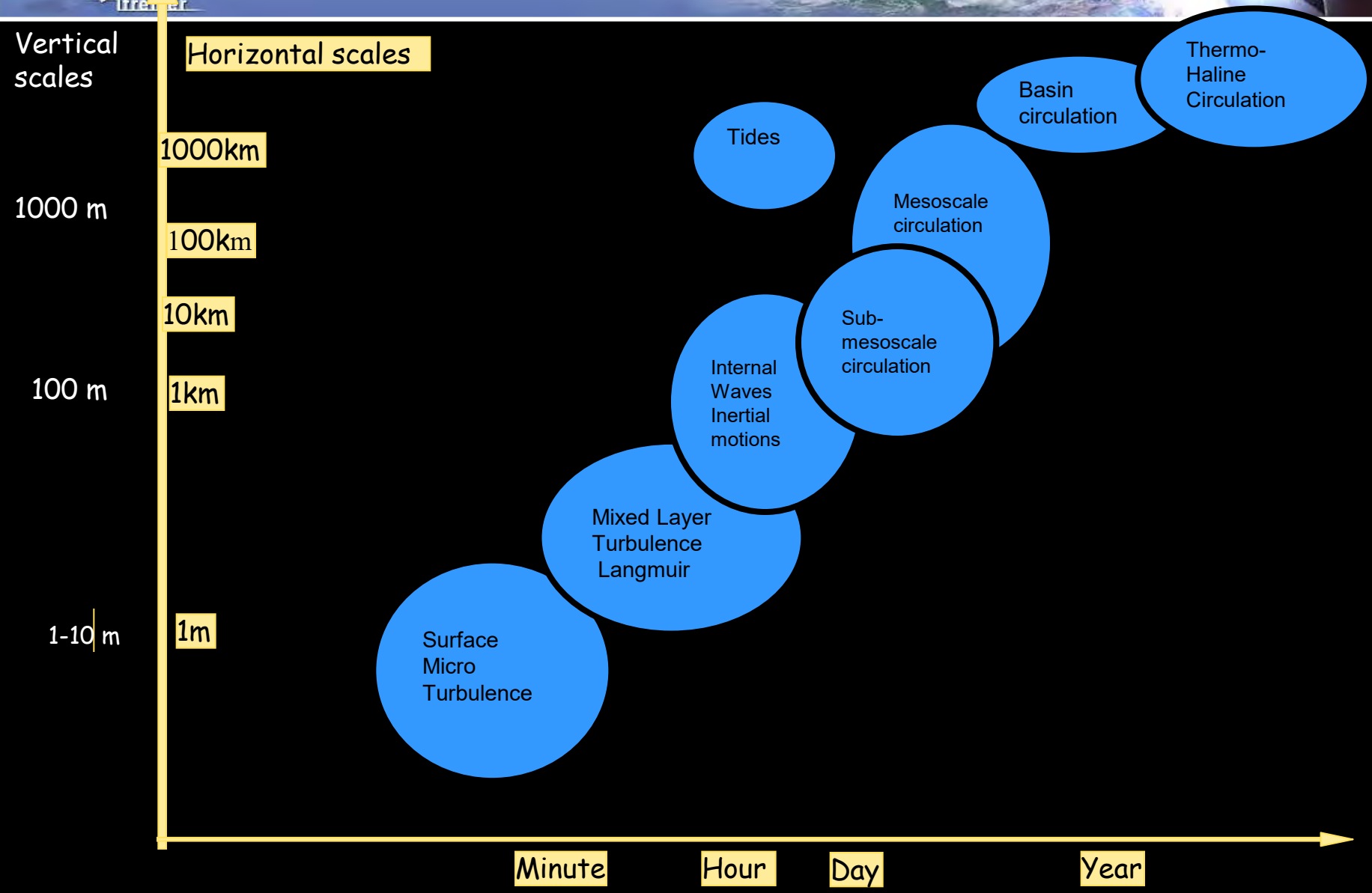

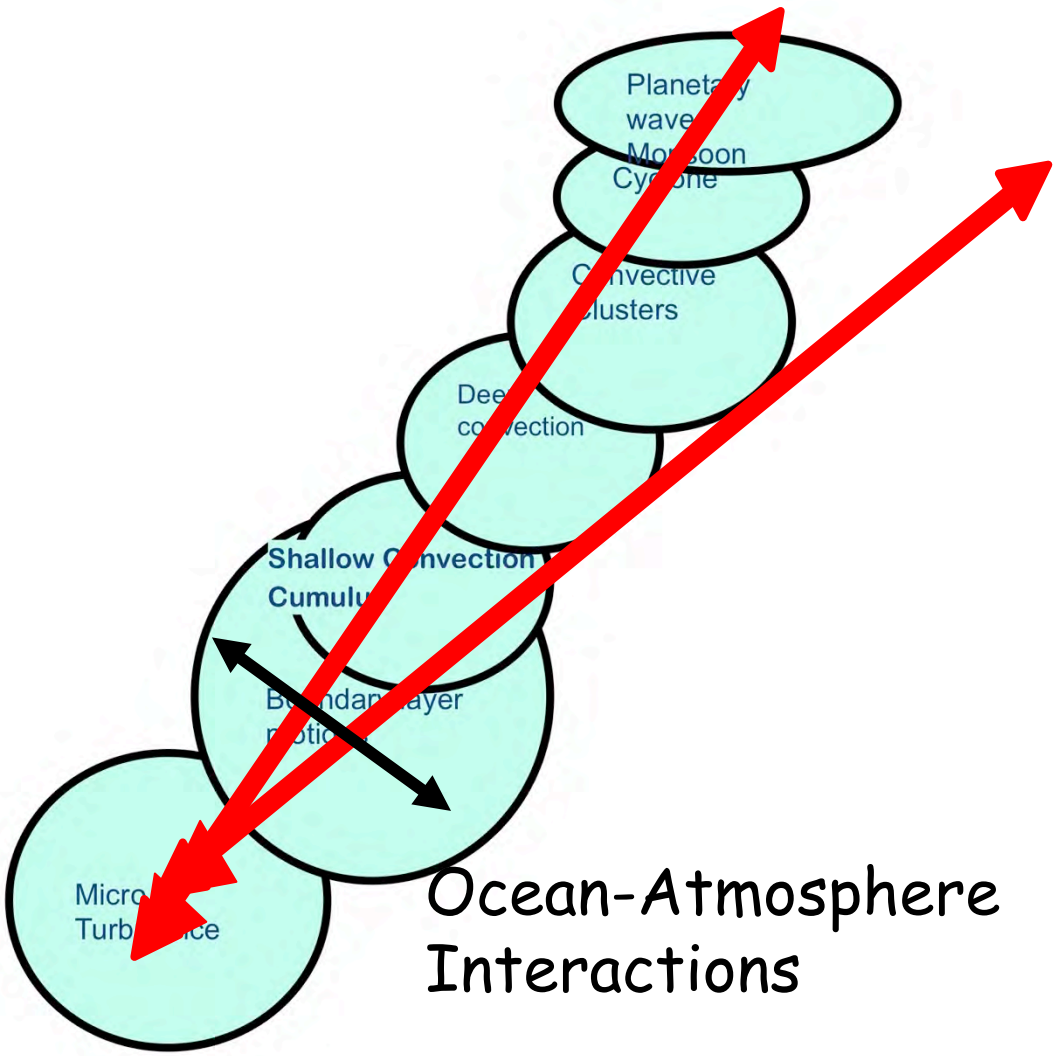

Ocean-Atmosphere Interactions

Upper ocean atmospheric forcing monitoring

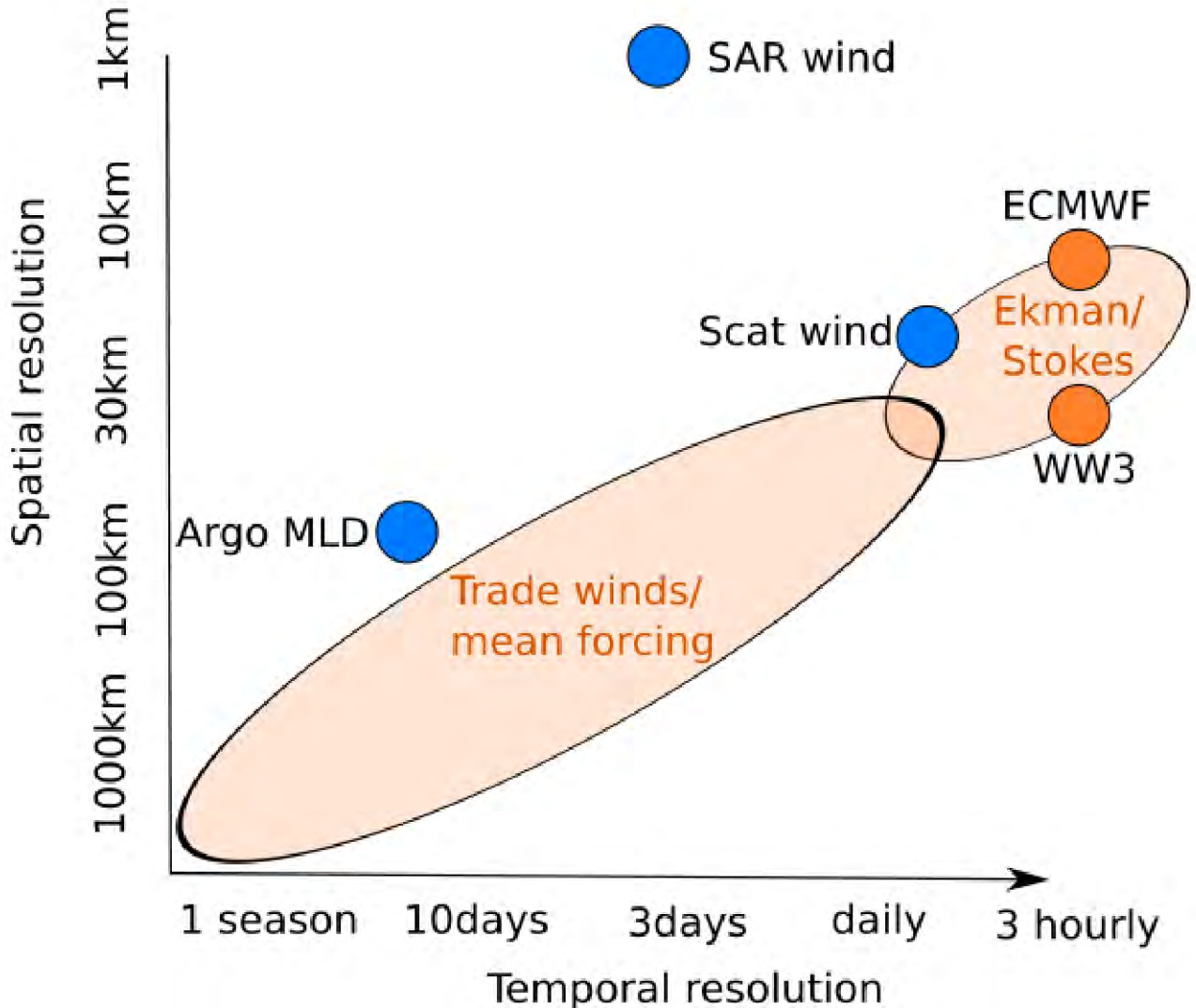

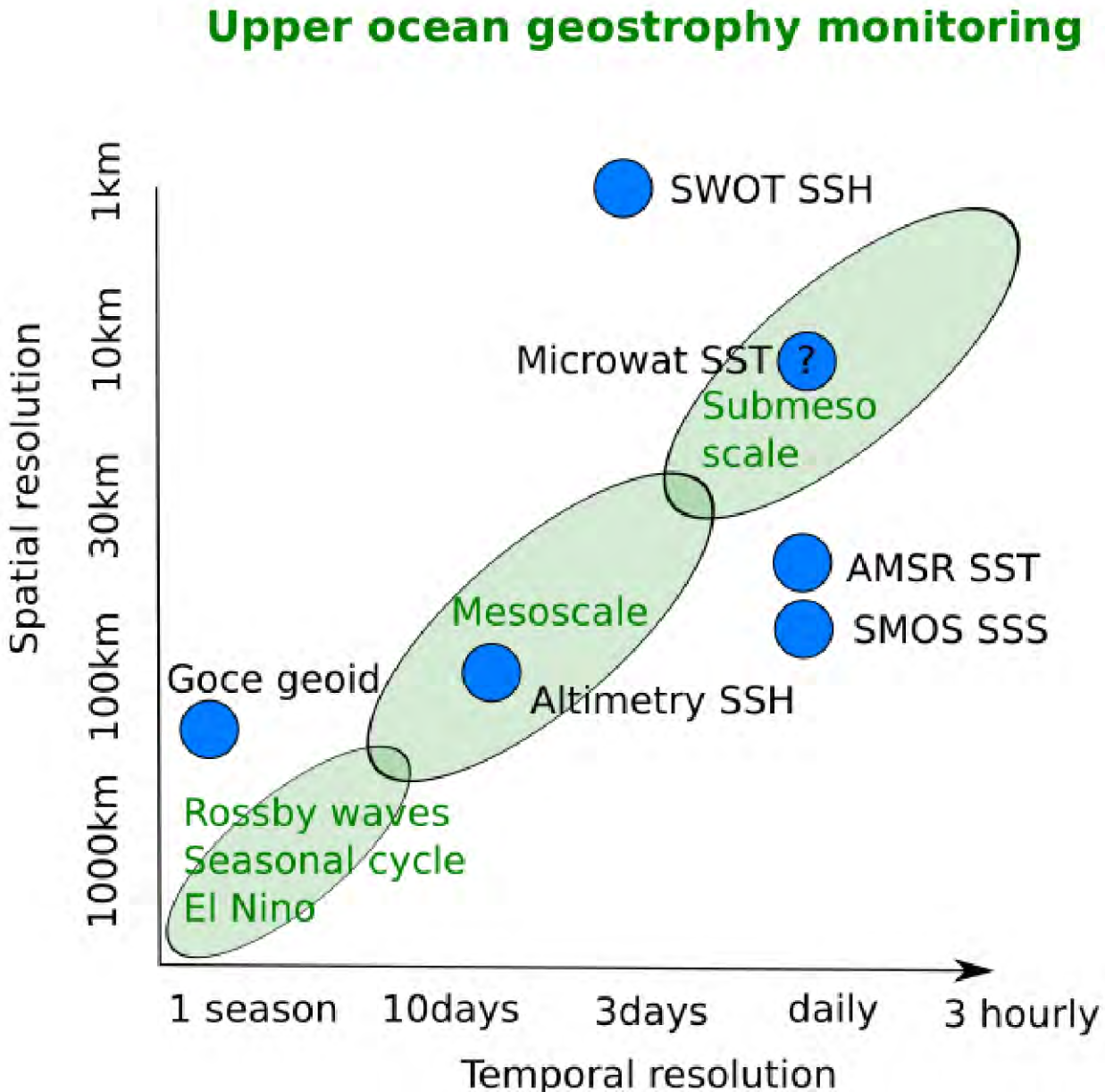
Upper ocean geostrophy monitoring
SWOT SSH
Microwat SST
?
Submeso
scale
AMSR SST
SMOS SSS
Mesoscale
Goce geoid
Altimetry SSH
Rossby waves
Seasonal cycle
El Nino
Spatial resolution
1km
10km
30km
100km
1000km
1 season
10days
3days
daily
3 hourly
Temporal resolution

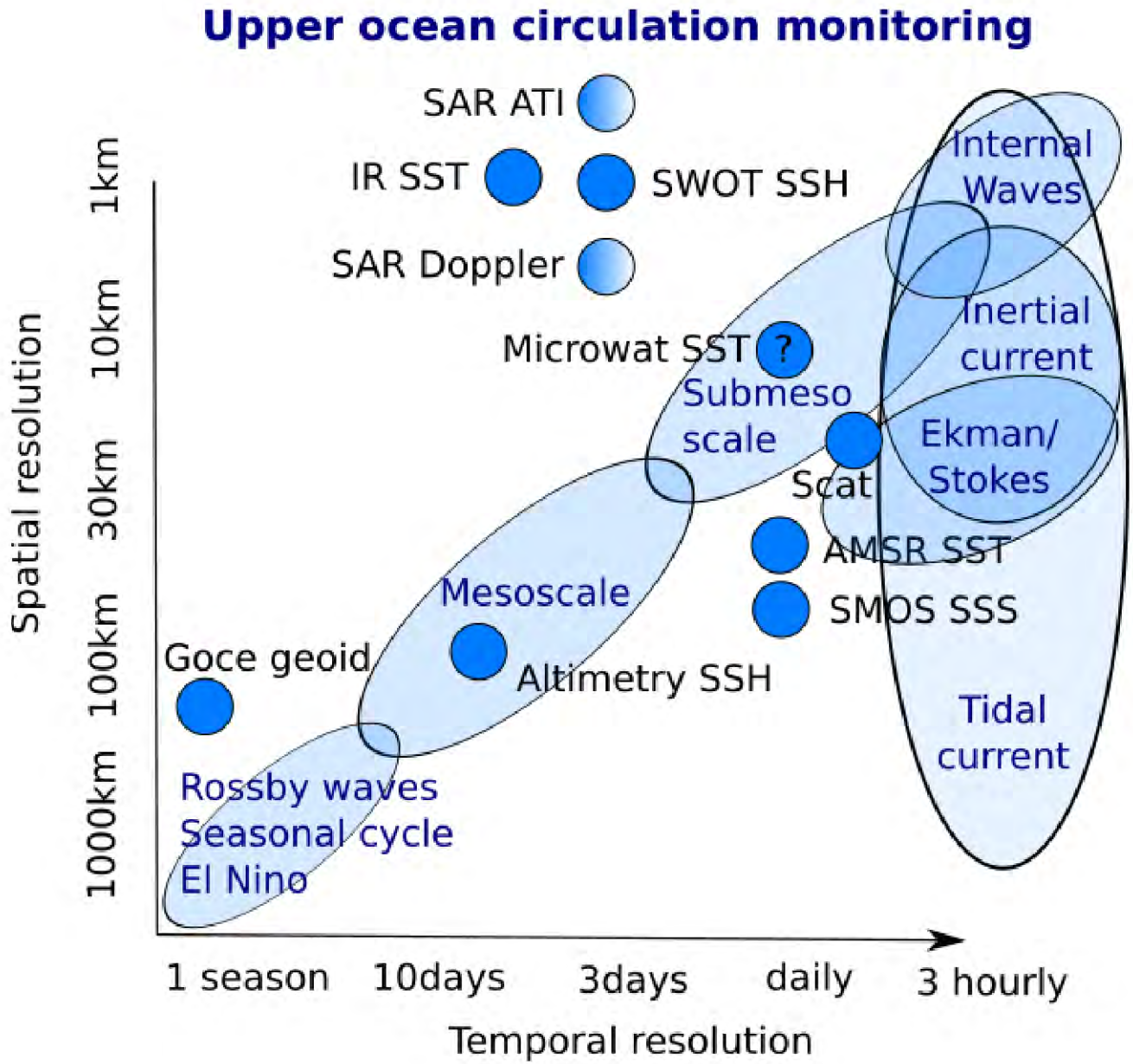
Upper ocean circulation monitoring
SAR ATI
IR SST
SWOT SSH
SAR Doppler
Microwat SST
?
Submeso scale
Scat
AMSR SST
SMOS SSS
Mesoscale
Altimetry SSH
Goce geoid
Rossby waves
Seasonal cycle
El Nino
Internal Waves
Inertial current
Ekman/ Stokes
Tidal current
Spatial resolution
1km
10km
30km
100km
1000km
1 season
10days
3days
daily
3 hourly
Temporal resolution

Upper ocean ageostrophic current monitoring

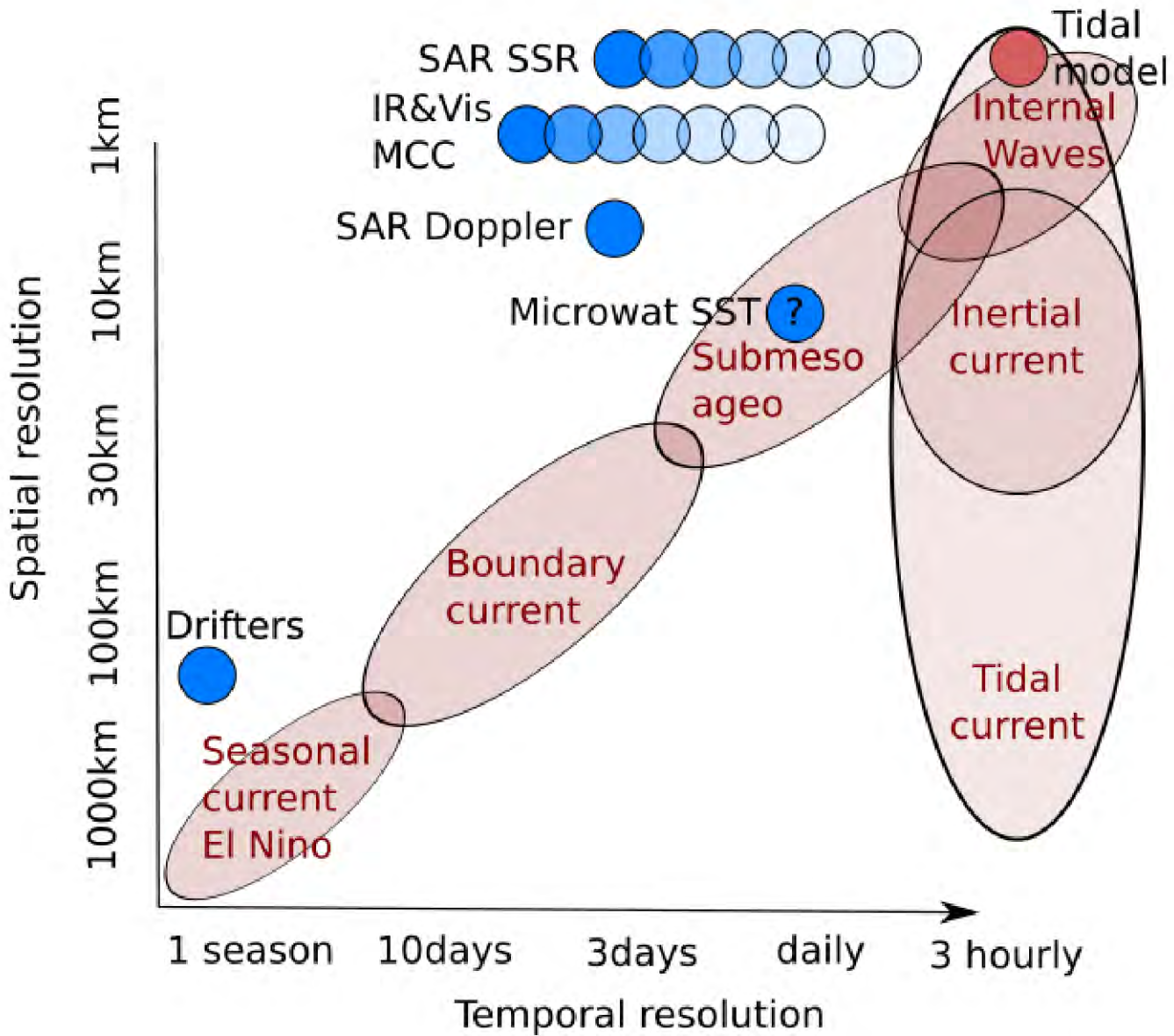

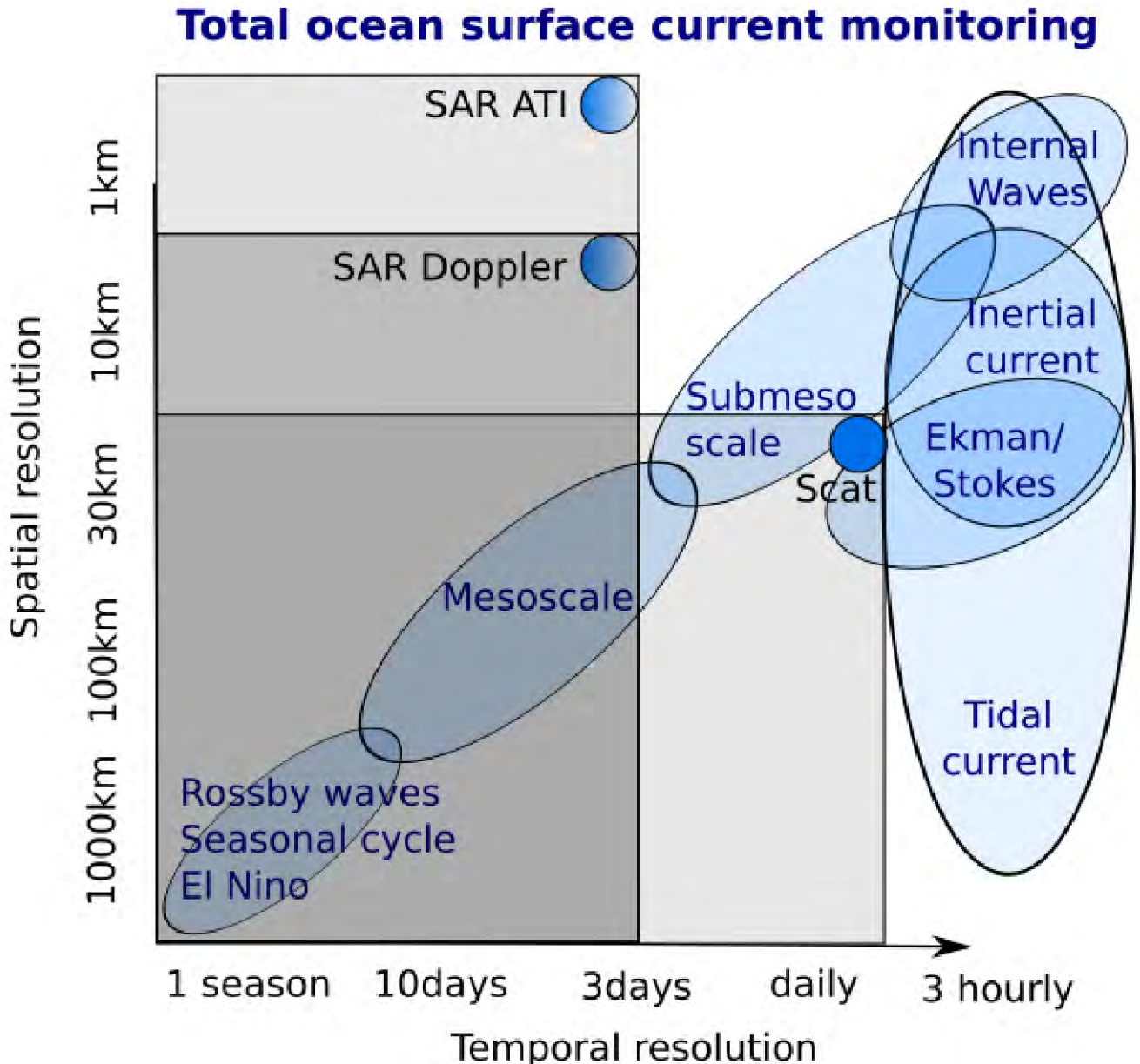
Total ocean surface current monitoring
SAR ATI
SAR Doppler
Internal Waves
Inertial current
Submeso scale
Ekman/ Stokes
Scat
Mesoscale
Tidal current
Rossby waves
Seasonal cycle
El Nino
Spatial resolution
1km
10km
30km
100km
1000km
1 season
10days
3days
daily
3 hourly
Temporal resolution

Main message …

- Today ideal instrument … (wide-swath, high-resolution, topography, roughness, Doppler, emissivity, reflectance, …) = the combined use of observations, including in situ measurements
- Very (too) large number of spatio-temporal scales under local and non-local interactions
- Improved technologies (instruments, resolution, computer capabilities, storage, dissemination) all contribute to improved combined analysis
- Theoretical frameworks and numerical simulations can be used to assess the causes and contexts of the different observations (including sensor physics, observability conditions and instrument capabilities), to refine dynamical/statistical gap filling methods
- New challenges, new altimeter instruments (SARAL, Sentinel-3, SWOT, …, CubeSat opportunities) and combined roughness contrasts as local quantitative proxies to trace strong surface gradient areas

Et encore ... Towards an observation-driven framework

- Thematically-driven Mining applications shall rapidly emerge to avoid the data deluge, and to emphasize the synergy between observations (in situ and satellite), numerical simulations and theoretical developments
- 'collaborative' efforts to promote future developments to avoid (limit) computation burden and/or (redundant) archive volume growth.
- Data on an EO-'cloud' and software utilities/applications more efficiently developed to search, process, visualize, analyze the data in a common approach.
- Usual discussions – the need for standard data formats, metadata conventions, open access etc.

Data Ecosystem

In situ

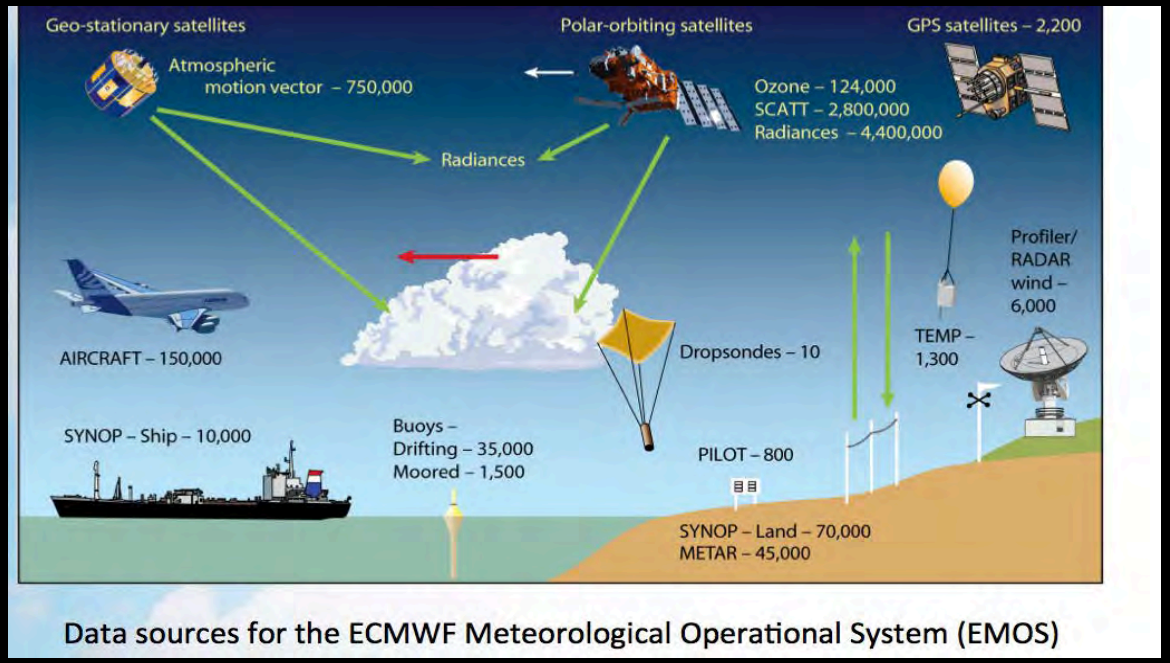

Data sources for the ECMWF Meteorological Operational System (EMOS)

In vivo

Données sociétales et économiques

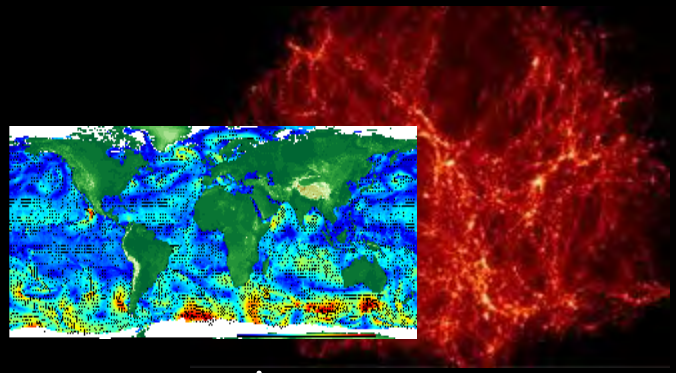

In silico

Interdisciplinary crossings

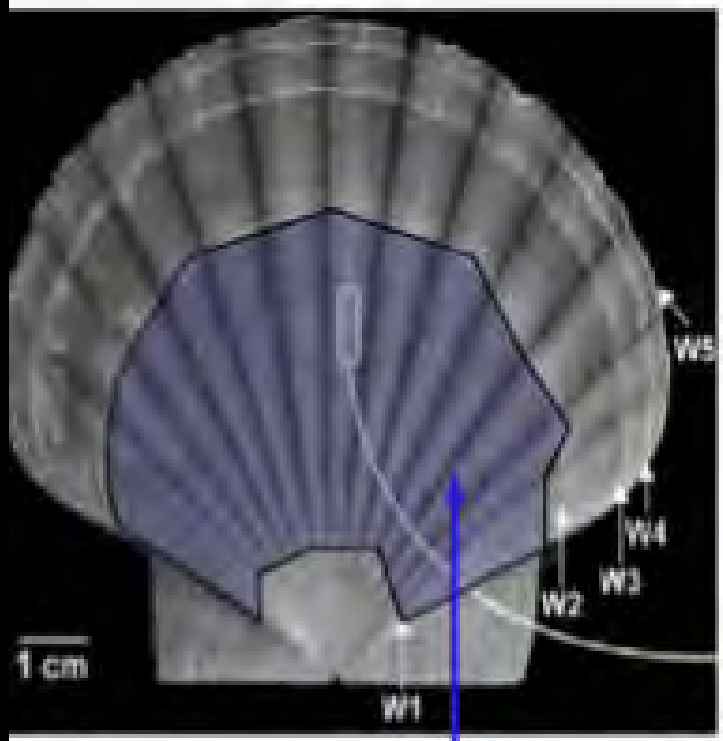

class 1

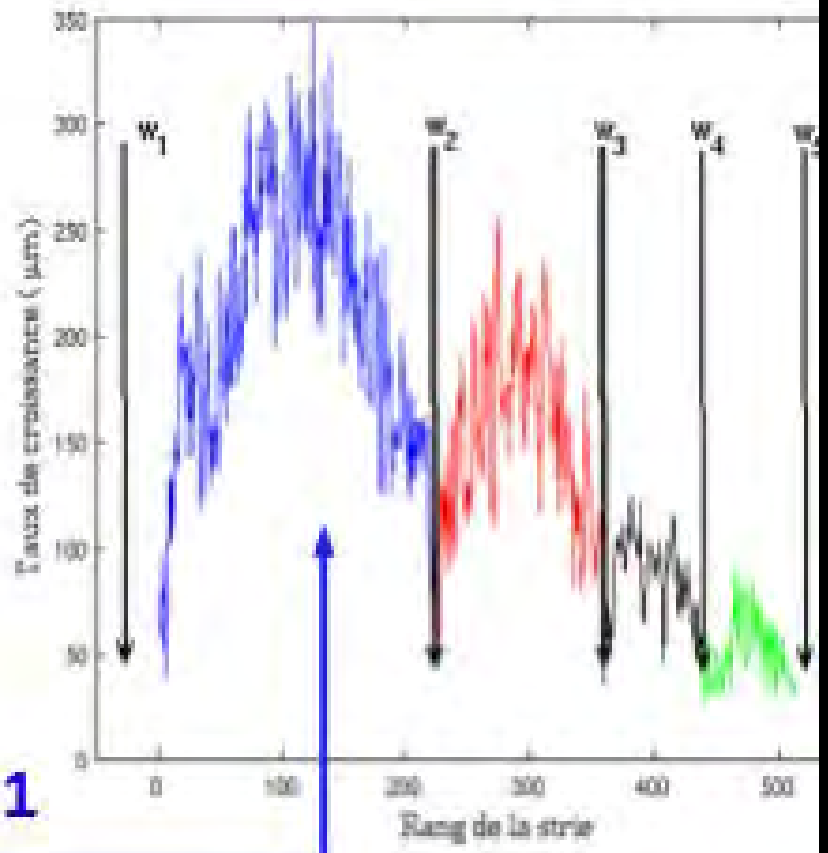

Biogeochemical campaigns

ARTICLE

doi:10.1038/nature11229

Deep carbon export from a Southern Ocean iron-fertilized diatom bloom

Victor Smetacek[1,2]*, Christine Klaas[1]*, Volker H. Strass[1], Philipp Assmy[1,3], Marina Montresor[4], Boris Cisewski, Adrian Webb[8], Francesco d'Ovidio[9], Jesús M. Arrieta[10,11], Ulrich Bathmann[1,12], Richard Bellerby[13,14], Gry Peter Croot[16,17], Santiago Gonzalez[10], Joachim Henjes[1,18], Gerhard J. Herndl[10,19], Linn J. Hoffmann[16], Harry J

→biogeochemical campaigns increasingly require the identification of transport and mixing structures

→ The precision of the biogeochemical budgets directly depends on the precision of altimery

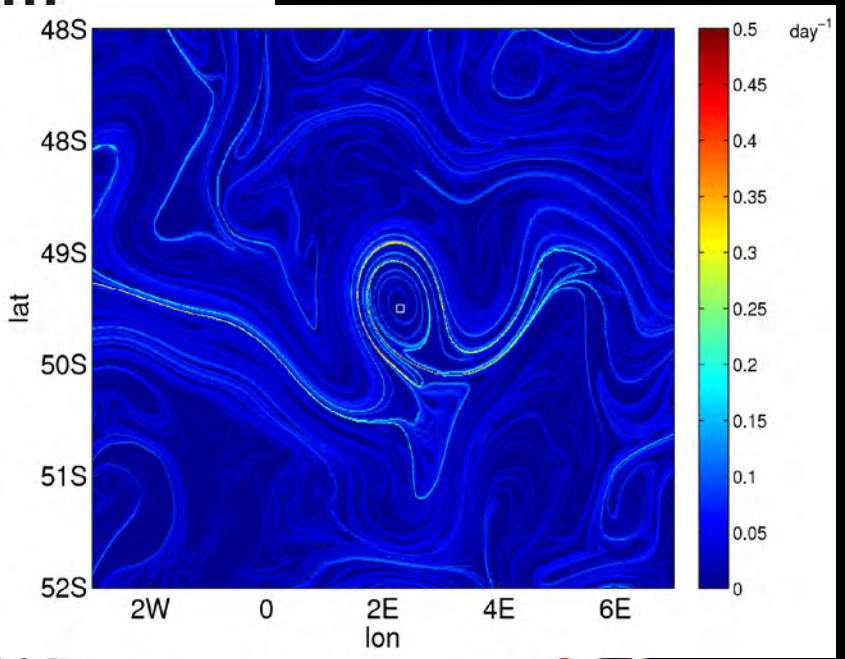

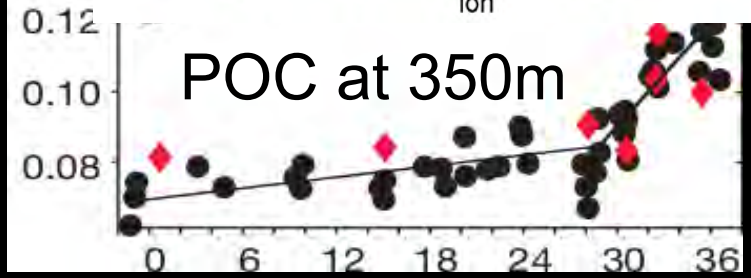

Altimetry for ecology 2: the invisible landscape

LETTER

doi:10.1038/nature10082

Tracking apex marine predator movements in a dynamic ocean

B. A. Block[1], I. D. Jonsen[2], S. J. Jorgensen[1], A. J. Winship[2], S. A. Shaffer[3], S. J. Bograd[4], E. L. Hazen[4], D. G. Foley[4], G. A. Breed[2,5], A.-L. Harrison[5], J. E. Ganong[1], A. Swithenbank[1], M. Castleton[1], H. Dewar[6], B. R. Mate[7], G. L. Shillinger[1], K. M. Schaefer[8], S. R. Benson[9], M. J. Weise[5], R. W. Henry[5] & D. P. Costa[5]

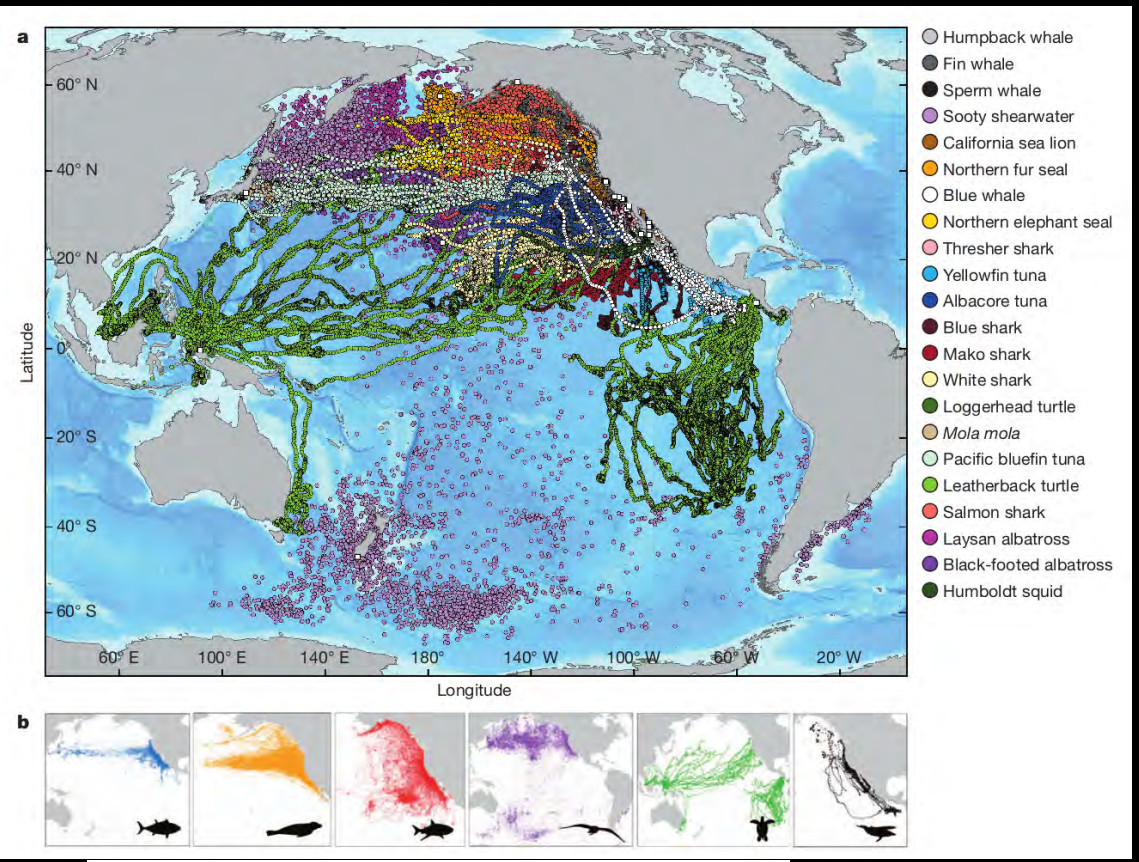

NATURE | VOL 475 | 7 JULY 2011

In their displacements, top predators encounter environmental heterogeneity at multiple scales.

Until now, observations where sparse, and matched large-scale current information was enough

The blended satellite products allow to estimate the impact of surface currents on the biogeochemical transport, on the dispersion of pollutants and oil spills

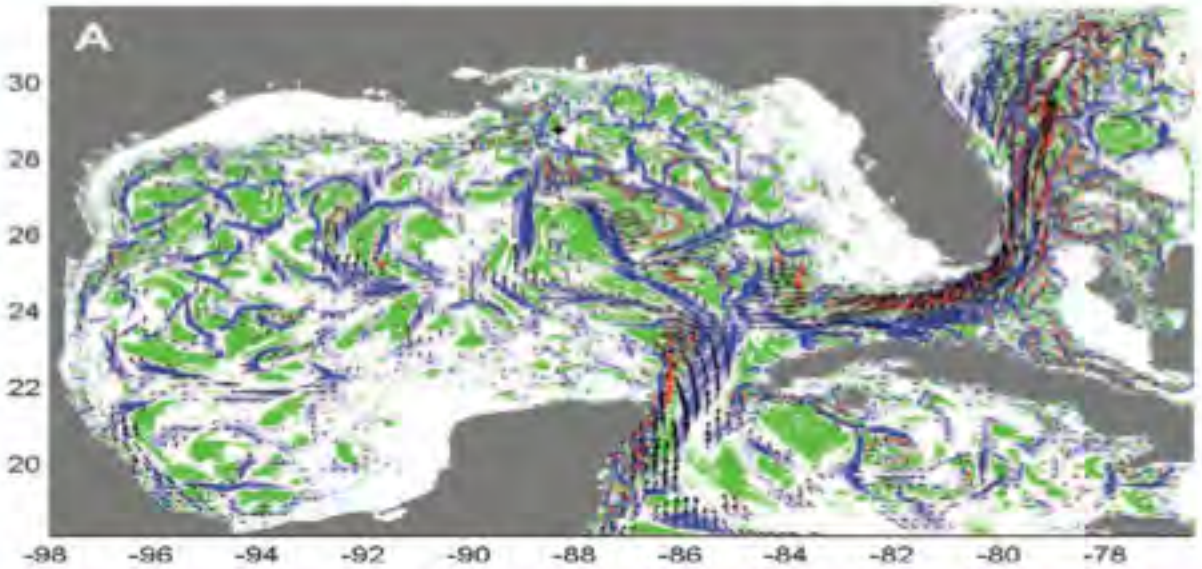

Forecast of oil spill dispersion in the Gulf of Mexico on 25 june 2010: red and blue show regions of strong oil dispersion within 3 days. This diagnosis, based on altimetric data, compared well with what was observed (Mezic et al, Science, 2010).

However these satellite datasets (altimetric and microwave data) cannot capture ocean dynamics at scales smaller than 100 km because of the resolution (or/and noise level).

Extracting new knowledge

Analysis of altimeter wave forms :
ERS 1 & 2, Envisat, Jason 1 & 2, Cryosat, AltiKa (12 TB)

Disposing of a sandbox with permanent access to all data and processing power greatly ease bridging the gap between initial idea and full demonstration / long term assessment

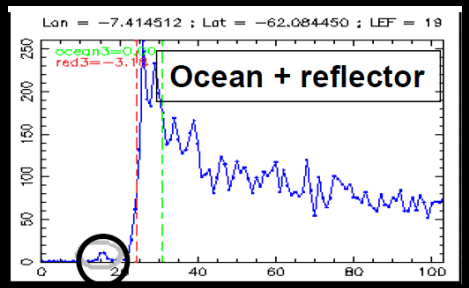

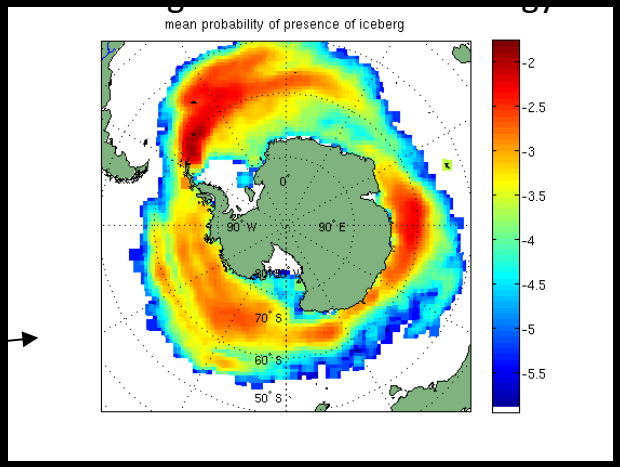

Ship detection

Lake ice thickness

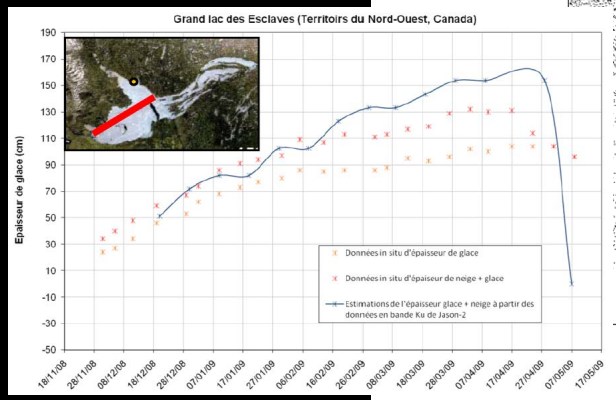

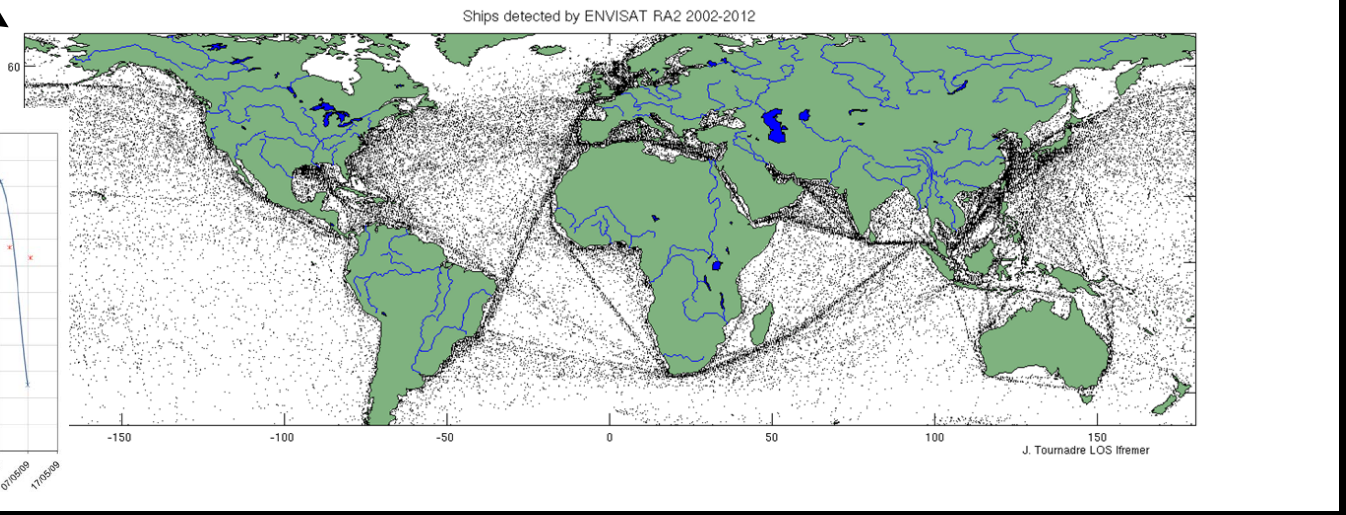

Big questions....

Are storms more numerous and intensifying with climate

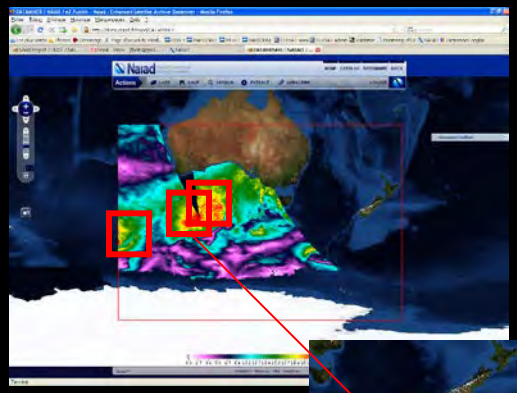

Scatterometer and SAR (20 years)

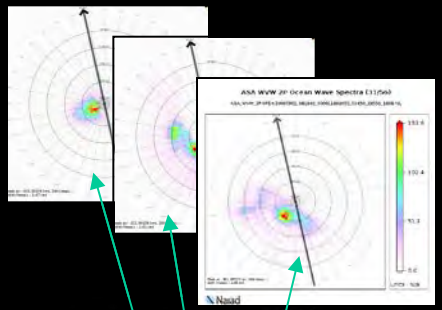

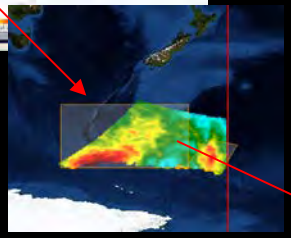

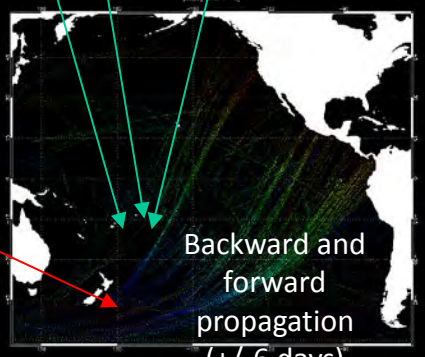

Backward and forward propagation (+/-6 days)

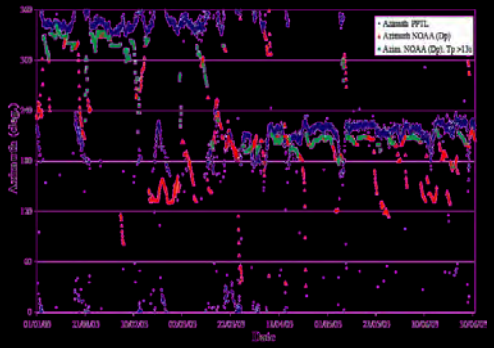

Seismic noise (50 years)

Buoys (30 years)

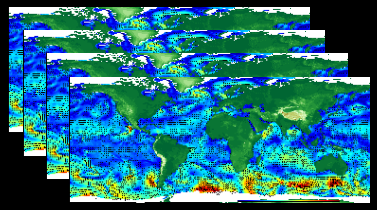

Weather model (25 years)

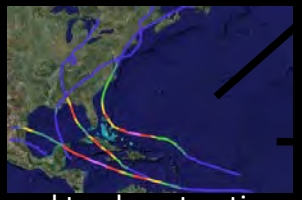

Feature and tracks extraction

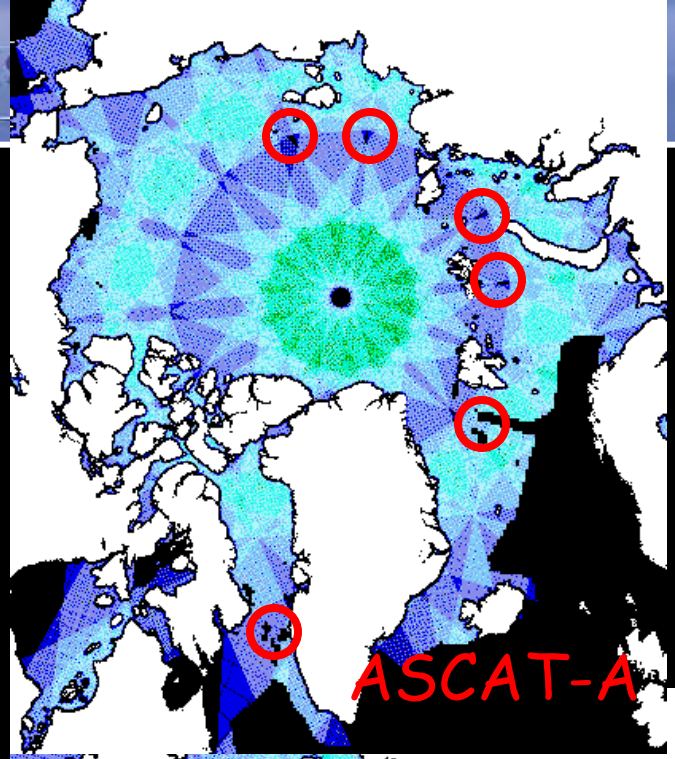

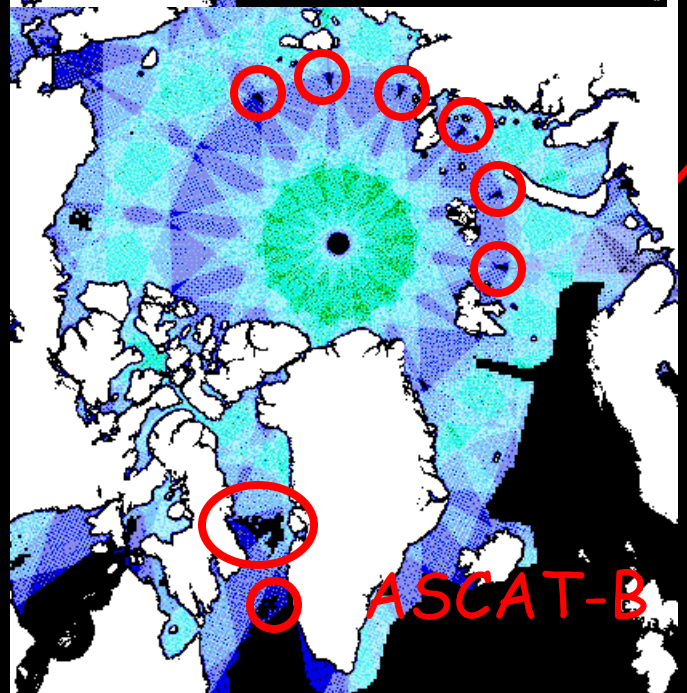

ASC

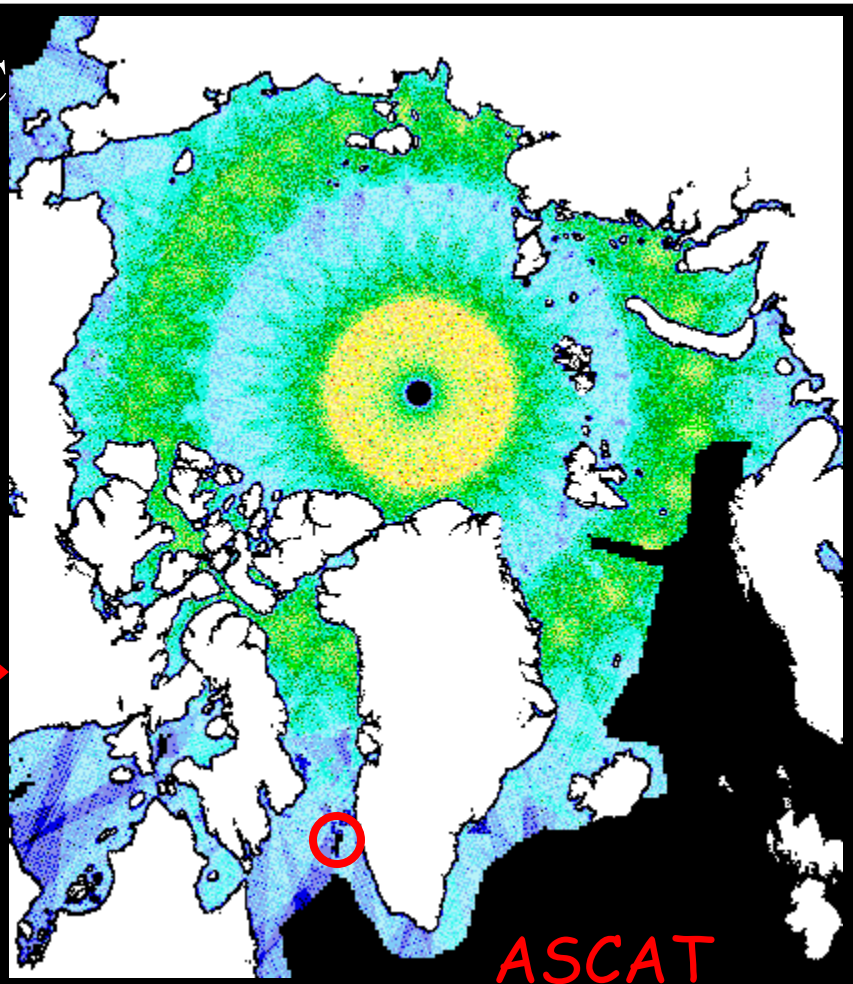

Backscatter data

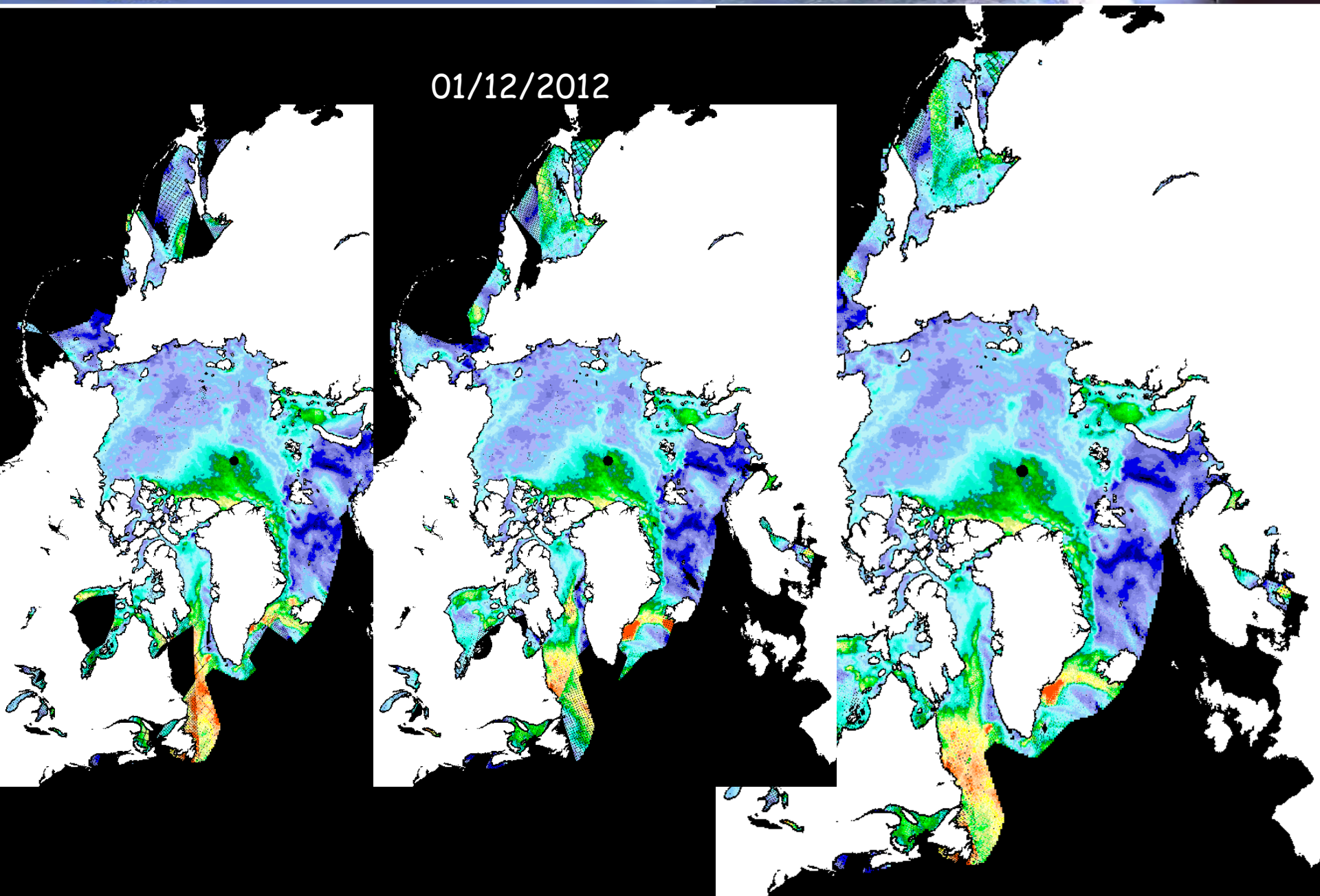

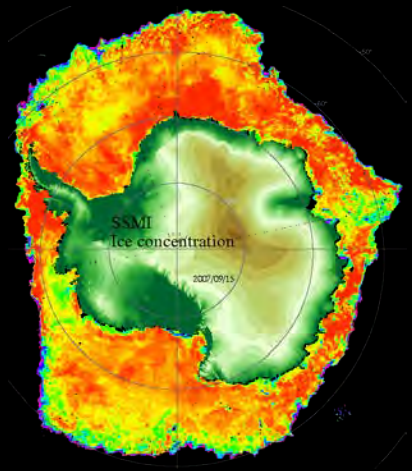
SSMI
Ice concentration
2007/09/15

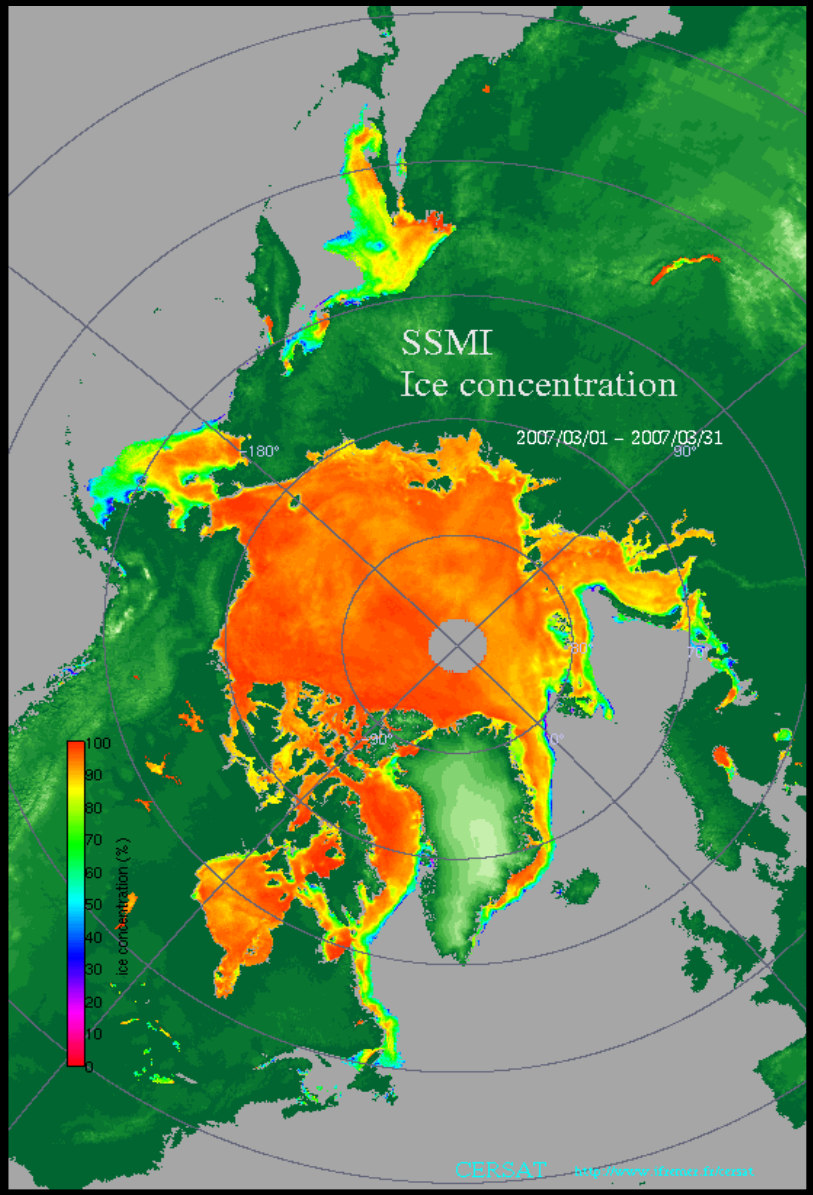
SSMI
Ice concentration
2007/03/01 – 2007/03/31
180°
90°
100
90
80
70
60
50
40
30
20
10
0
Ice concentration (%)
CERSAT

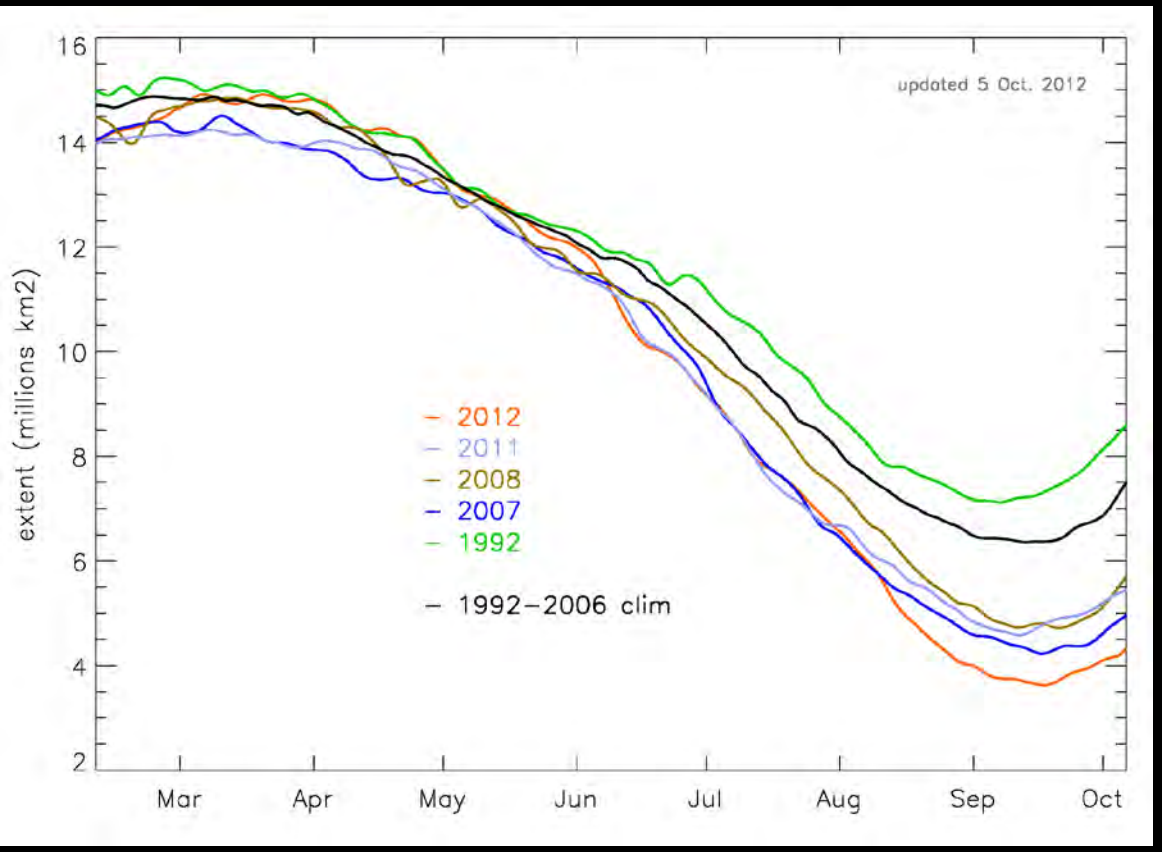
updated 5 Oct. 2012
extent (millions km2)
16
14
12
10
8
6
4
2
Mar
Apr
May
Jun
Jul
Aug
Sep
Oct
2012
2011
2008
2007
1992
1992–2006 clim


1992–2006 clim
2007
2012
Russia
Greenland
Canada

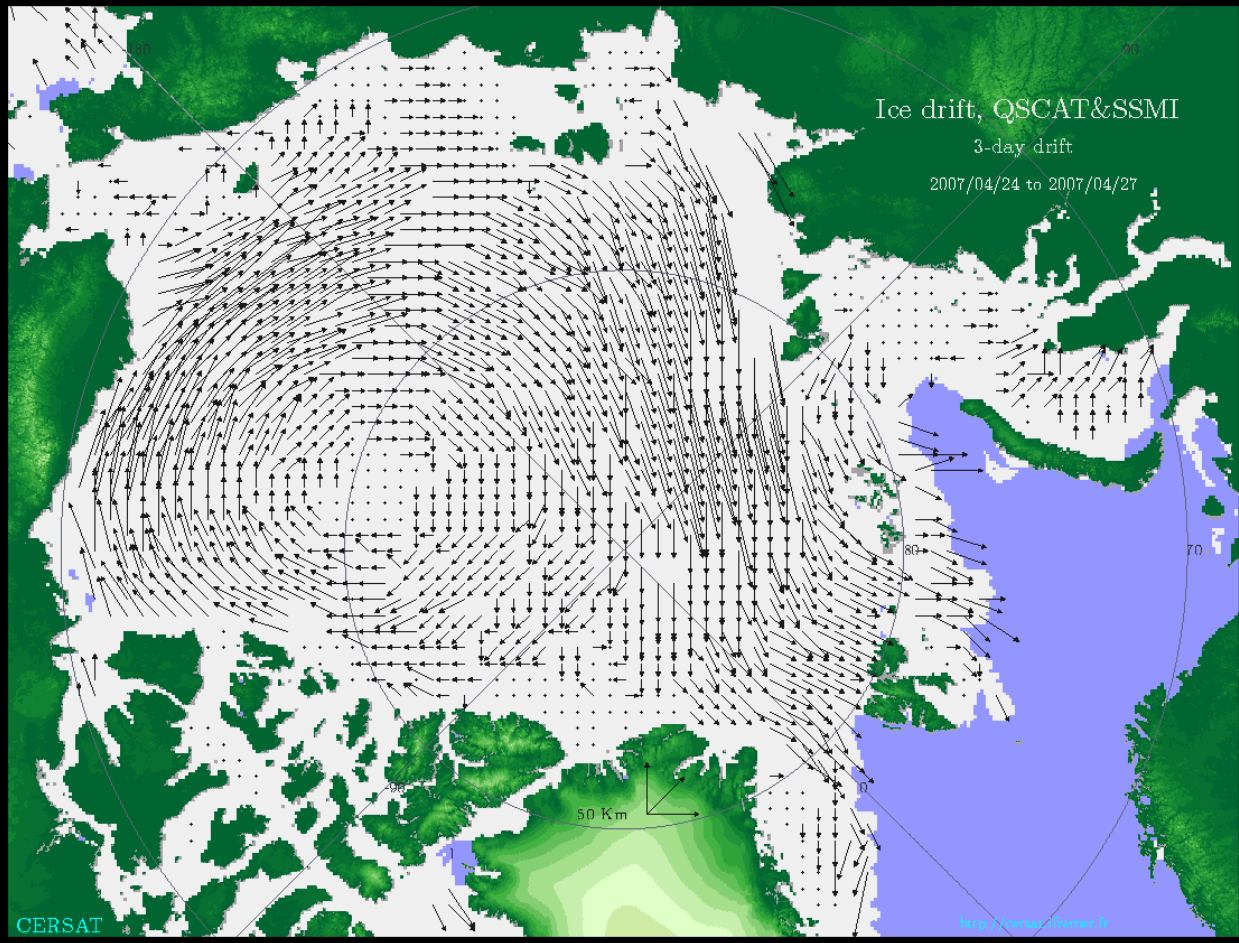
Ice drift, QSCAT&SSMI
3-day drift
2007/04/24 to 2007/04/27
50 Km
CERSAT

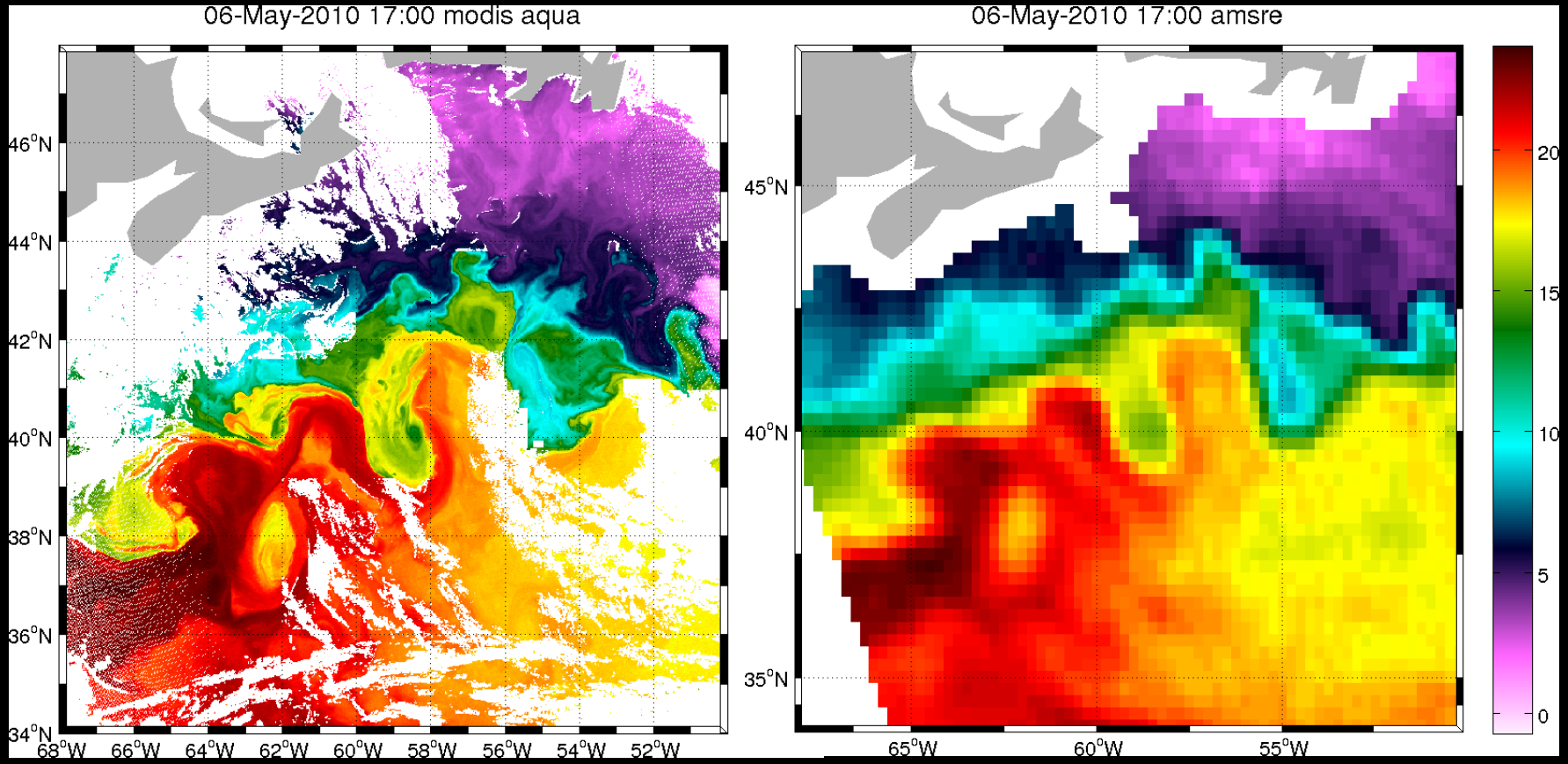
06-May-2010 17:00 modis aqua
06-May-2010 17:00 amsre
46°N
44°N
42°N
40°N
38°N
36°N
34°N
68°W
66°W
64°W
62°W
60°W
58°W
56°W
54°W
52°W
45°N
40°N
35°N
65°W
60°W
55°W
20
15
10
5
0

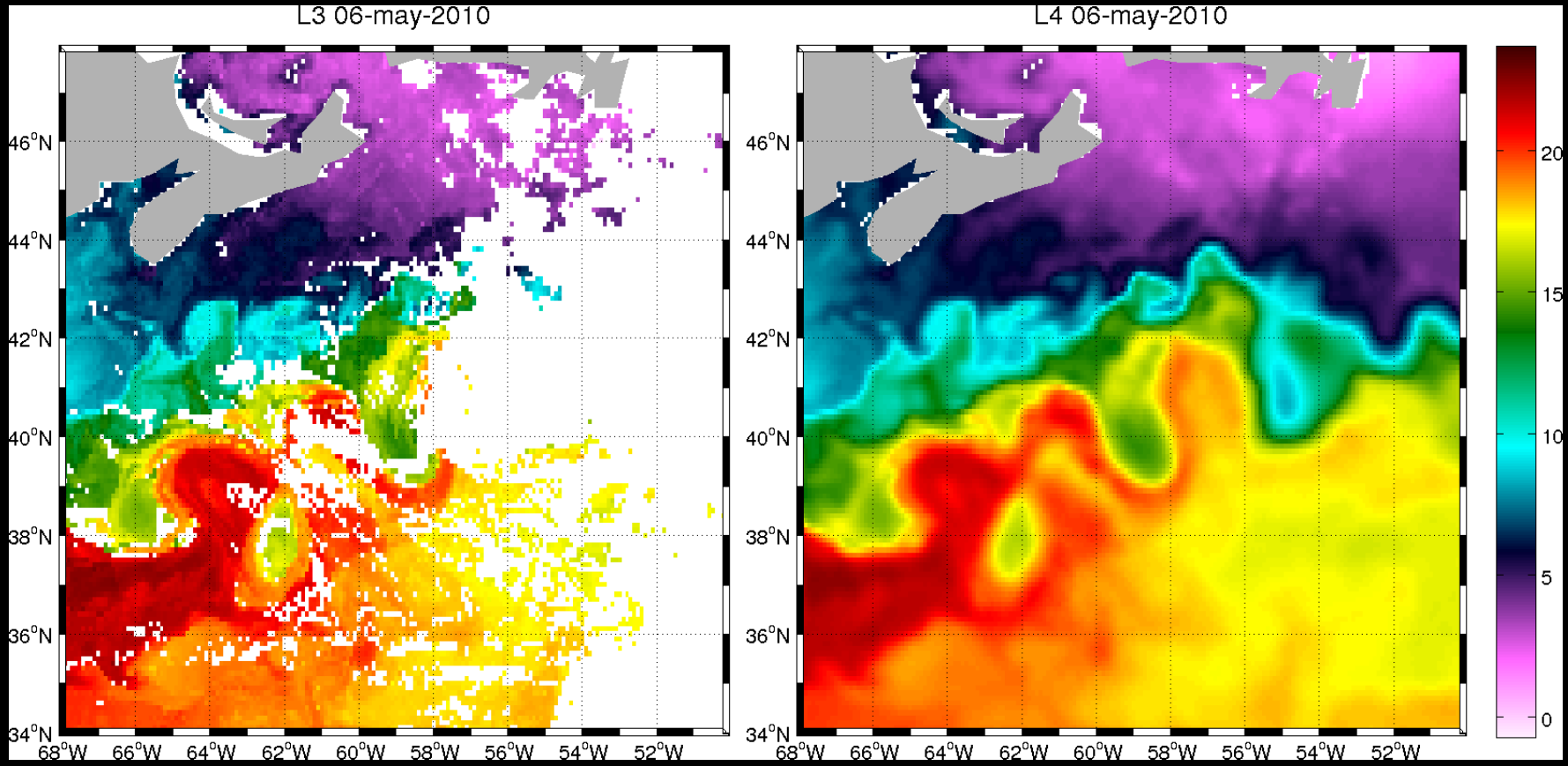
L3 06-may-2010
L4 06-may-2010
46°N
44°N
42°N
40°N
38°N
36°N
34°N
68°W
66°W
64°W
62°W
60°W
58°W
56°W
54°W
52°W
20
15
10
5
0

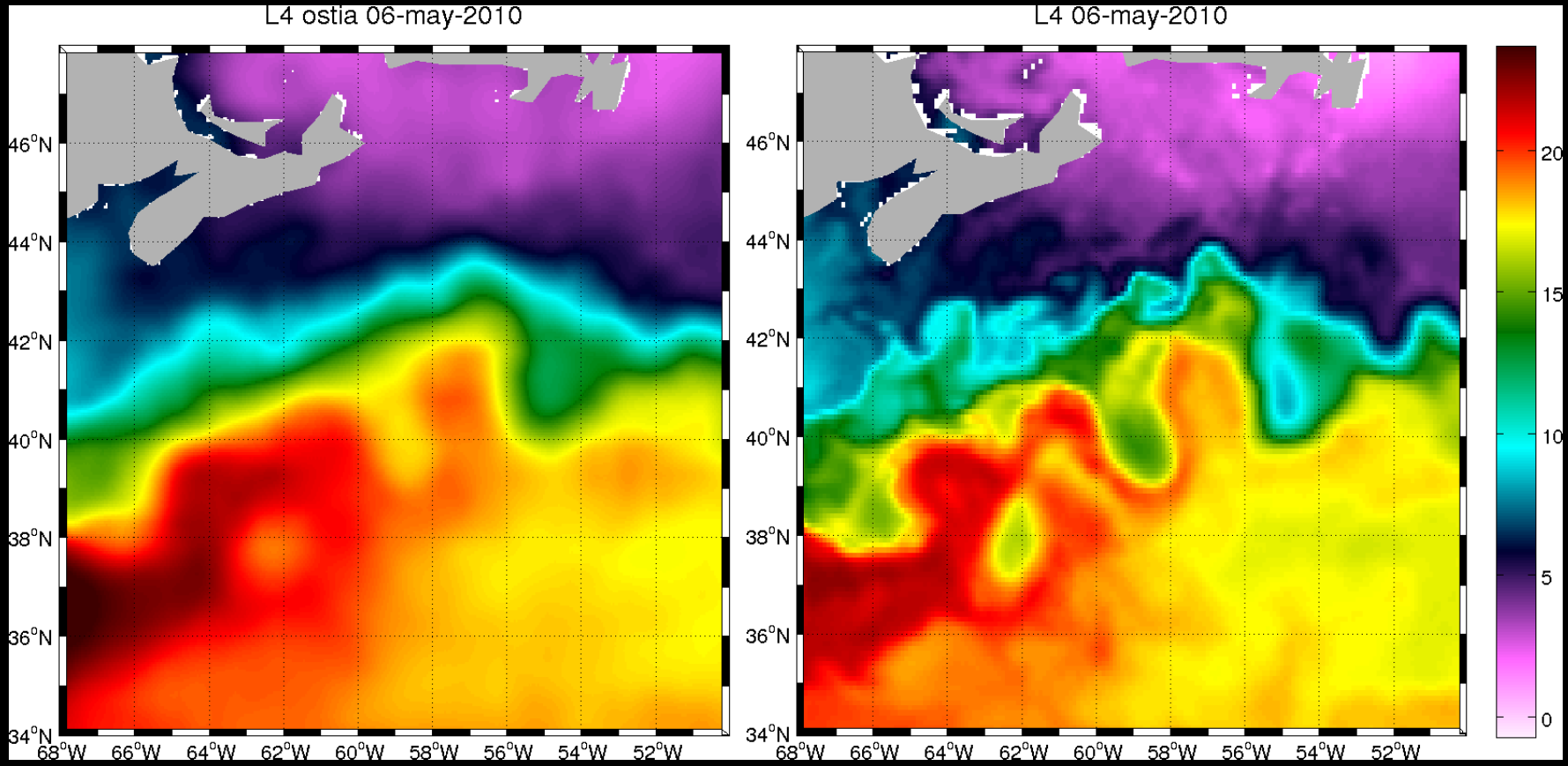
L4 ostia 06-may-2010
L4 06-may-2010
46°N
44°N
42°N
40°N
38°N
36°N
34°N
68°W
66°W
64°W
62°W
60°W
58°W
56°W
54°W
52°W
20
15
10
5
0

Global SST

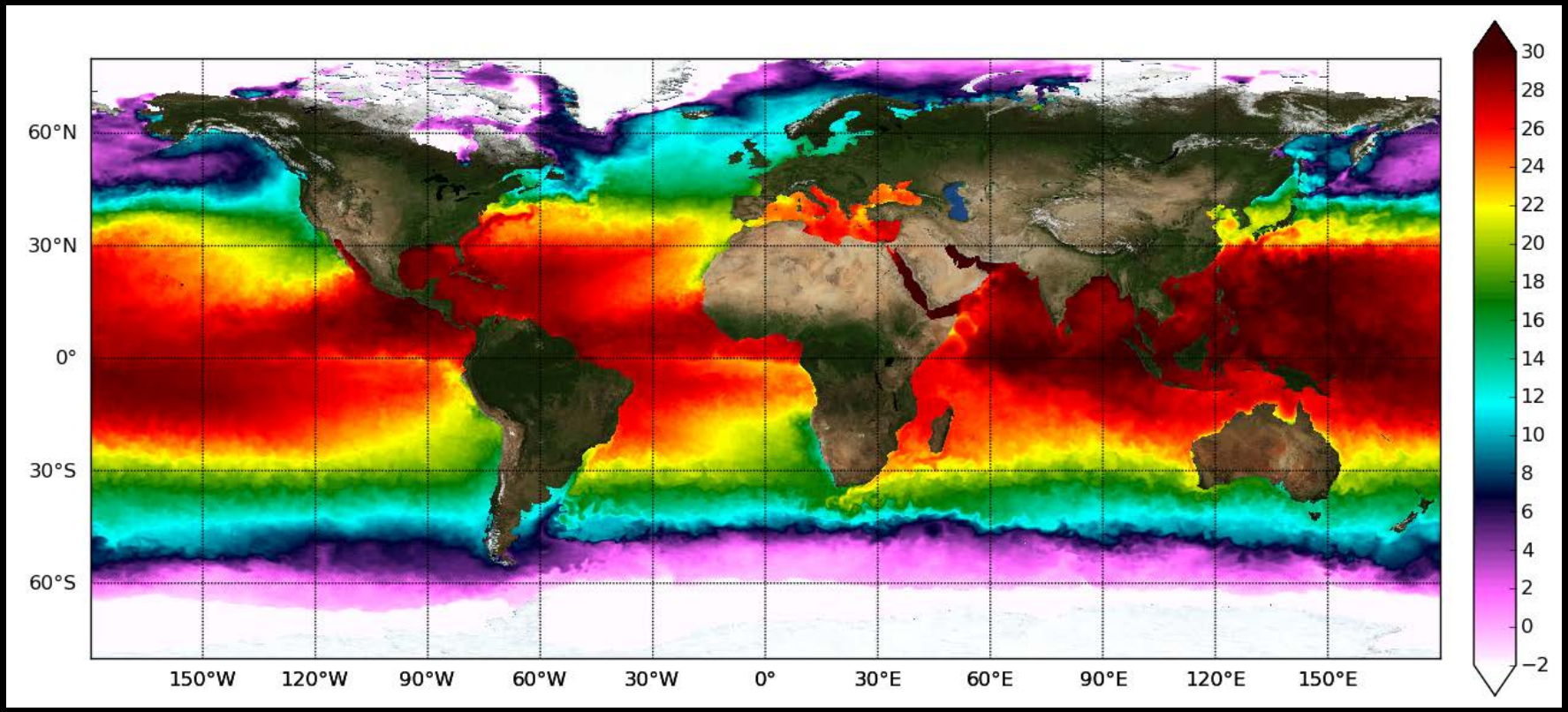

Global reanalysis 2006-present
at 10 km resolution

Lagrangian Diagnostics

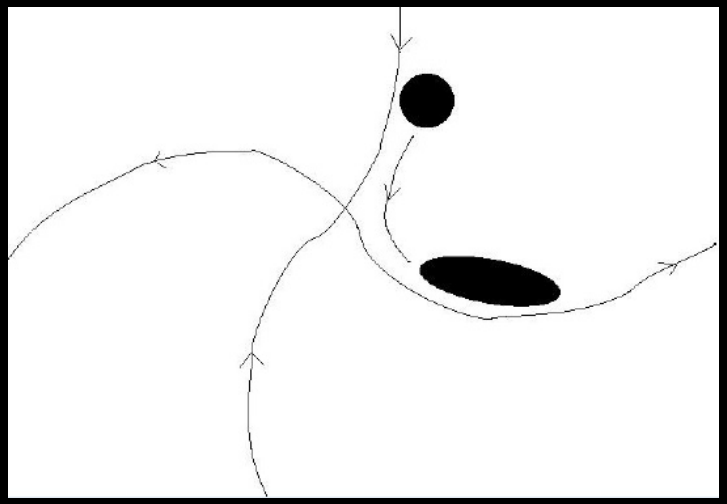

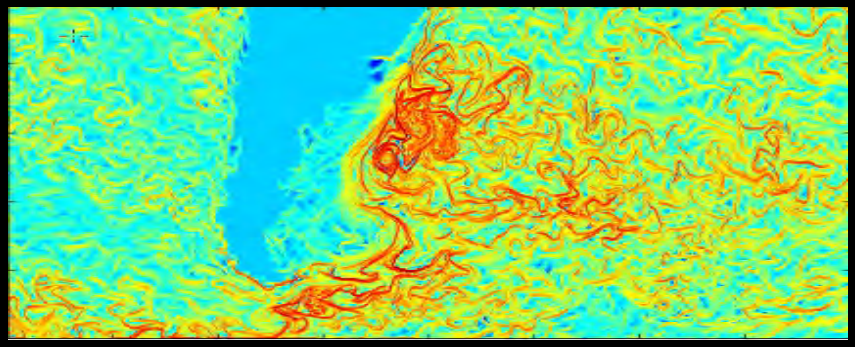

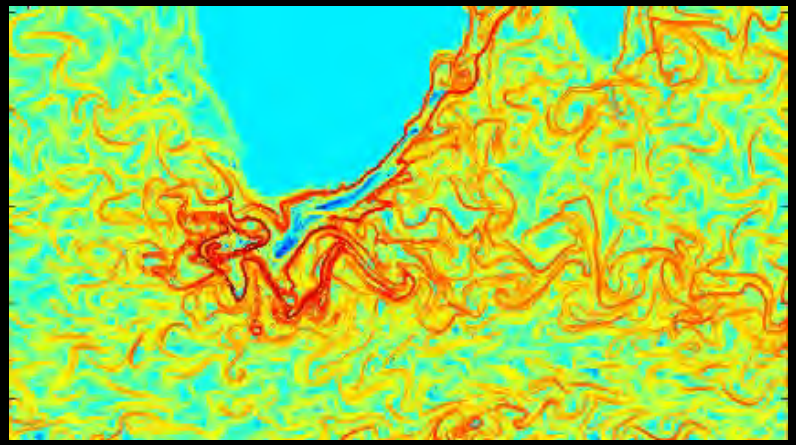

Lyapunov exponents from particle backtracking using medium resolution velocity fields (e.g., D'Ovidio et al., 2008)

Small scales / mesoscale

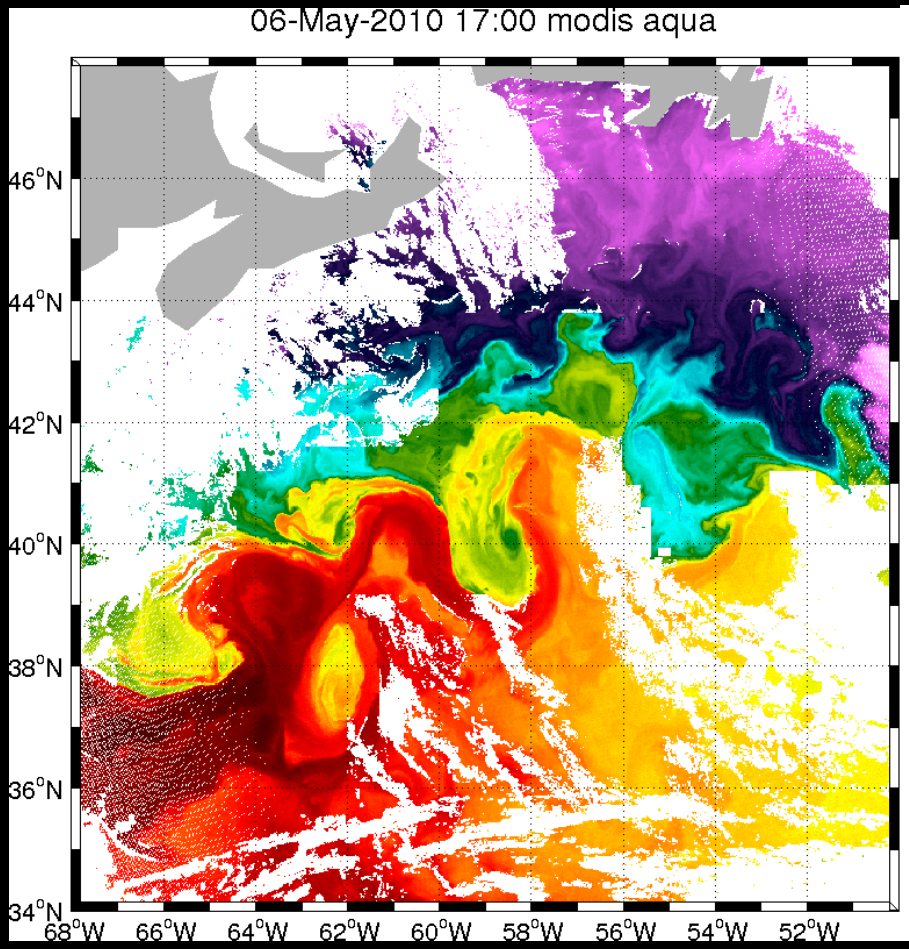

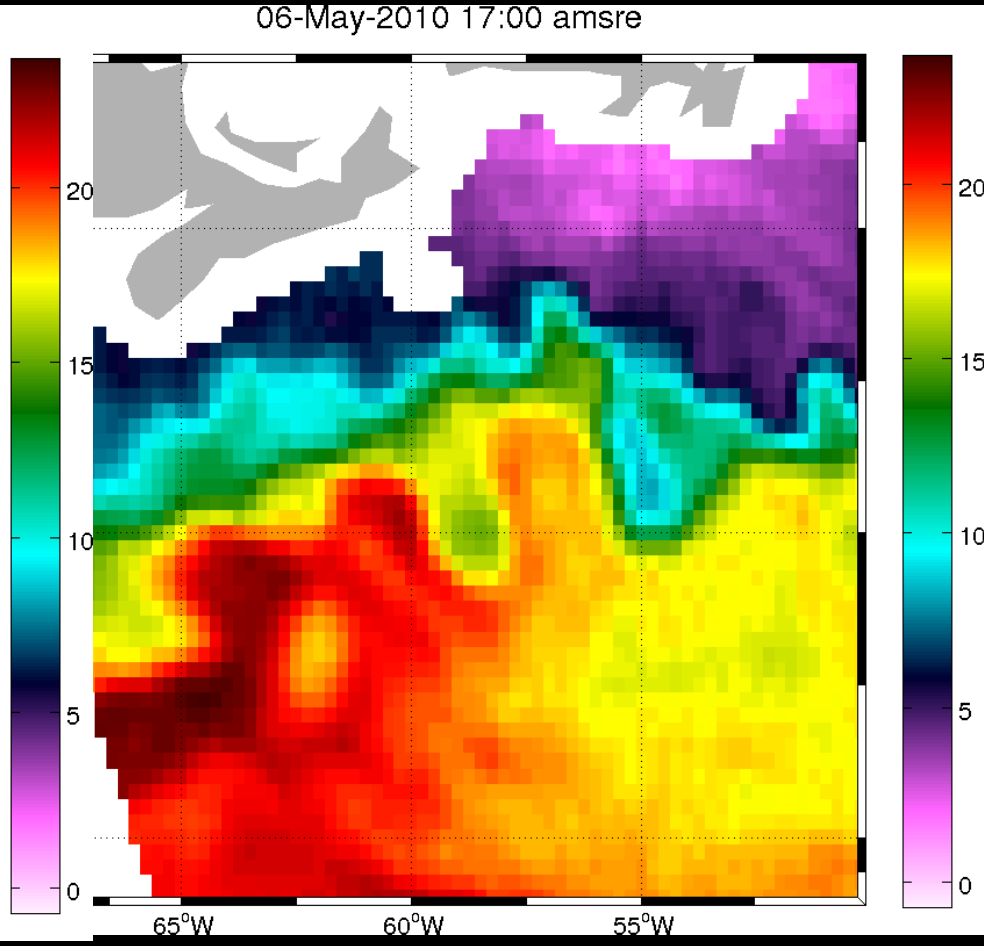

Small scales / mesoscale

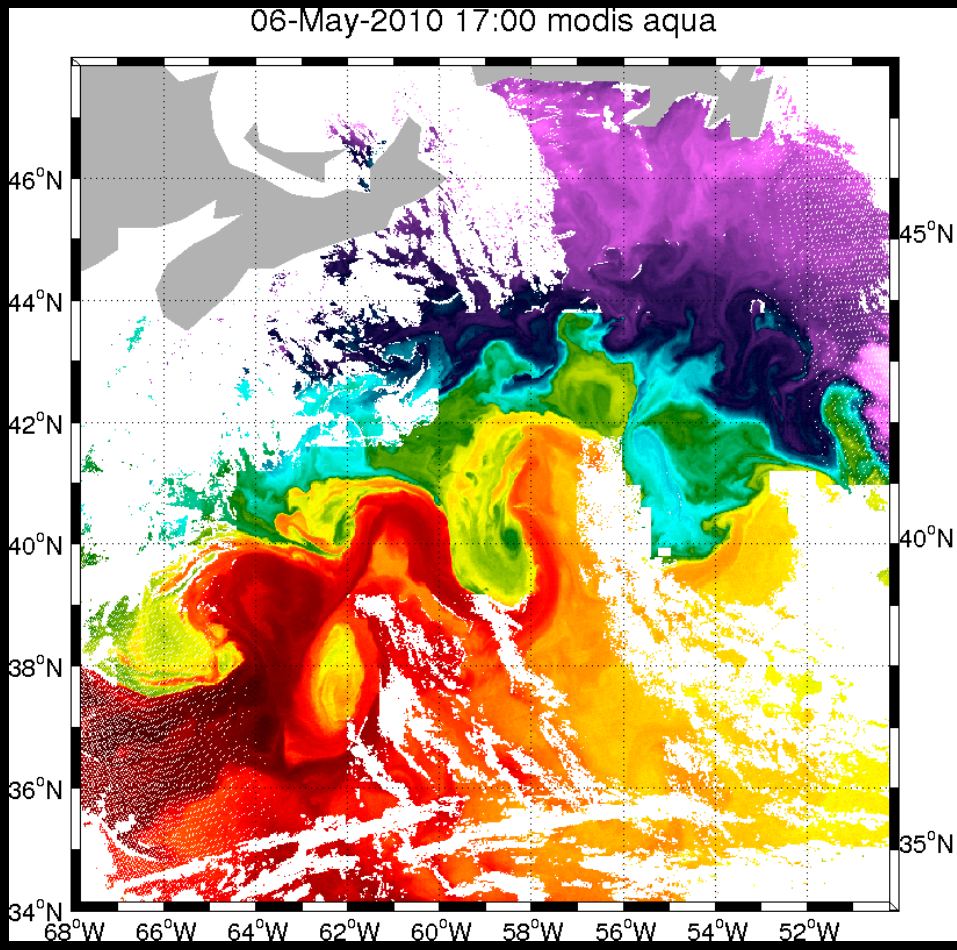

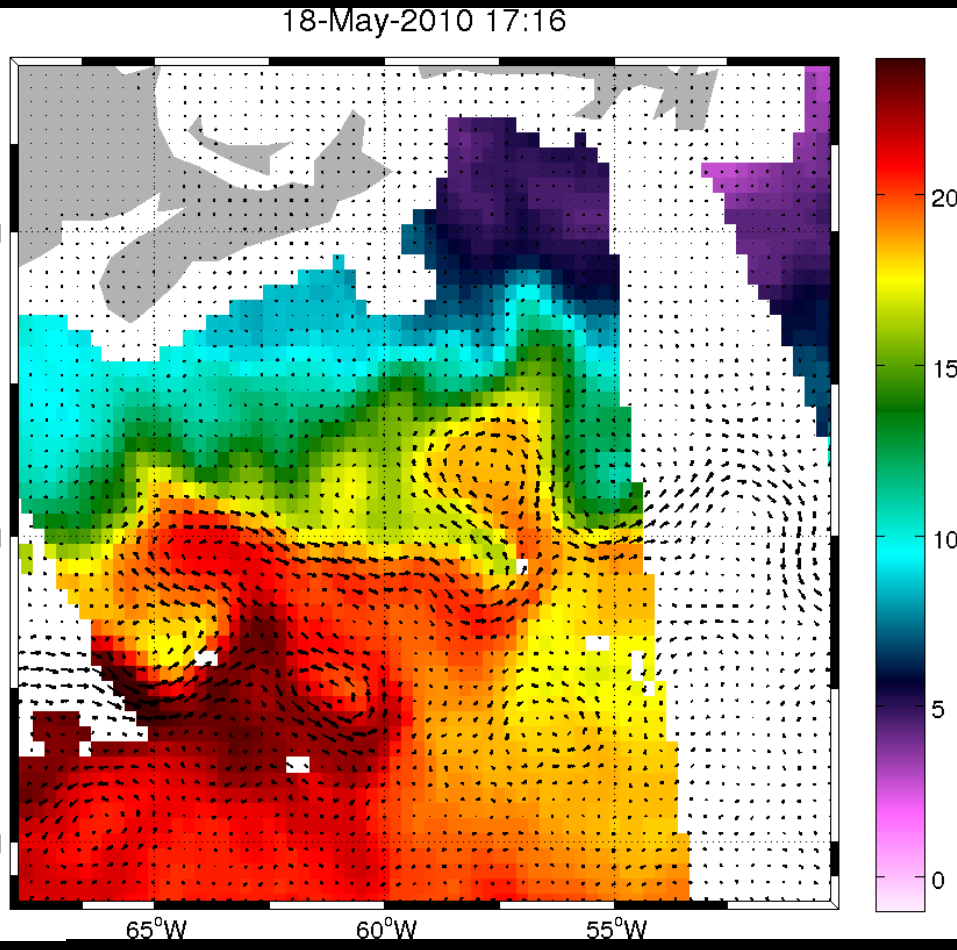

Small scales / mesoscale

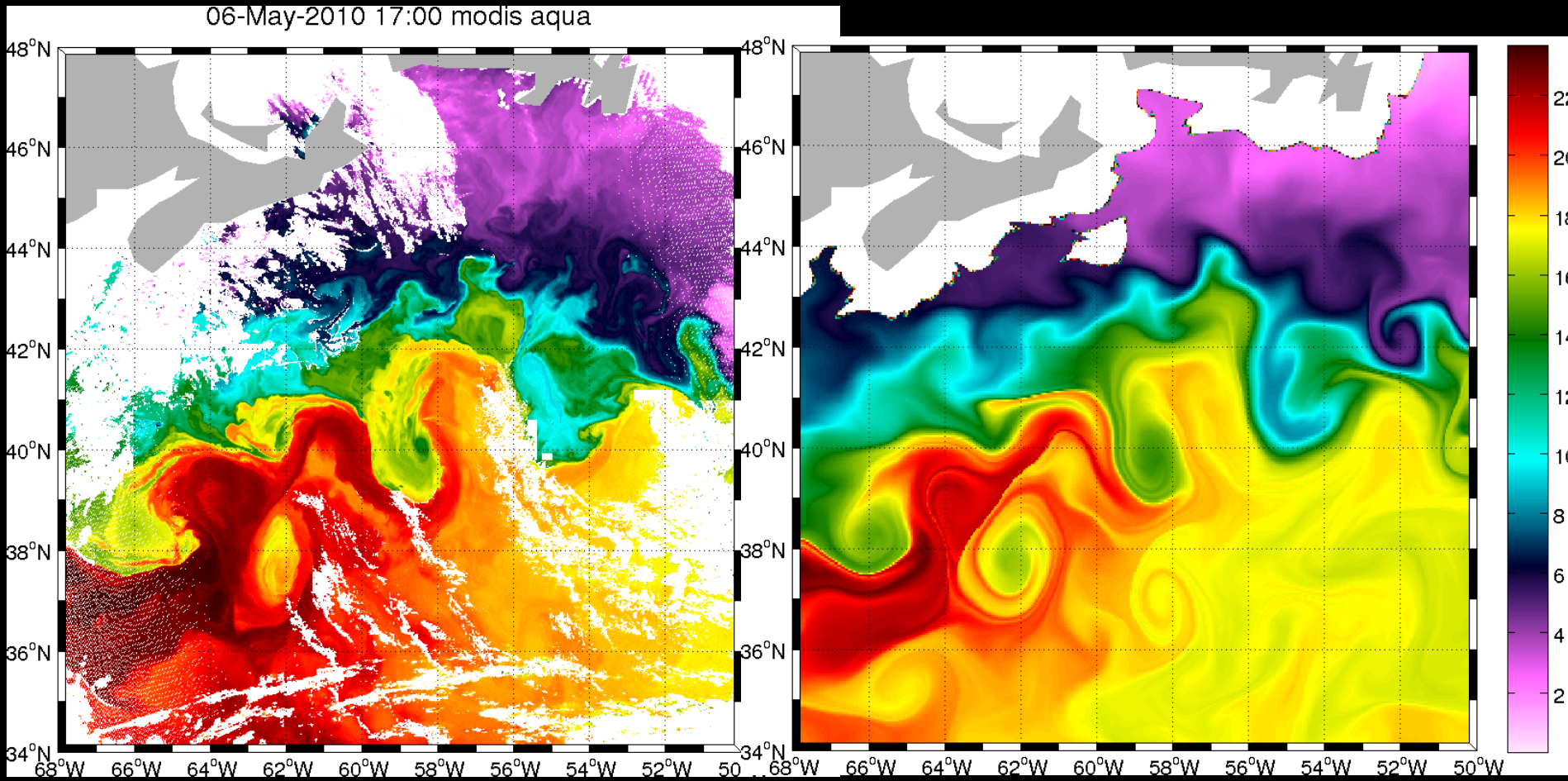

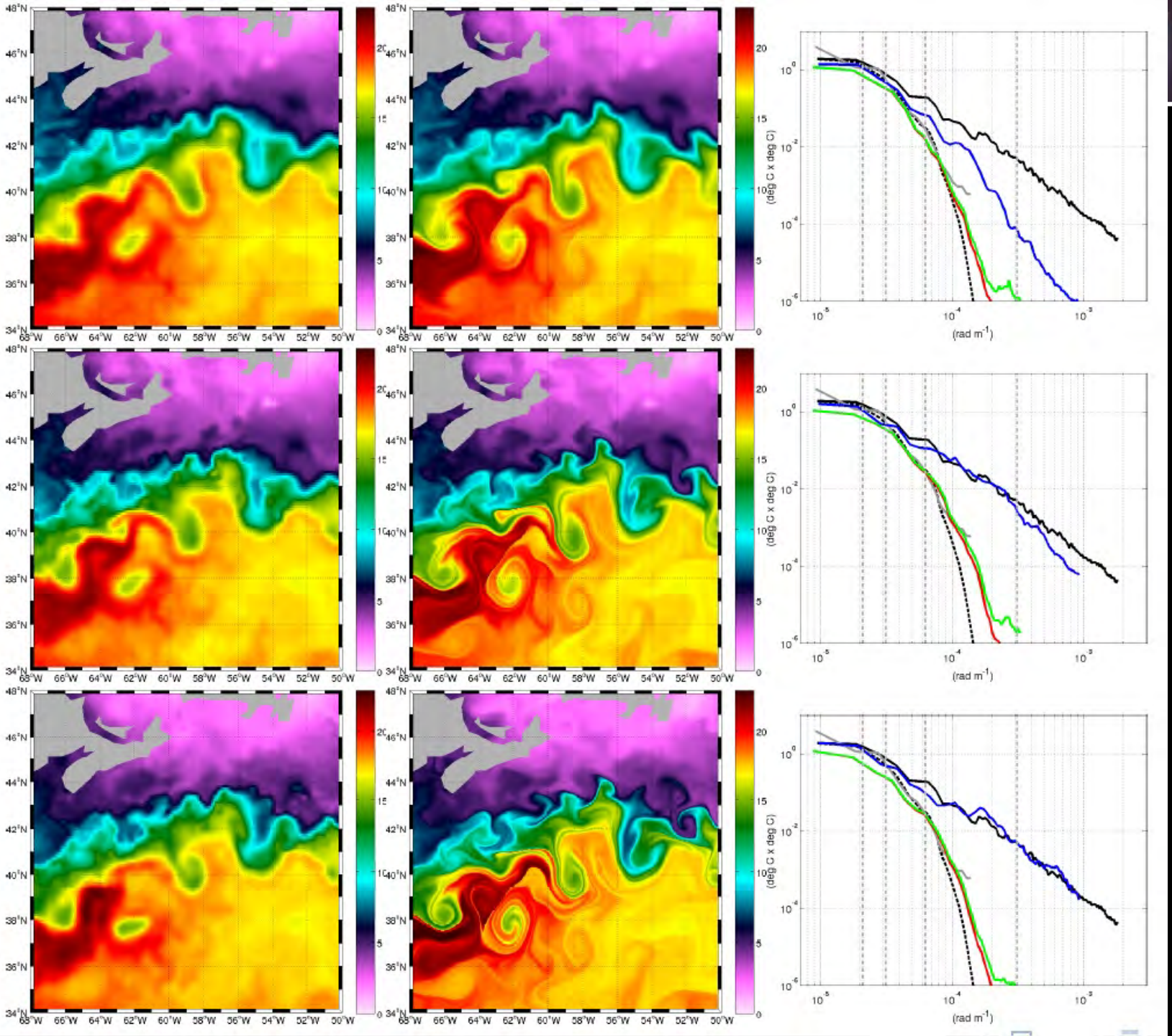
48°N
46°N
44°N
42°N
40°N
38°N
36°N
34°N
68°W
66°W
64°W
62°W
60°W
58°W
56°W
54°W
52°W
50°W
20
15
10
5
0
(deg C x deg C)
(rad m-1)

Sea Surface Salinity from Space

Ionosphere

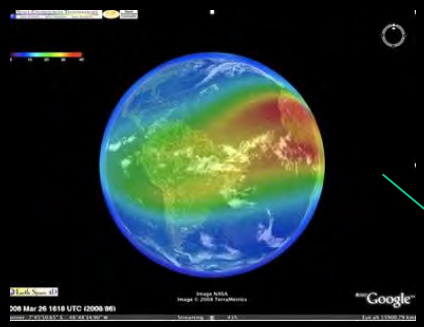

SMOS

Galactic Brigthness

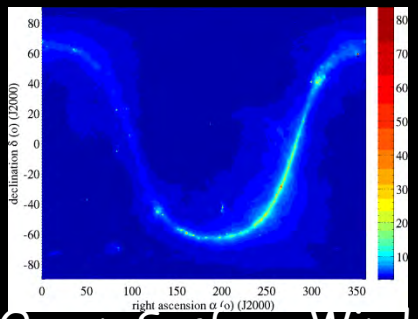

Electromagnetic Models

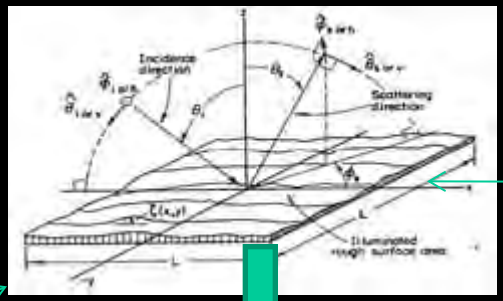

Ocean Surface Winds

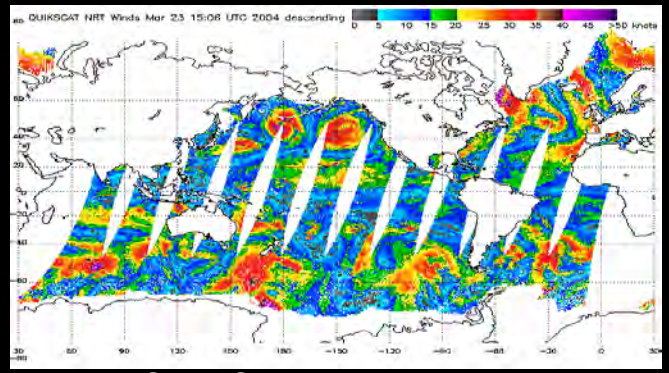

Sea Surface Temperature

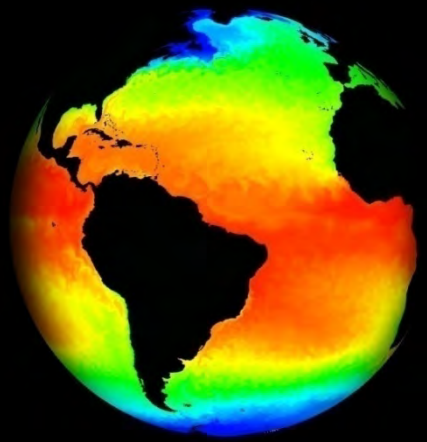

Sea State

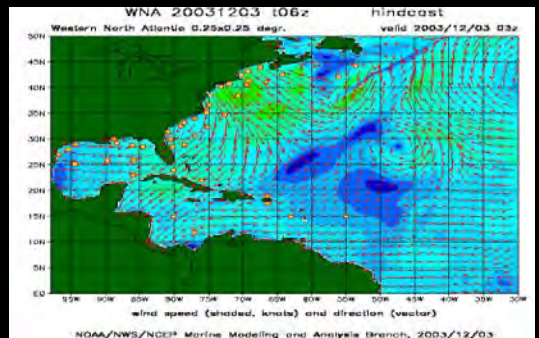

Sea Surface Salinity

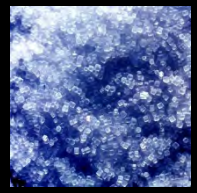

SSS Monthly Composite Jan 2010-0.5°x0.5°

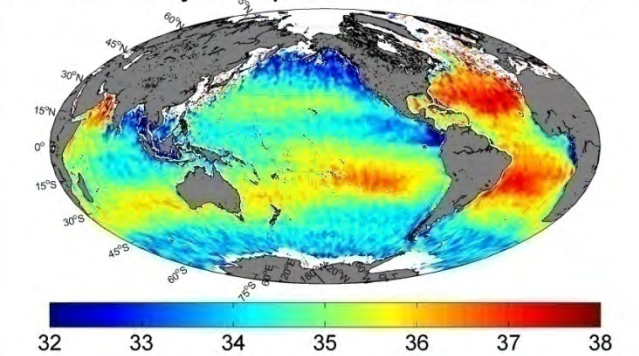

SSS Monthly Composite Feb 2010-0.5°x0.5°

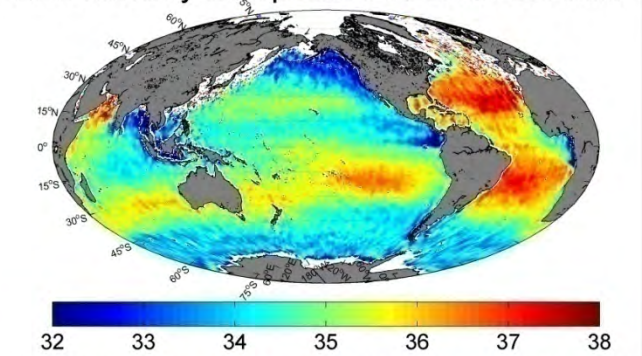

SSS Monthly Composite Mar 2010-0.5°x0.5°

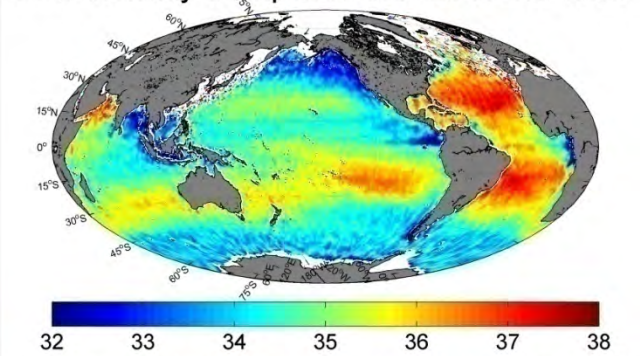

SSS Monthly Composite Apr 2010-0.5°x0.5°

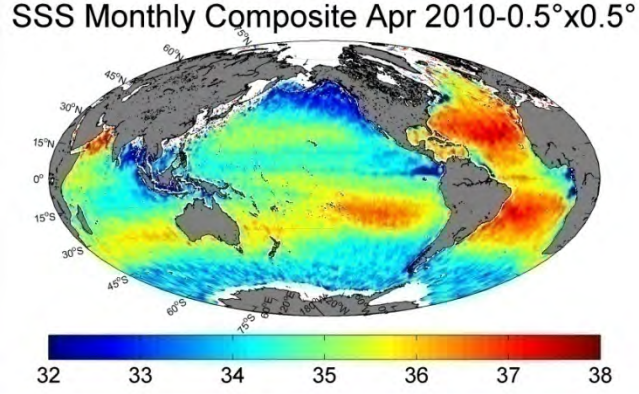

SSS Monthly Composite May 2010-0.5°x0.5°

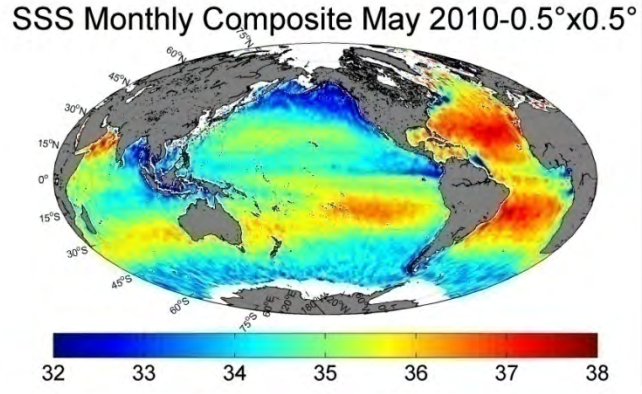

SSS Monthly Composite Jun 2010-0.5°x0.5°

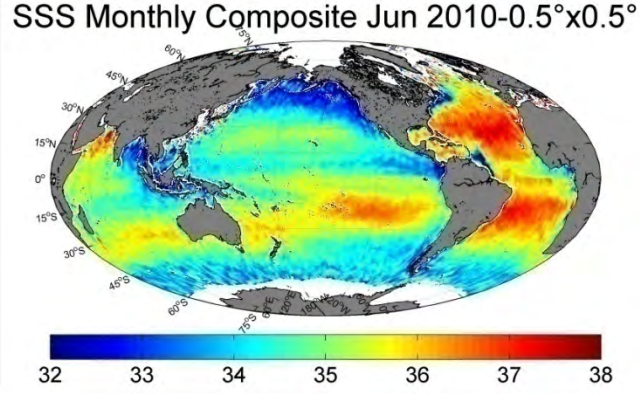

SSS Monthly Composite Jul 2010-0.5°x0.5°

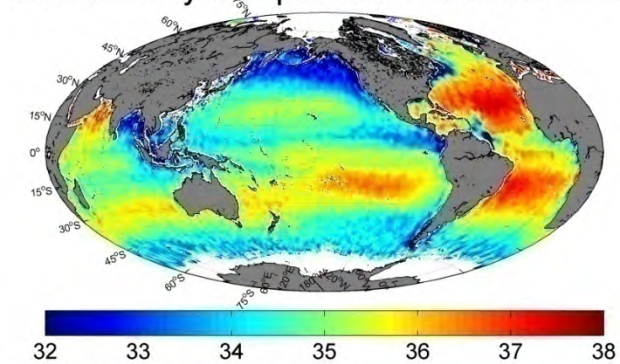

SSS Monthly Composite Aug 2010-0.5°x0.5°

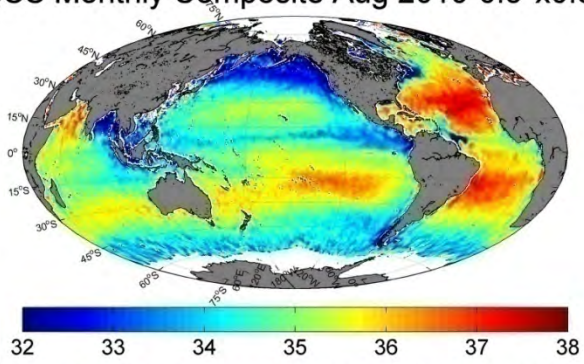

SSS Monthly Composite Sep 2010-0.5°x0.5°

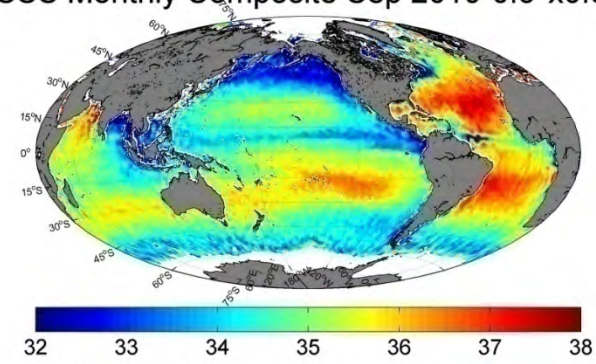

SSS Monthly Composite Oct 2010-0.5°x0.5°

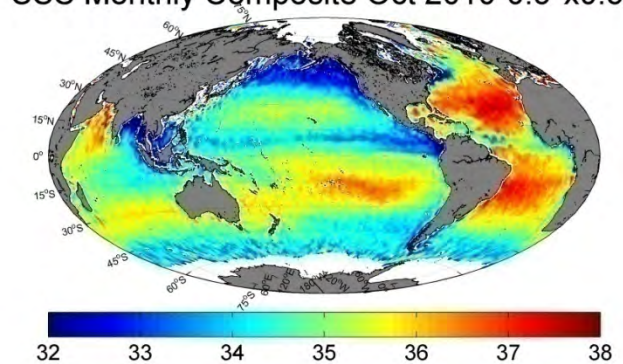

SSS Monthly Composite Nov 2010-0.5°x0.5°

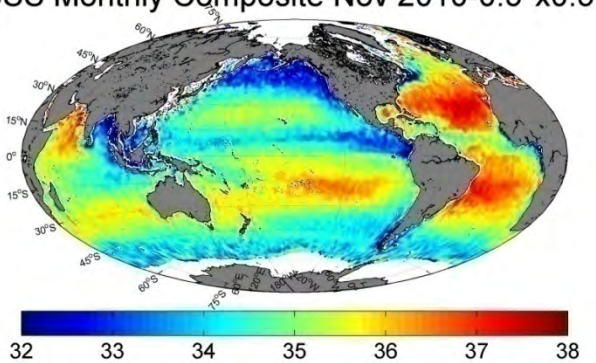

SSS Monthly Composite Dec 2010-0.5°x0.5°

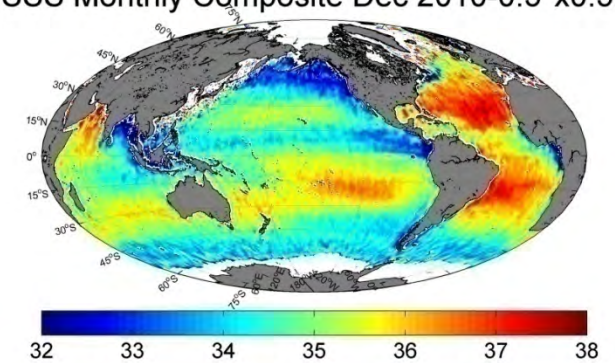

SMOS SSS (color)+ currents (vector) from 03/03 to 17/03 2012

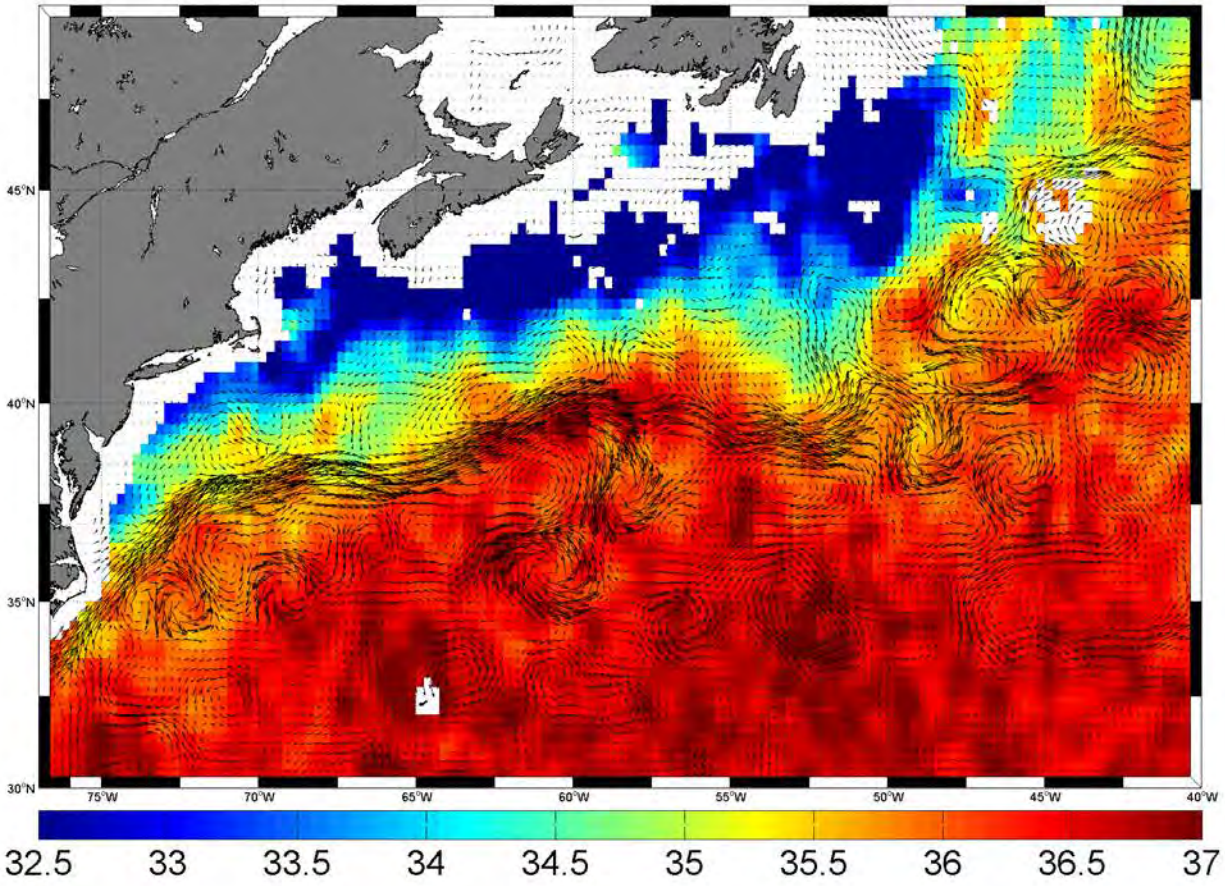

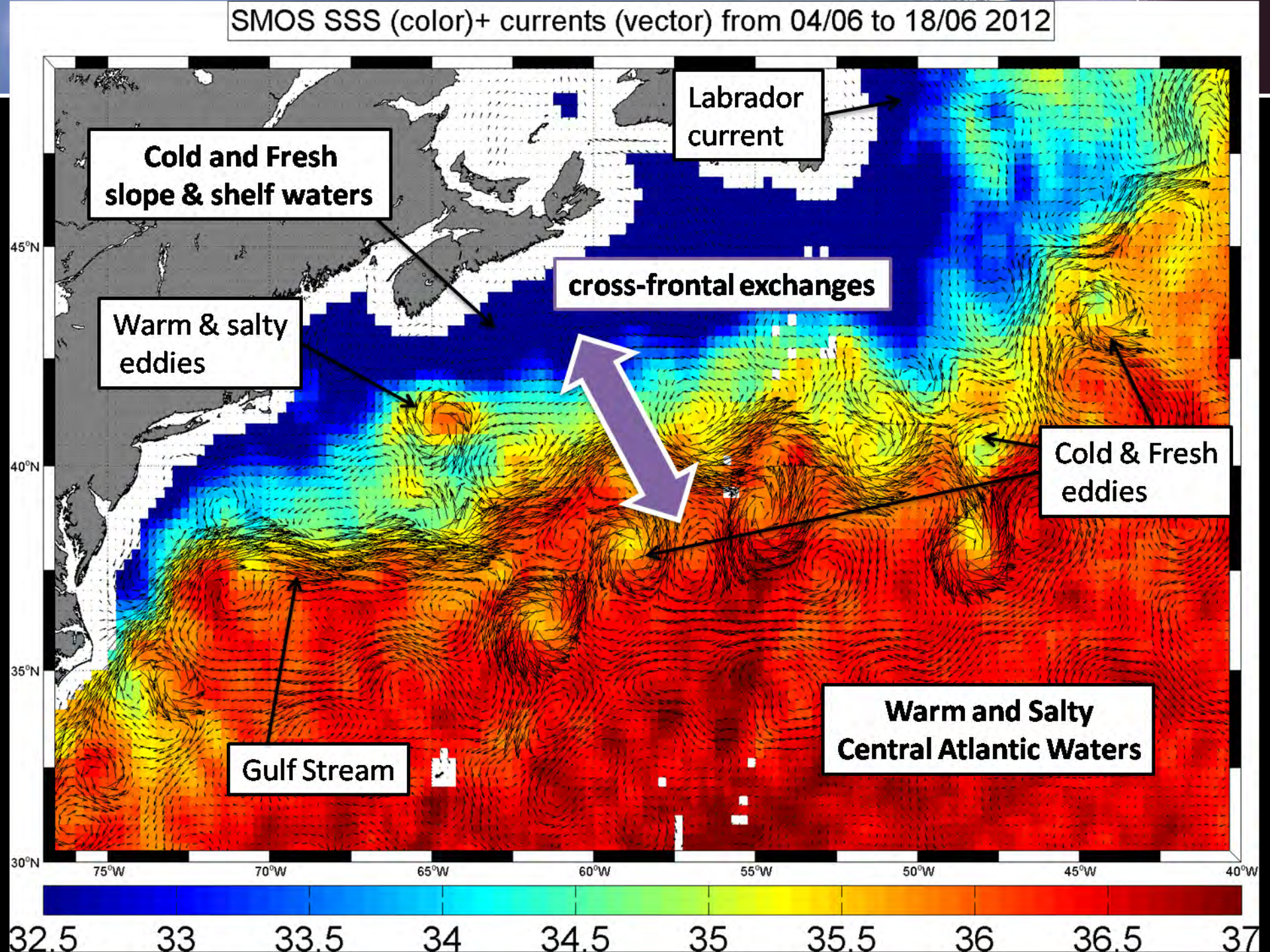
SMOS SSS (color)+ currents (vector) from 04/06 to 18/06 2012
Labrador current
Cold and Fresh slope & shelf waters
cross-frontal exchanges
Warm & salty eddies
Cold & Fresh eddies
Gulf Stream
Warm and Salty Central Atlantic Waters
45°N
40°N
35°N
30°N
75°W
70°W
65°W
60°W
55°W
50°W
45°W
40°W
32.5
33
33.5
34
34.5
35
35.5
36
36.5
37

Synergy SSS (SMOS+AMSR-E)+Altimeter-derived surface currents +SST (GHRSST)+ Ocean Colour (CDOM MERIS/MODIS)

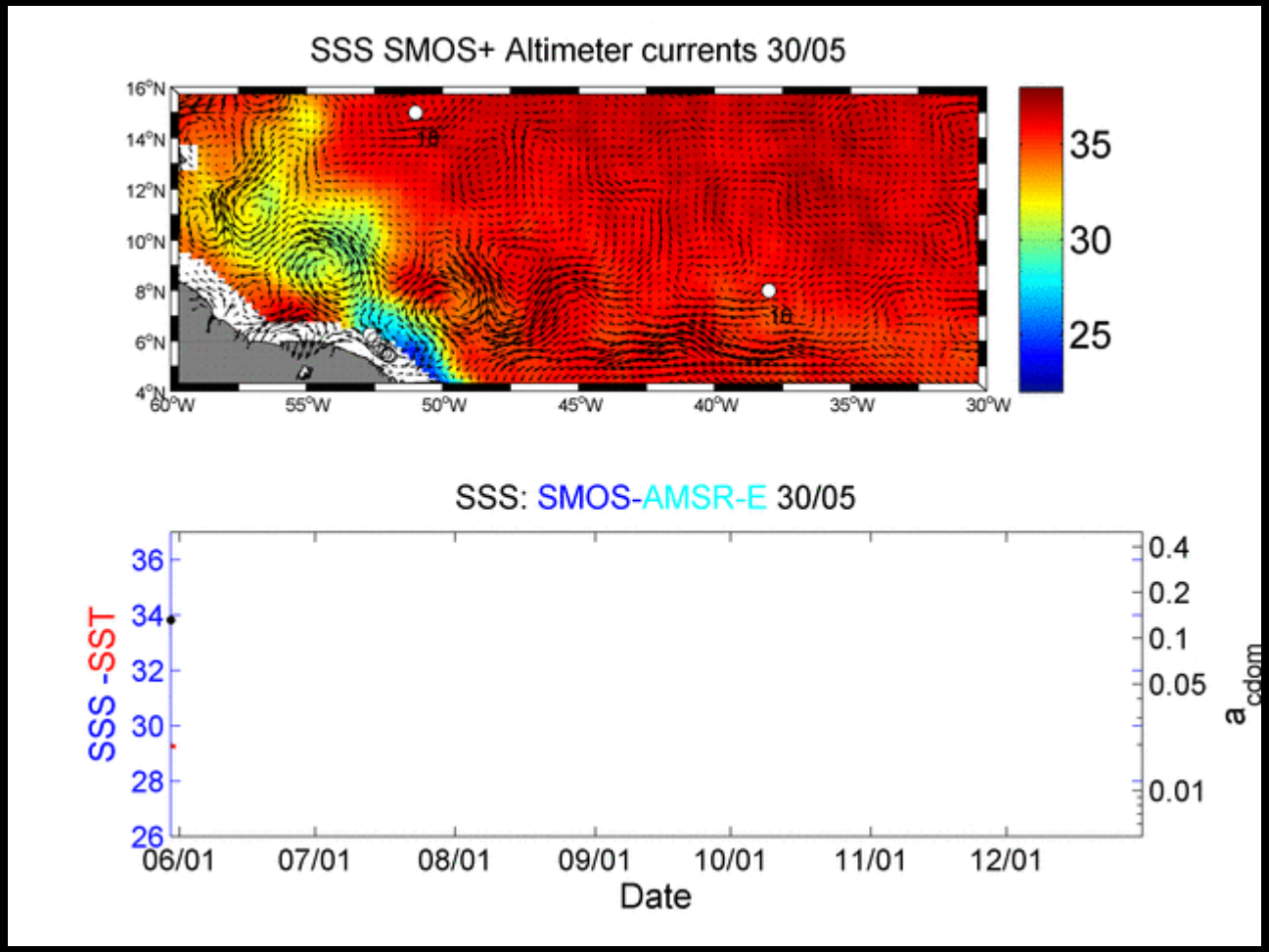

Lagangian Optical-Physical properties

SSS Averaged from Jun 04 through Jun 14

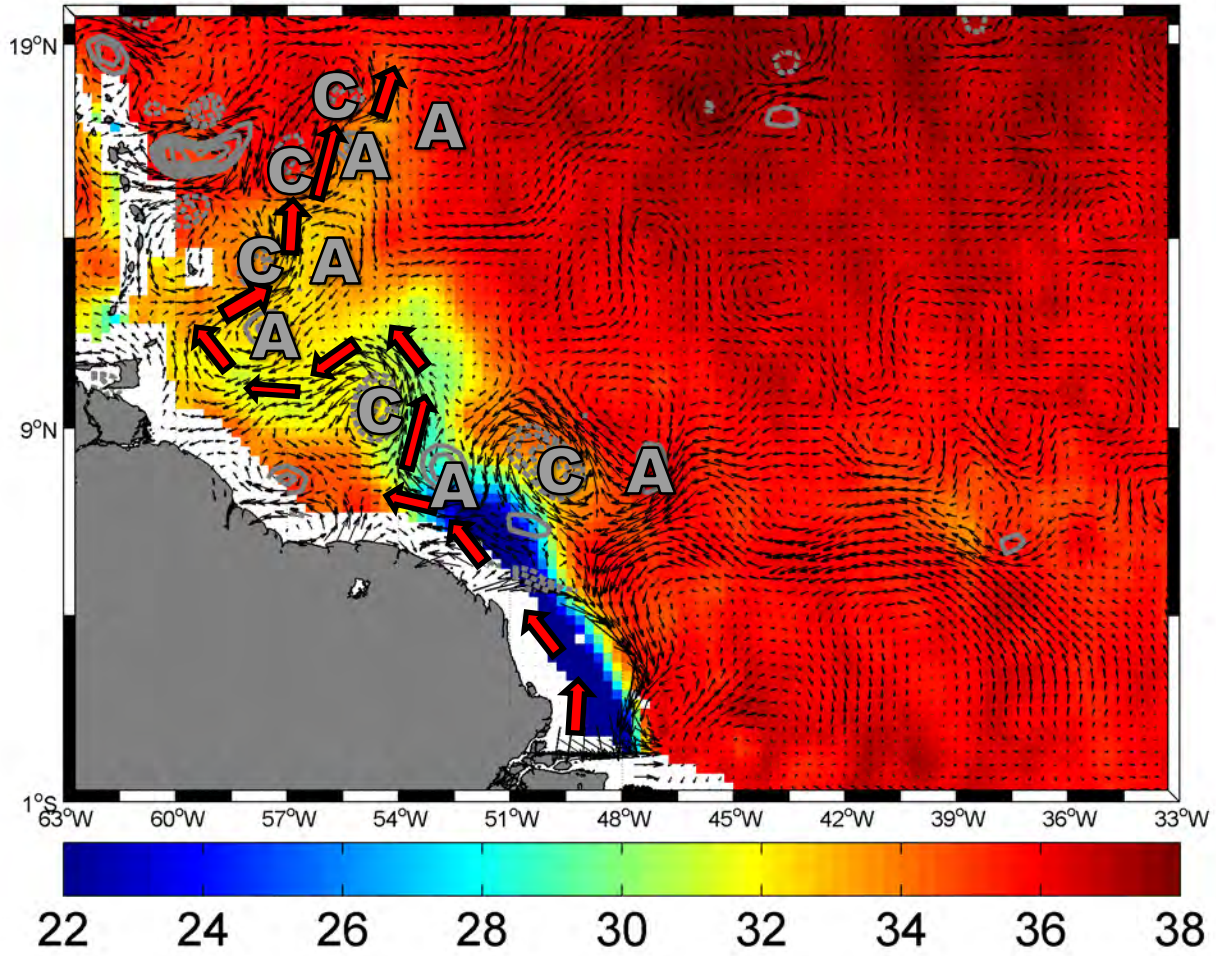

Time series of ocean color and salinity along plume trajectories

Analysis locations based on segments of low salinity plume trajectory (proximal: 0-600km, distal: 1200-1800km)

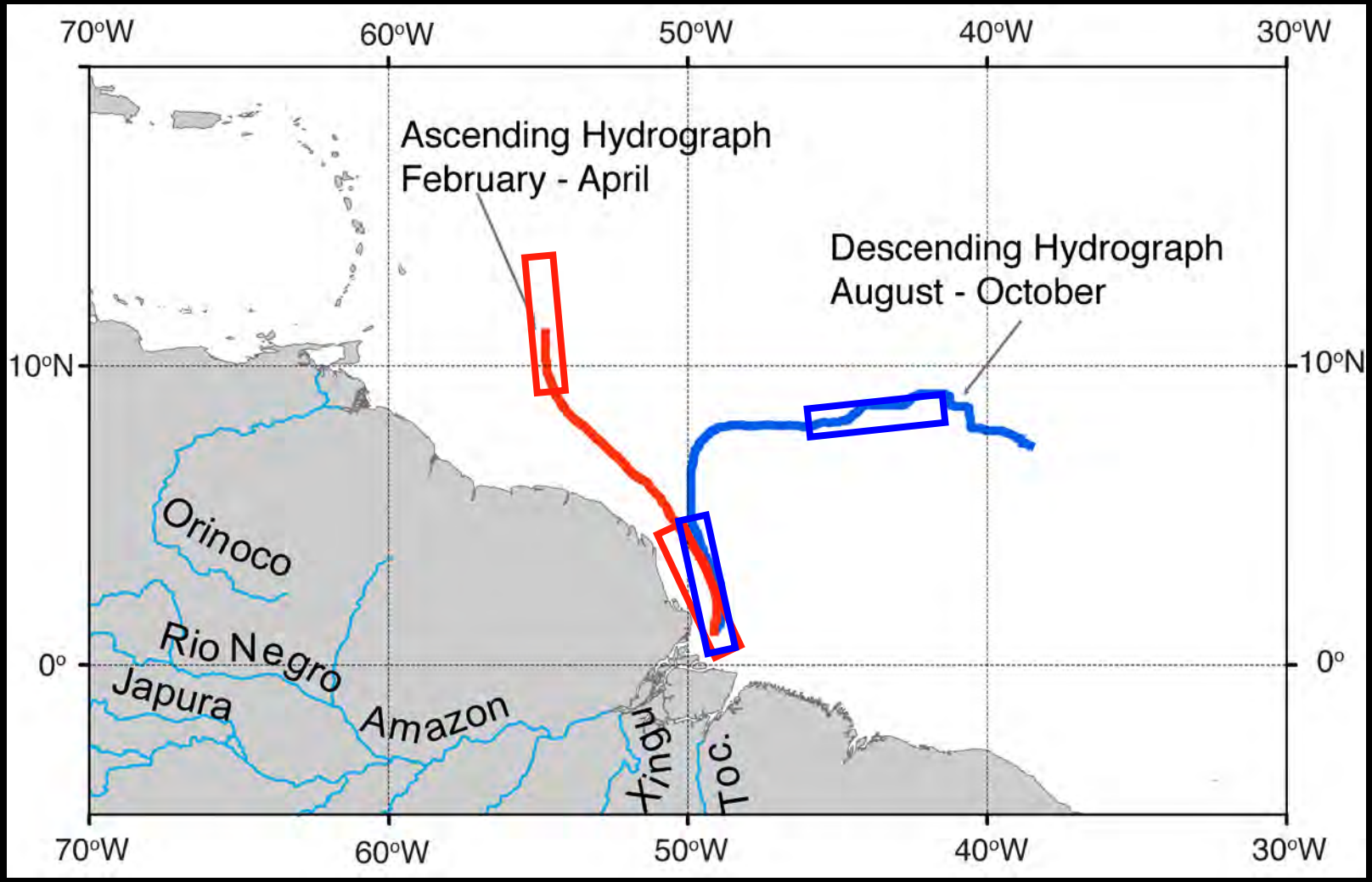

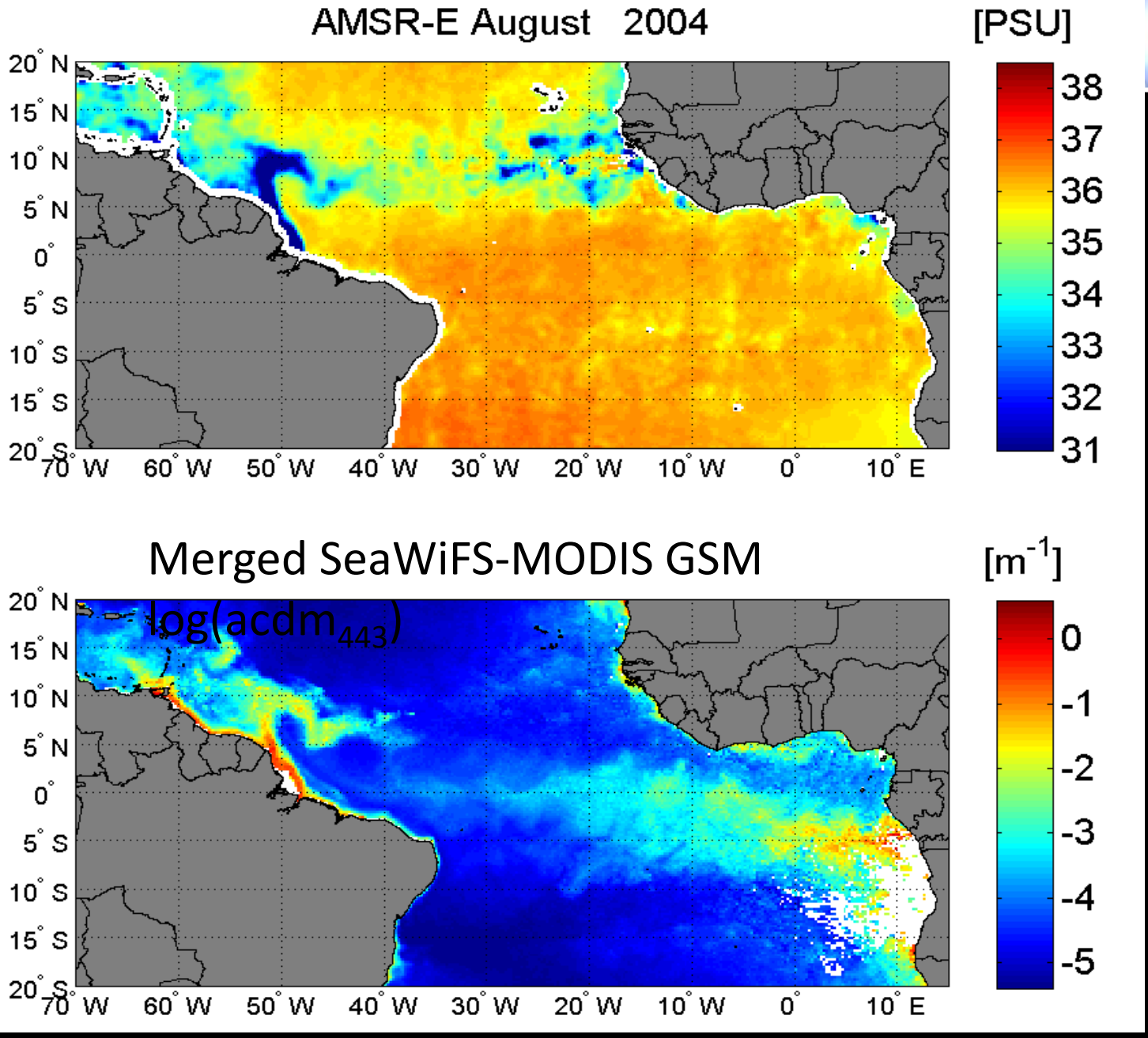
AMSR-E August 2004
[PSU]
38
37
36
35
34
33
32
31
20° N
15° N
10° N
5° N
0°
5° S
10° S
15° S
20° S
70° W
60° W
50° W
40° W
30° W
20° W
10° W
0°
10° E
Merged SeaWiFS-MODIS GSM
log(acdm443)
[m-1]
0
-1
-2
-3
-4
-5

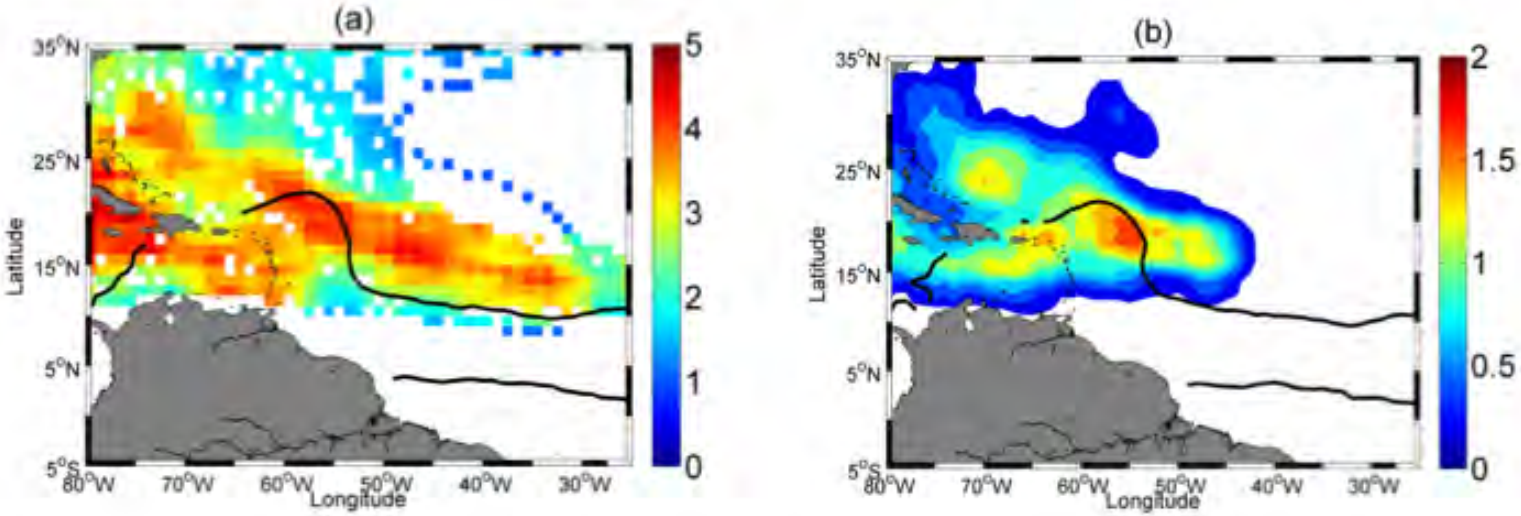

FIG.2 The number of 1950 through 2010 "best track" TC per one degree square (smoothed by a 3° x 3° block average) (a) that evolves as Cat 4-5 somewhere along their path and (b) that intensified locally to Cat 4-5. The black curve is showing the historical extent of the Amazon-Orinoco river plume during the hurricane peak season (August to October).

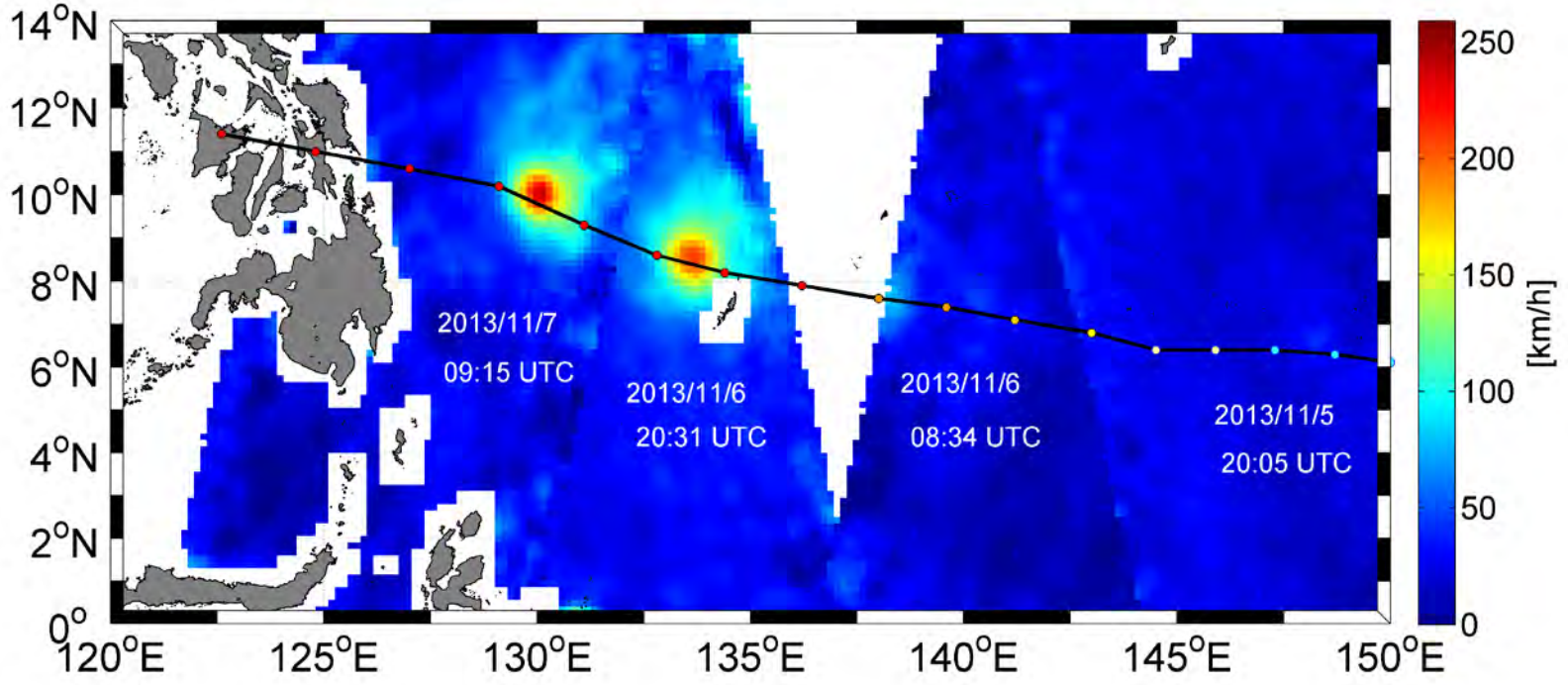
14°N
12°N
10°N
8°N
6°N
4°N
2°N
0°
120°E
125°E
130°E
135°E
140°E
145°E
150°E
2013/11/7
09:15 UTC
2013/11/6
20:31 UTC
2013/11/6
08:34 UTC
2013/11/5
20:05 UTC
250
200
150
100
50
0
[km/h]

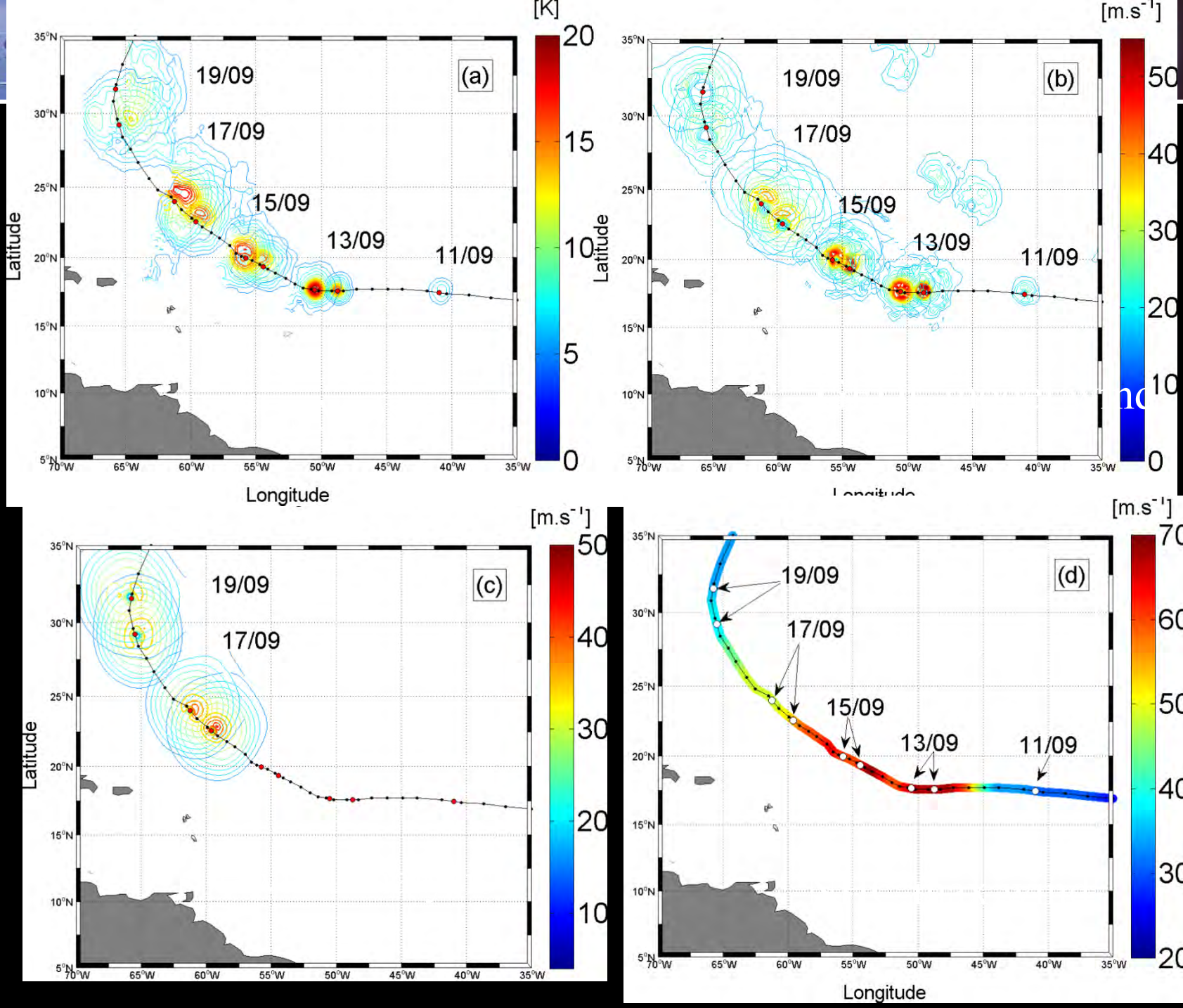
[K]
[m.s-1]
(a)
(b)
(c)
(d)
19/09
17/09
15/09
13/09
11/09
Latitude
Longitude
35°N
30°N
25°N
20°N
15°N
10°N
5°N
70°W
65°W
60°W
55°W
50°W
45°W
40°W
35°W
0
5
10
15
20
30
40
50
60
70

Surface area~ 89000 km^2> Lake Superior, the world largest freshwater lake: a transfer of 1 GTo of Salt in 5 days

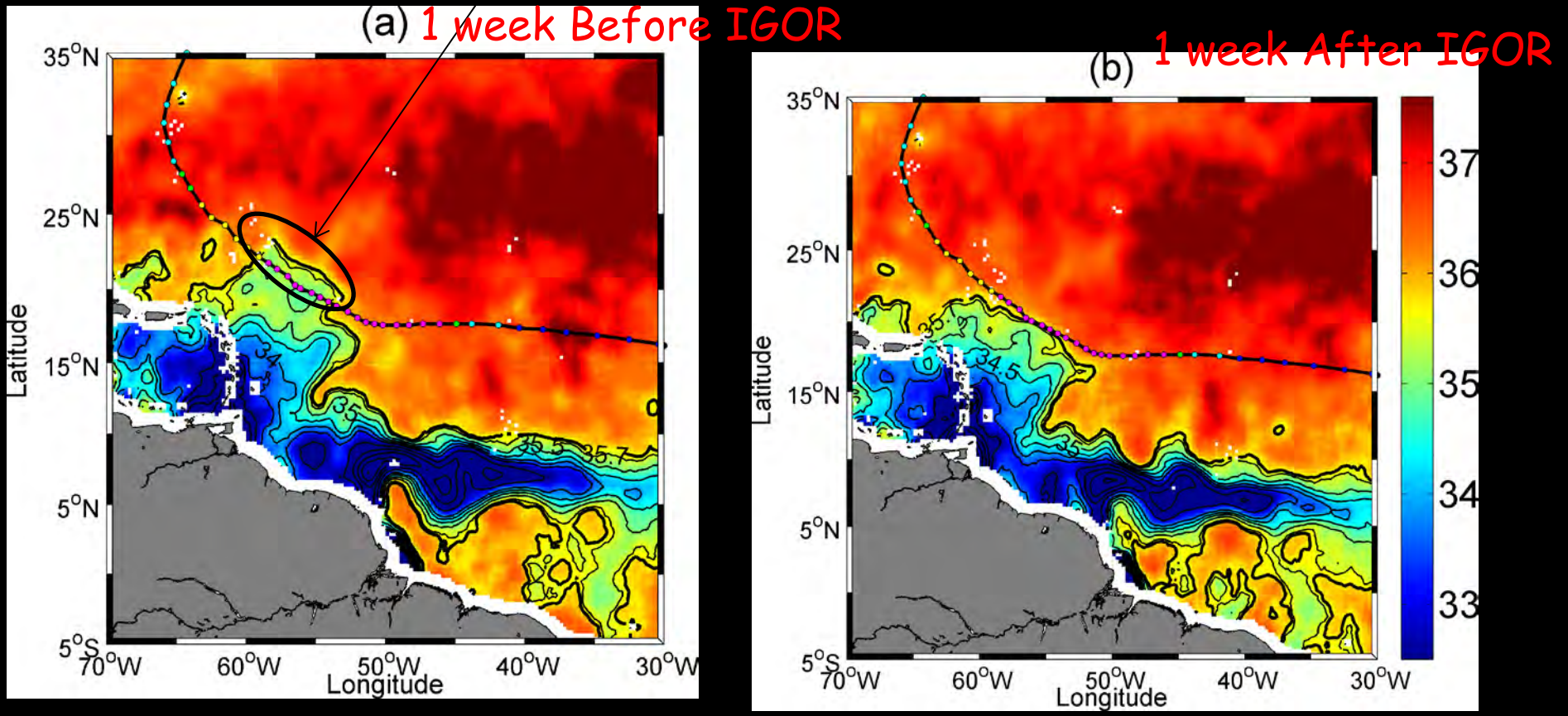

Figure 2: Two SMOS microwave satellite-derived SSS composite images of the Amazon plume region revealing the SSS conditions (a) before and (b) after the passing of Hurricane Igor, a category 5 hurricane that attained wind speeds of 136 knots in September 2010. Color-coded circles mark the successive hurricane eye positions and maximum 1-min sustained wind speed values in knots. Seven days of data centered on (a) 10 Sep 2010 and (b) 22 Sep 2010 have been averaged to construct the SSS images, which are smoothed by a 1° x 1° block average.

Surface wakes of Igor

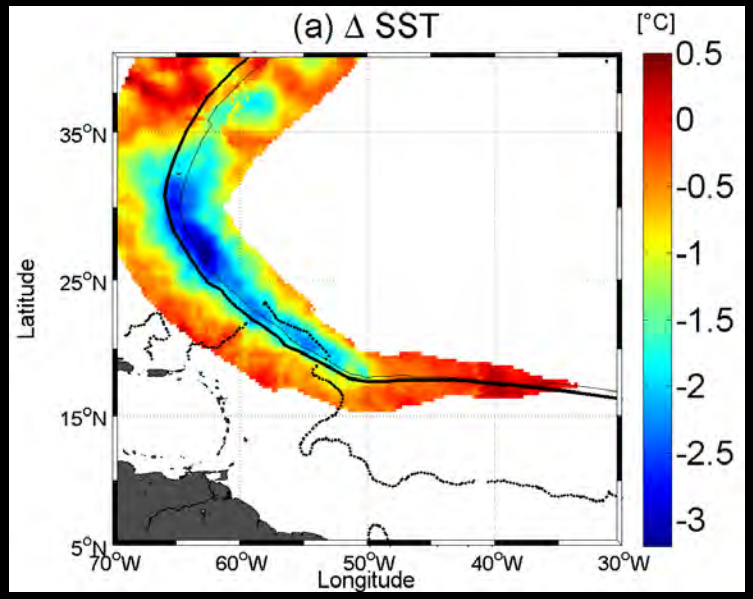

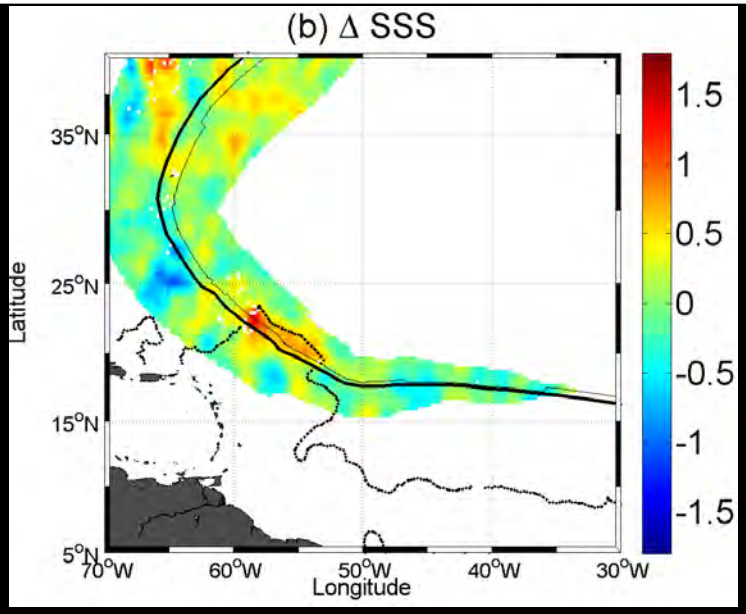

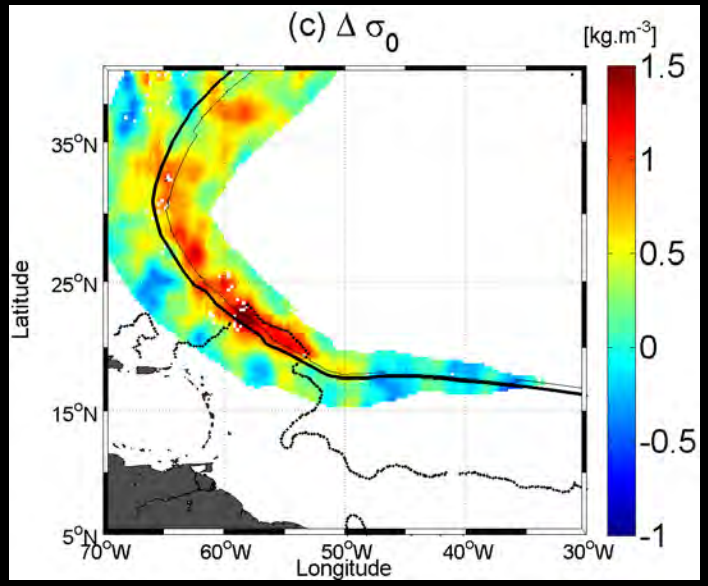

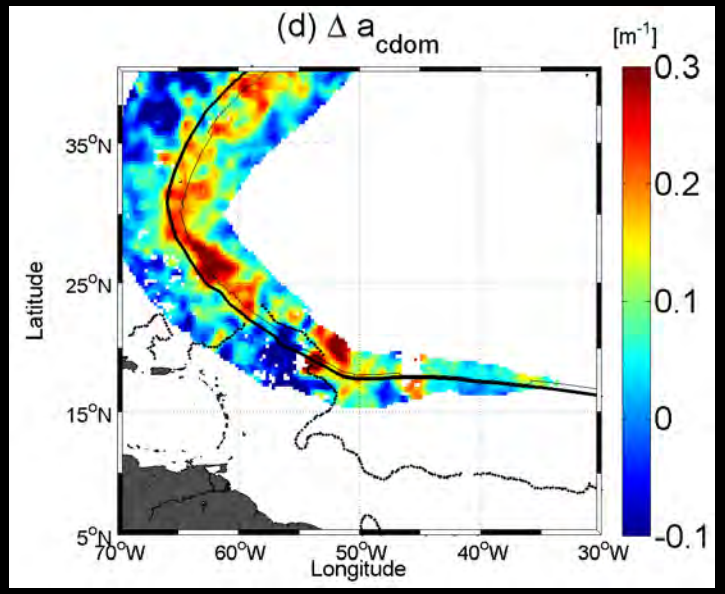

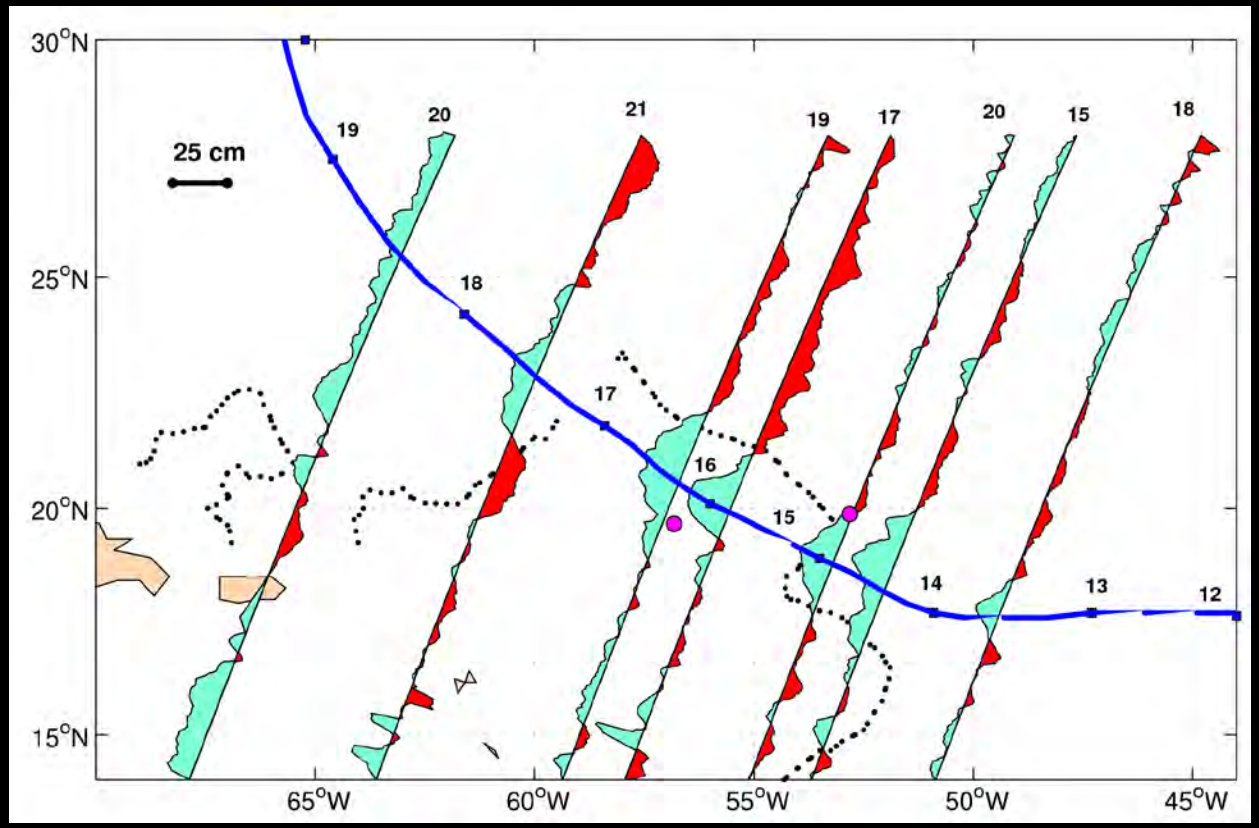
30°N
25°N
20°N
15°N
65°W
60°W
55°W
50°W
45°W
25 cm
19
20
21
19
17
20
15
18
18
17
16
15
14
13
12

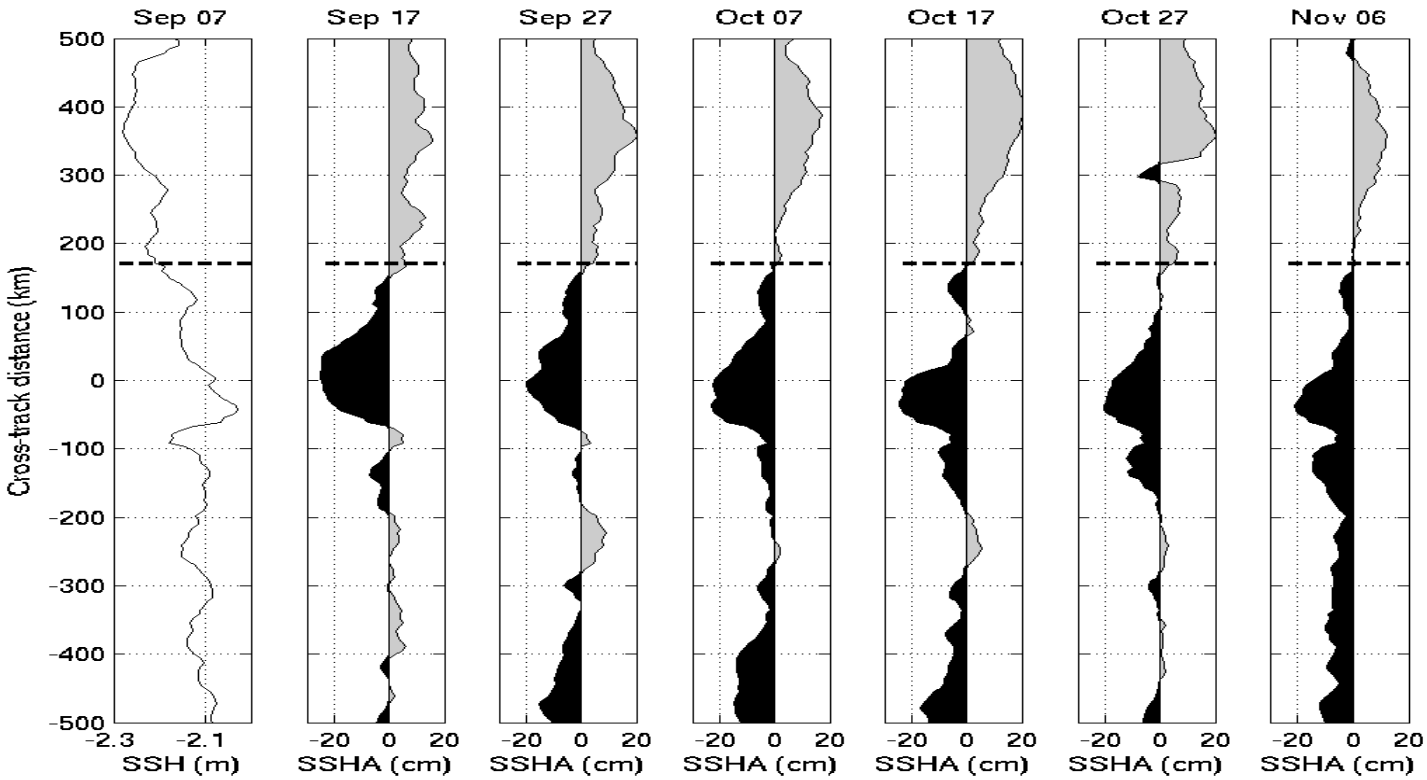
Sep 07
Sep 17
Sep 27
Oct 07
Oct 17
Oct 27
Nov 06
Cross-track distance (km)
500
400
300
200
100
0
-100
-200
-300
-400
-500
-2.3
-2.1
SSH (m)
-20
0
20
SSHA (cm)

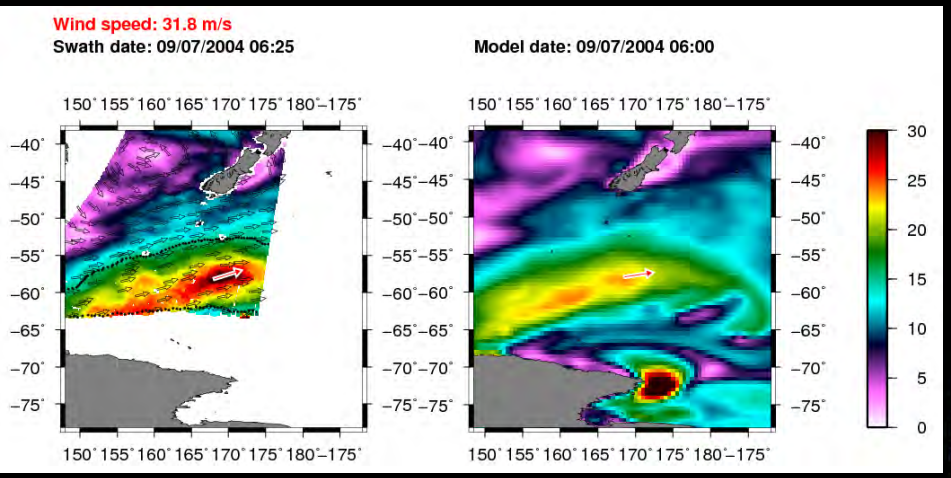

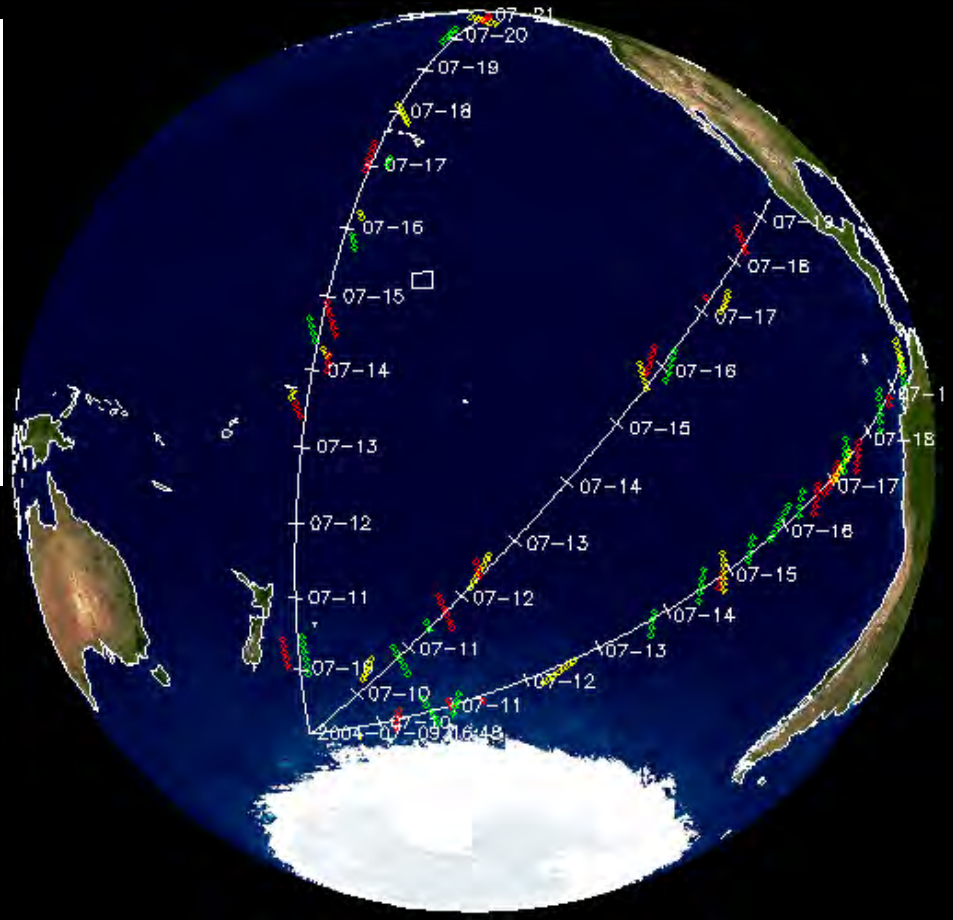

RED : ENVISAT ASAR
GREEN : ENVISAT RA2
YELLOW : JASON ALTIMETER

Fireworks

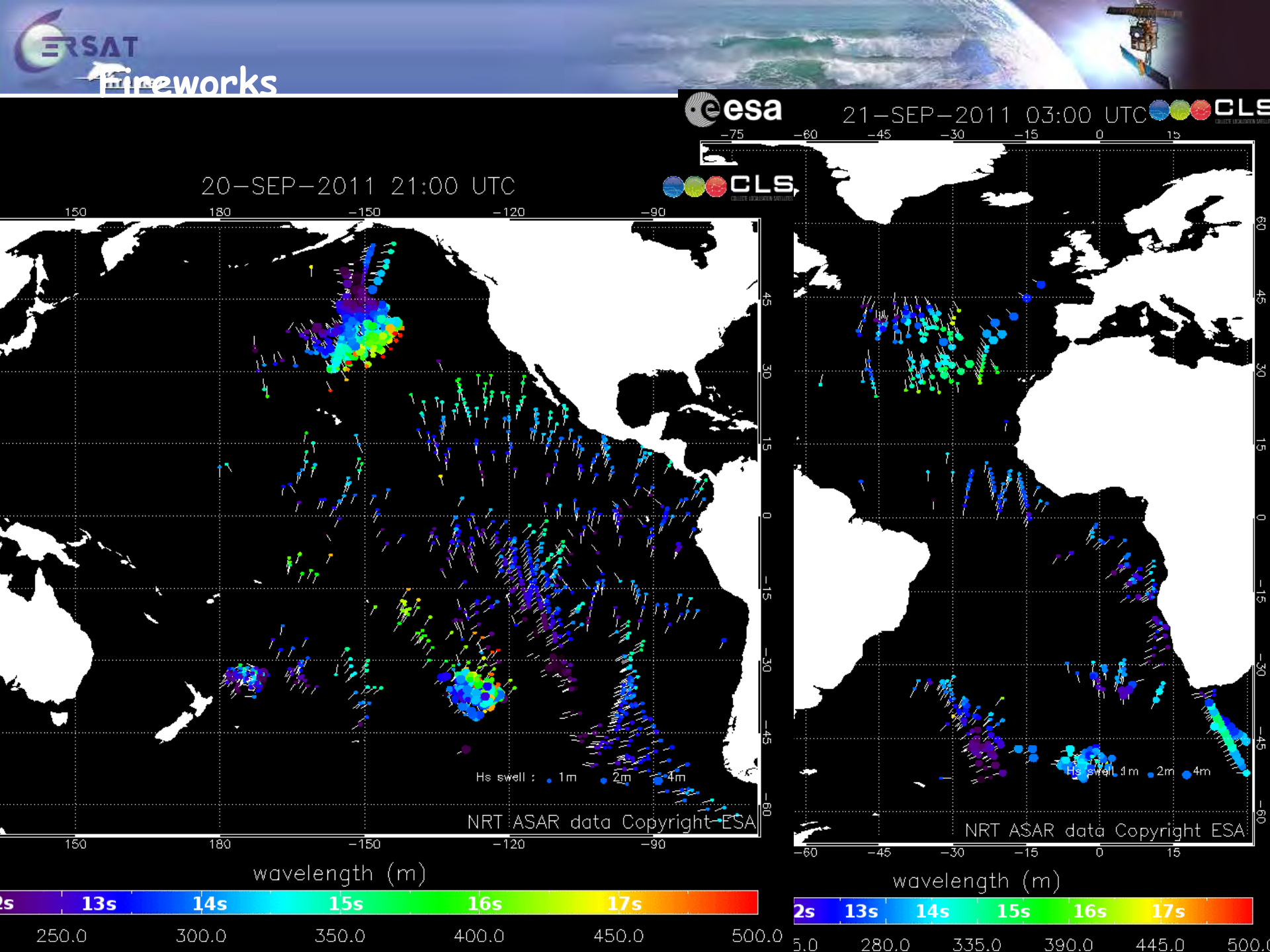
20-SEP-2011 21:00 UTC
21-SEP-2011 03:00 UTC
esa
CLS
Hs swell : 1m 2m 4m
NRT ASAR data Copyright ESA
wavelength (m)
13s 14s 15s 16s 17s
250.0 300.0 350.0 400.0 450.0 500.0
280.0 335.0 390.0 445.0

Consistency and storm severity

Example of seismic - SAR synergy

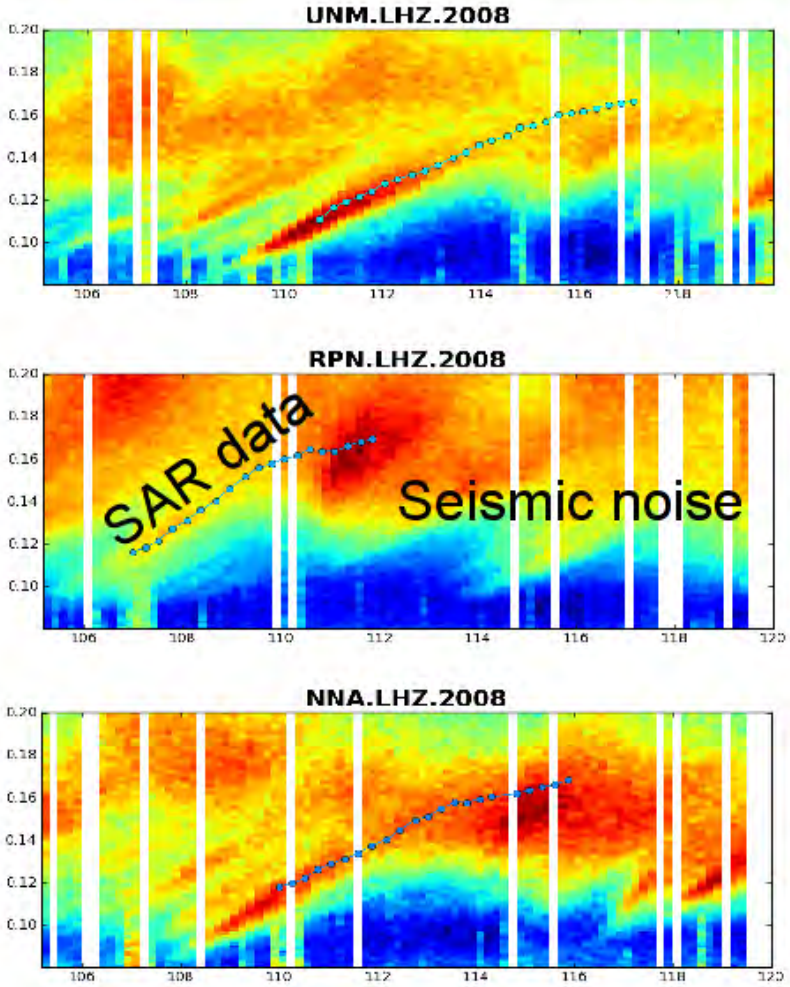

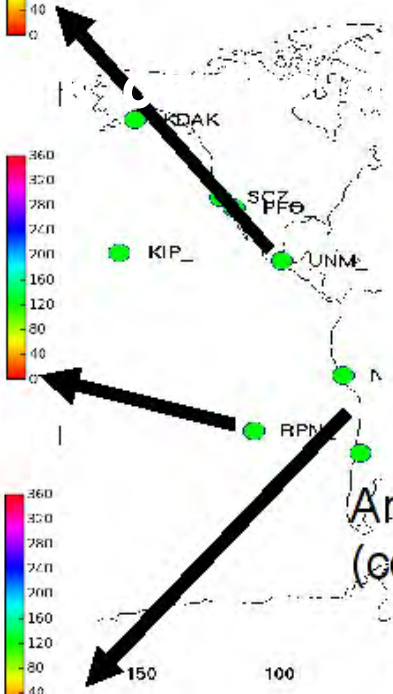

Storm location
From seismic (blue bands)

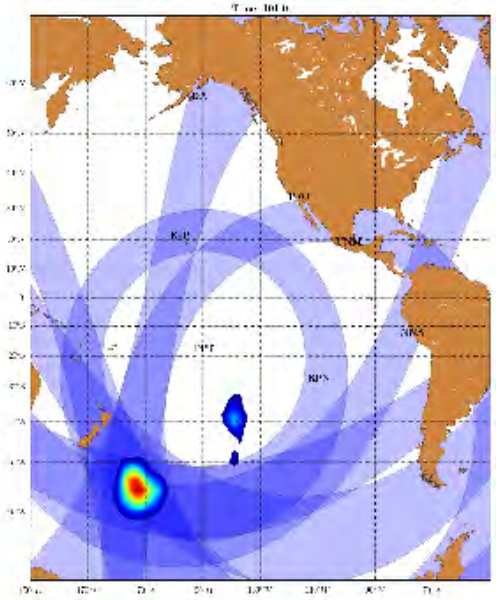

And location from SAR (colors)

Practical application medium SST resolution data

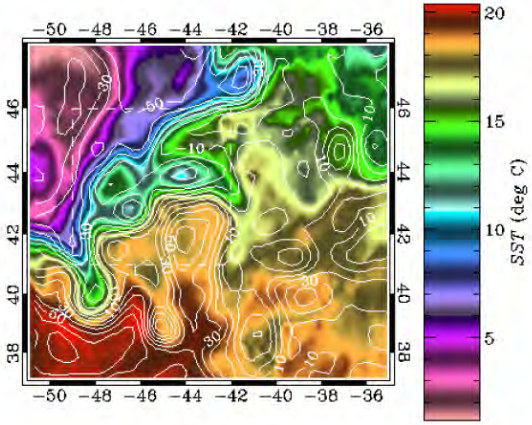

1. Given SST, ρ_s is computed using constant salinity.
2. Surface stream-function is computed $\hat{\psi}_e(\vec{k},0) \propto k^{-1}\hat{\rho}_s(\vec{k})$.
3. Results are compared to altimetry $\hat{\psi}_{altim}(\vec{k},0) \propto \hat{\eta}(\vec{k})$

$$\hat{E}_e \propto |\hat{\rho}_s|^2 \quad (6)$$

$$\hat{E}_{altim} \propto k^2|\hat{\eta}|^2 \quad (7)$$

- We focus on the band between 100 and 300 km.

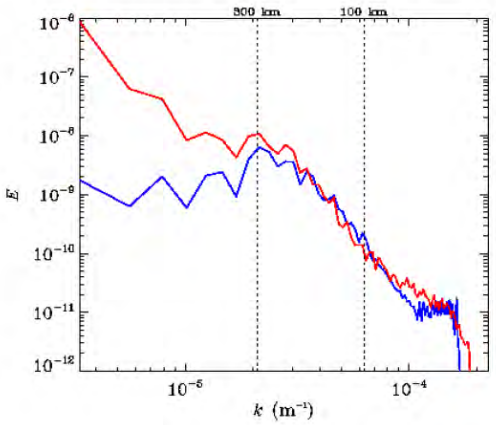

Practical application to medium SST resolution data

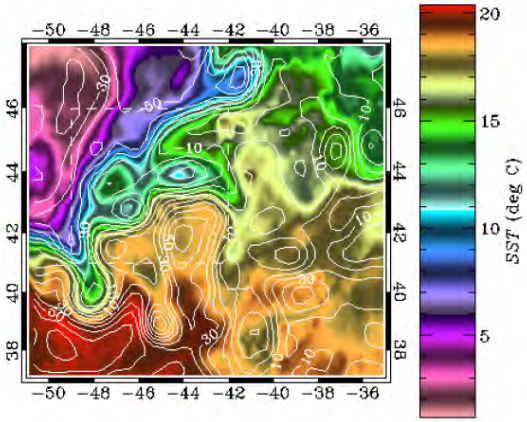

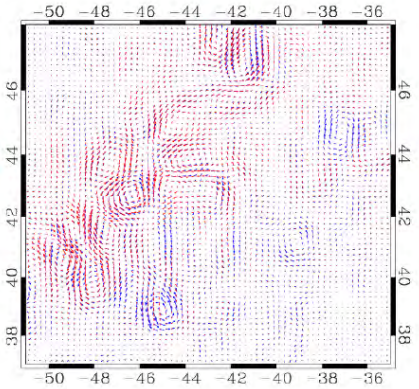

- N_1 is such that the scatter plot between $\vec{v}_e$ and $\vec{v}_{altim}$ has slope 1.
- Results are better for large thermal gradients.

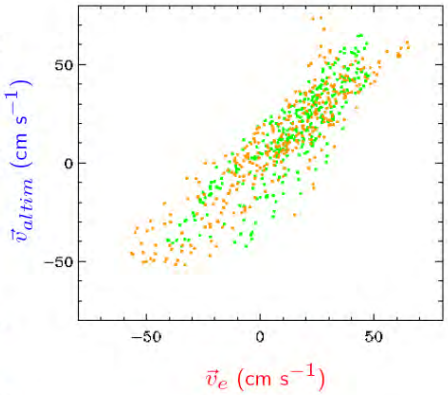

	Whole image		*Large thermal gradient*			
	R	ν	R	ν	$\langle R \rangle$	$\langle \nu \rangle$
u	0.71	0.49	0.87	0.24	0.71	0.50
v	0.67	0.55	0.90	0.19	0.69	0.53

SSH and SST in the 100-300 km band (montly mean Feb. 2008)

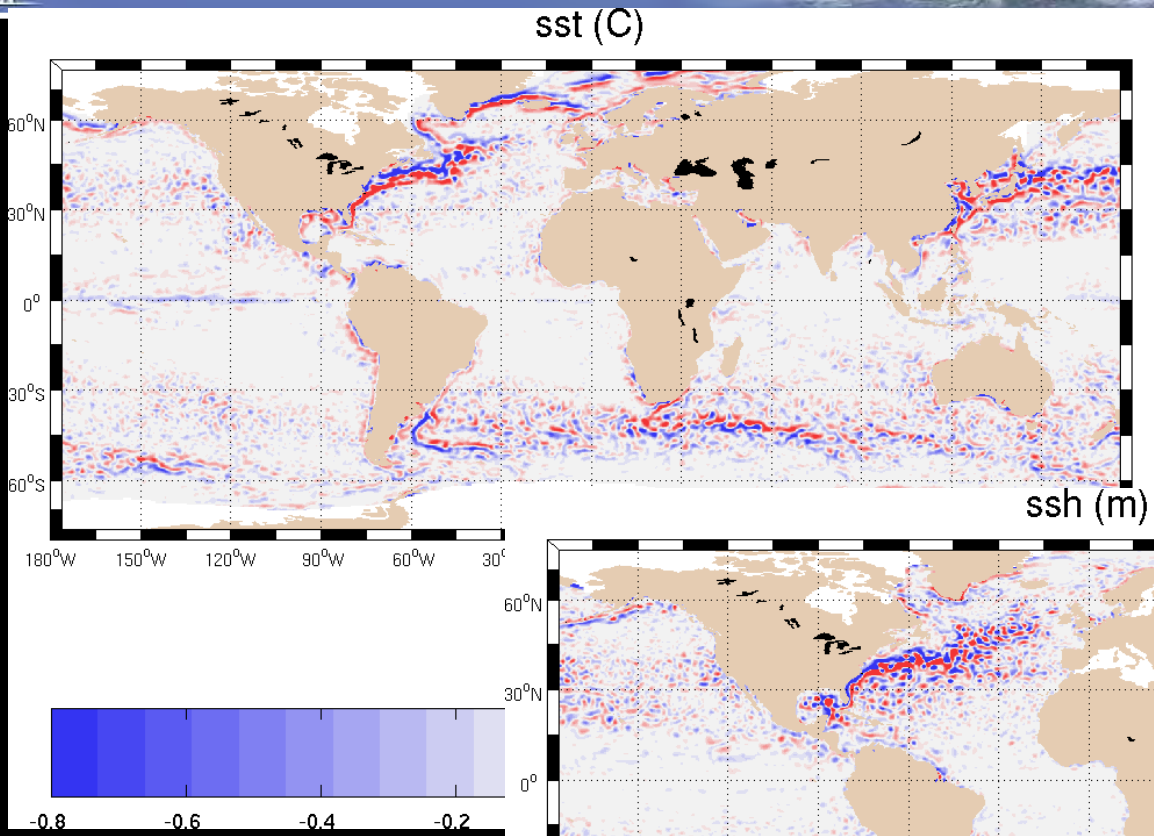

Monthly mean of SSH and SST, filtered

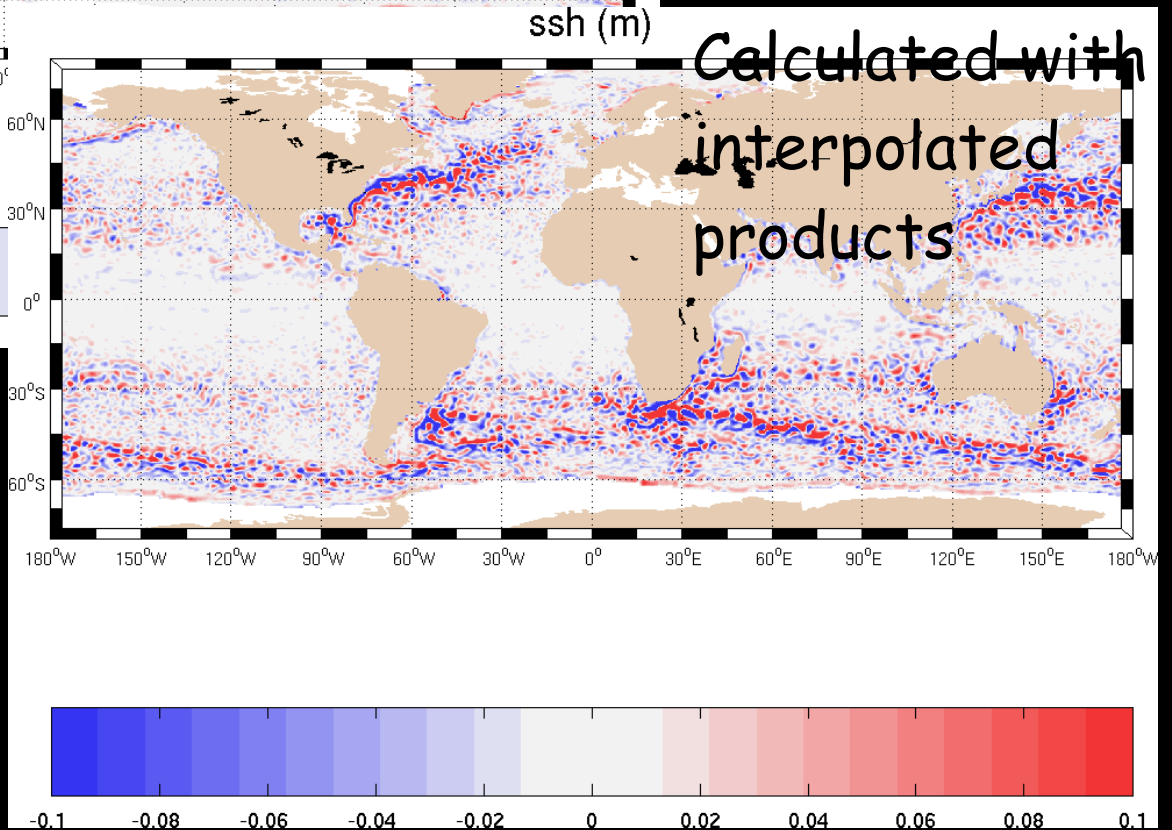

Calculated with interpolated products

SSH and SST variance in the 100-300 km band

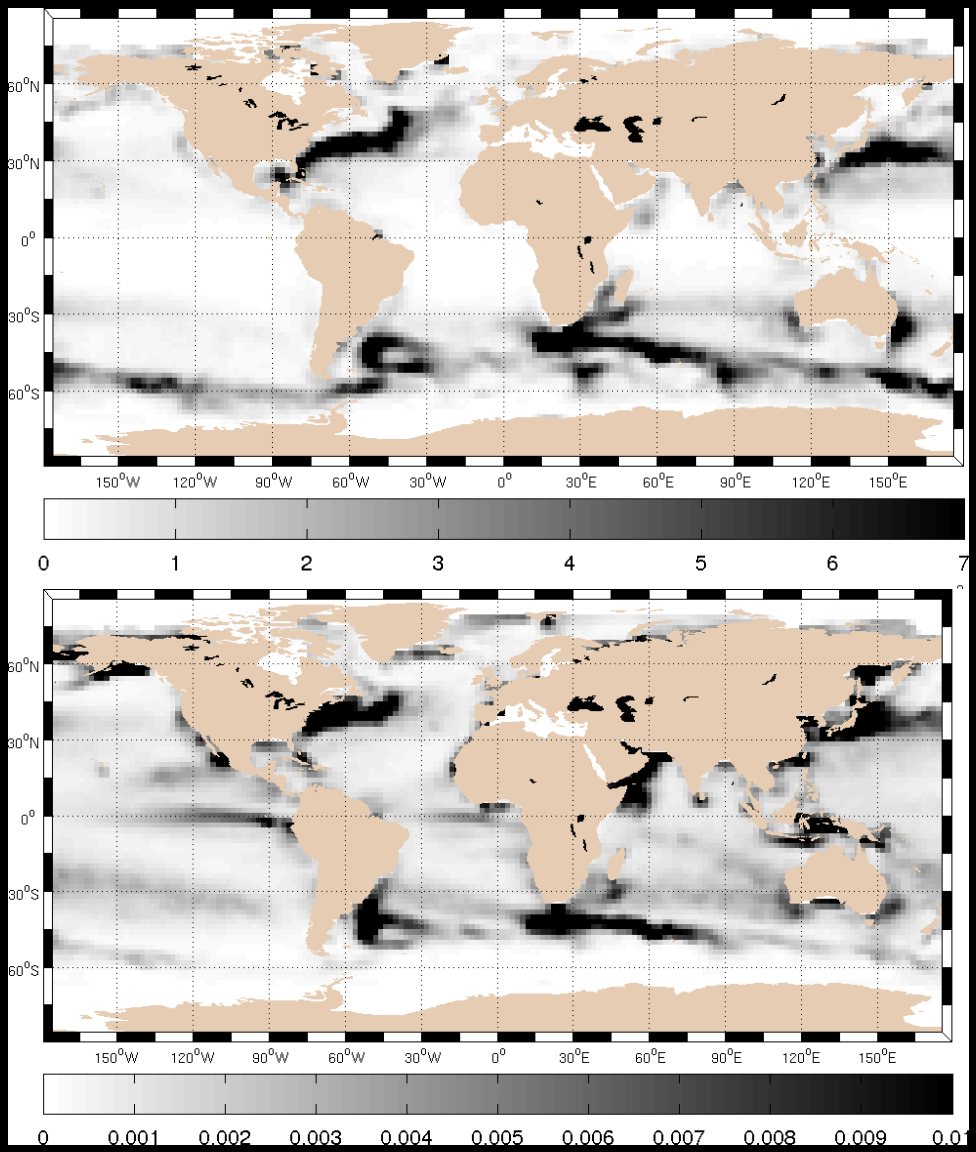

seasonal mean (Jul-Aug-Sep) of variance at 2° x2° grid resolution calculated from interpolated

SSH/SST correlation in the 100-300 km band

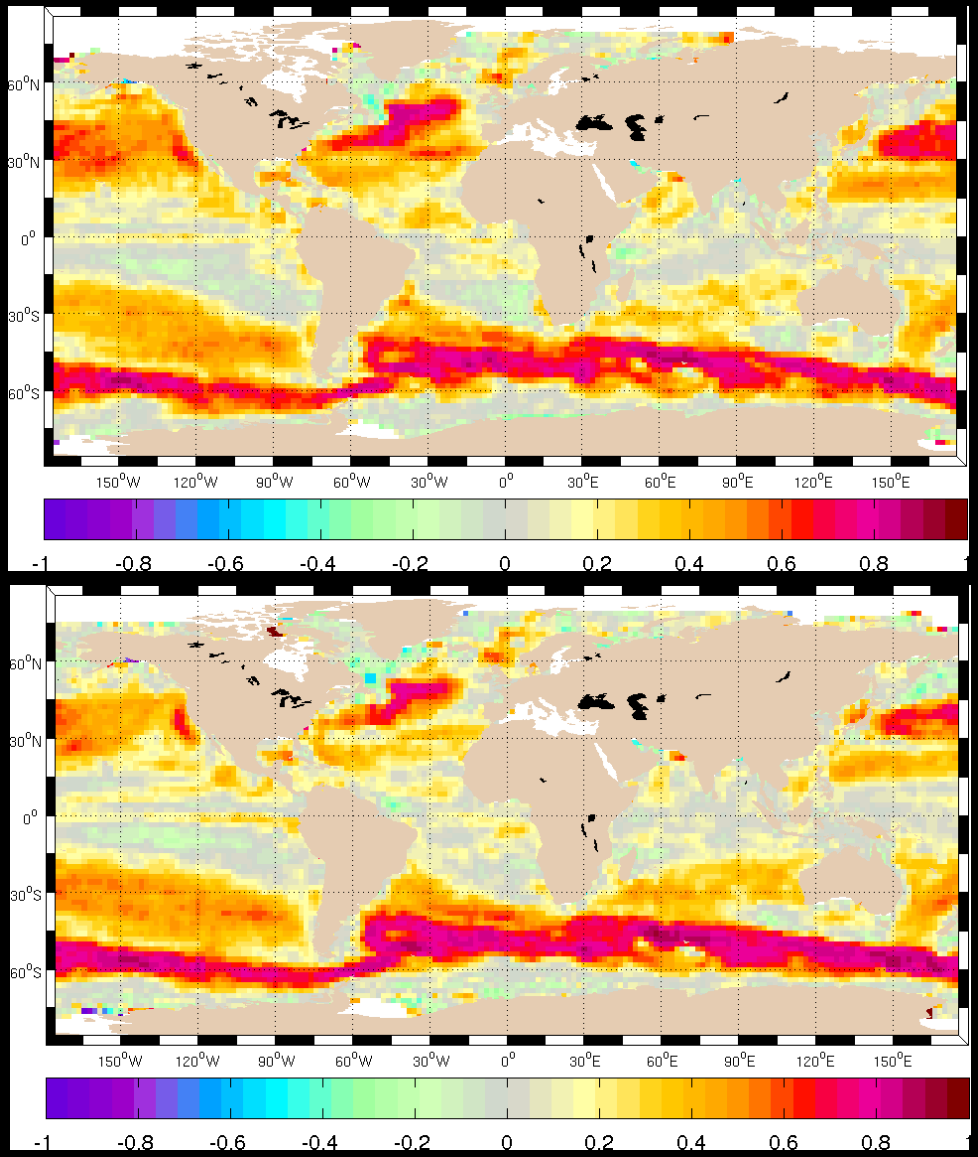

2003-2009 seasonal mean of correlation coefficients. Calulated from weekly 0.25° grid resolution OI products (MADT and AMSRE-TMI OI) within 8° x8° box at 2° x2° grid resolution

Characterizing the mesoscale - Spectral approach

SSH wavenumber spectral slopes in the 80-250 km band

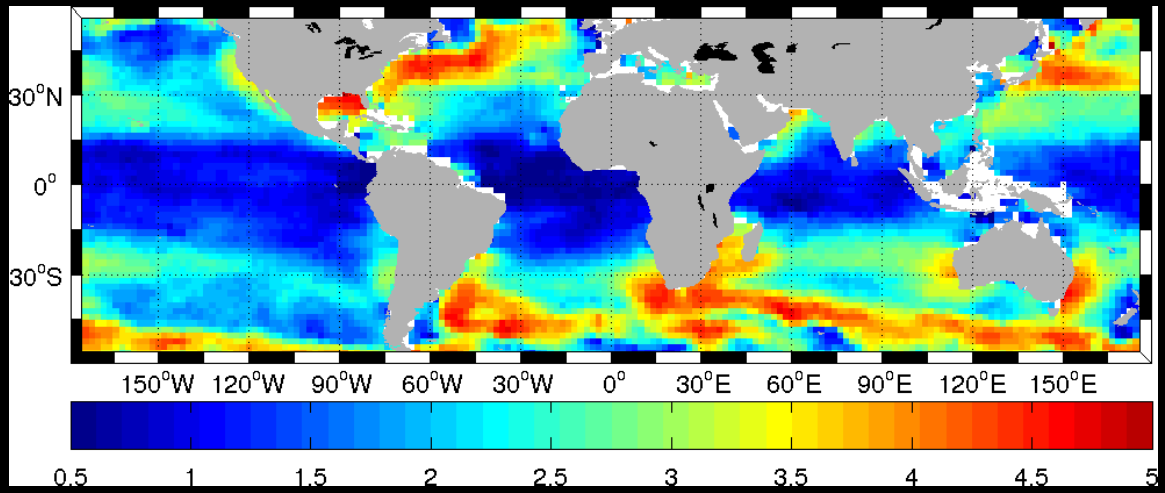

2003-2009 mean of the wavenumber spectral slope in the 80-250 km wavelength band calculated from

Jason

Track data (within 8° x8° box) at 2° x2° grid resolution~ global map proposed by Xu and Fu, 2011 and Xu and Fu, 2012

Characterizing the mesoscale - Spectral approach

SST wavenumber spectral slopes in the 80-250 km band

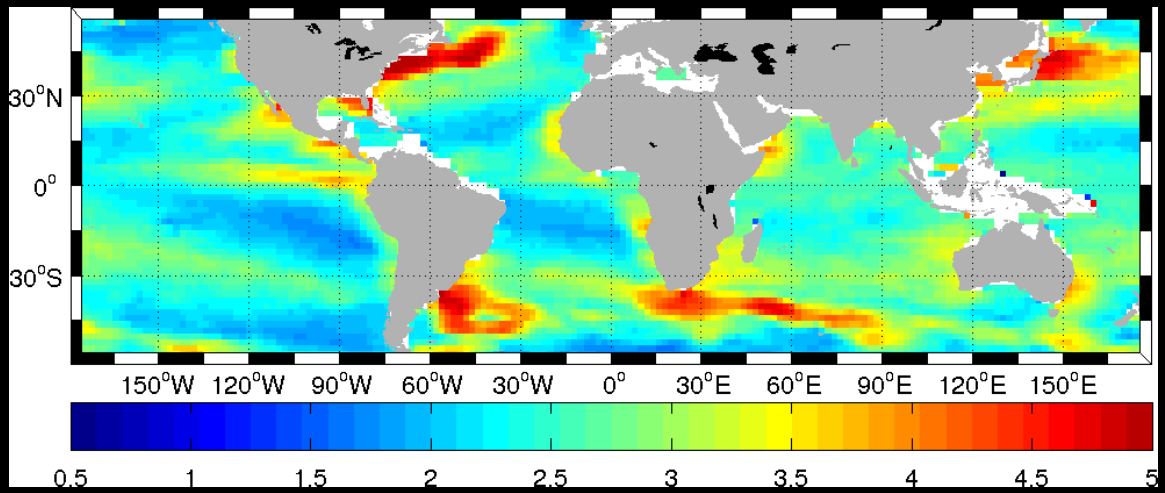

2003-2009 mean of the wavenumber spectral slope in the 80-250 km wavelength band calculated from AMSRE L3 data (within 8° x8° box) at 2° x2° grid resolution

Singularity exponents

- AMSR-E SST 3 day mean
- March 1, 2008
- More examples in Turiel et al, RSE 2008

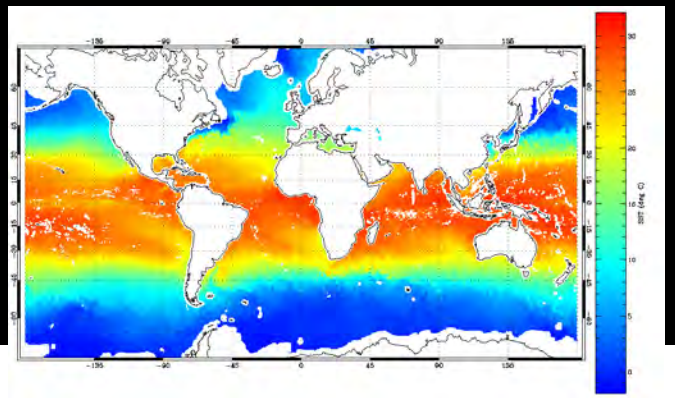

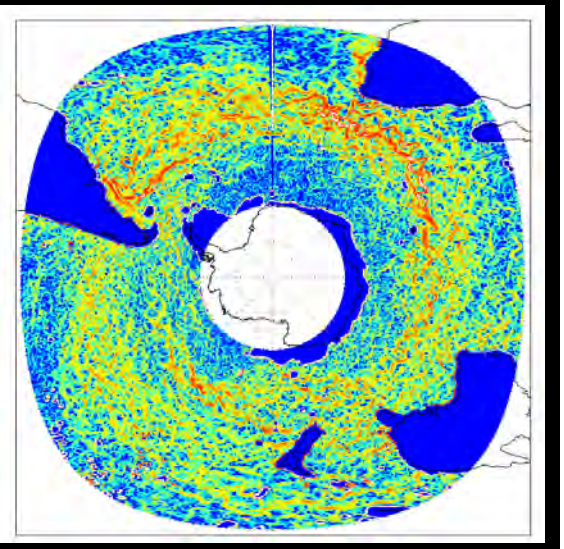

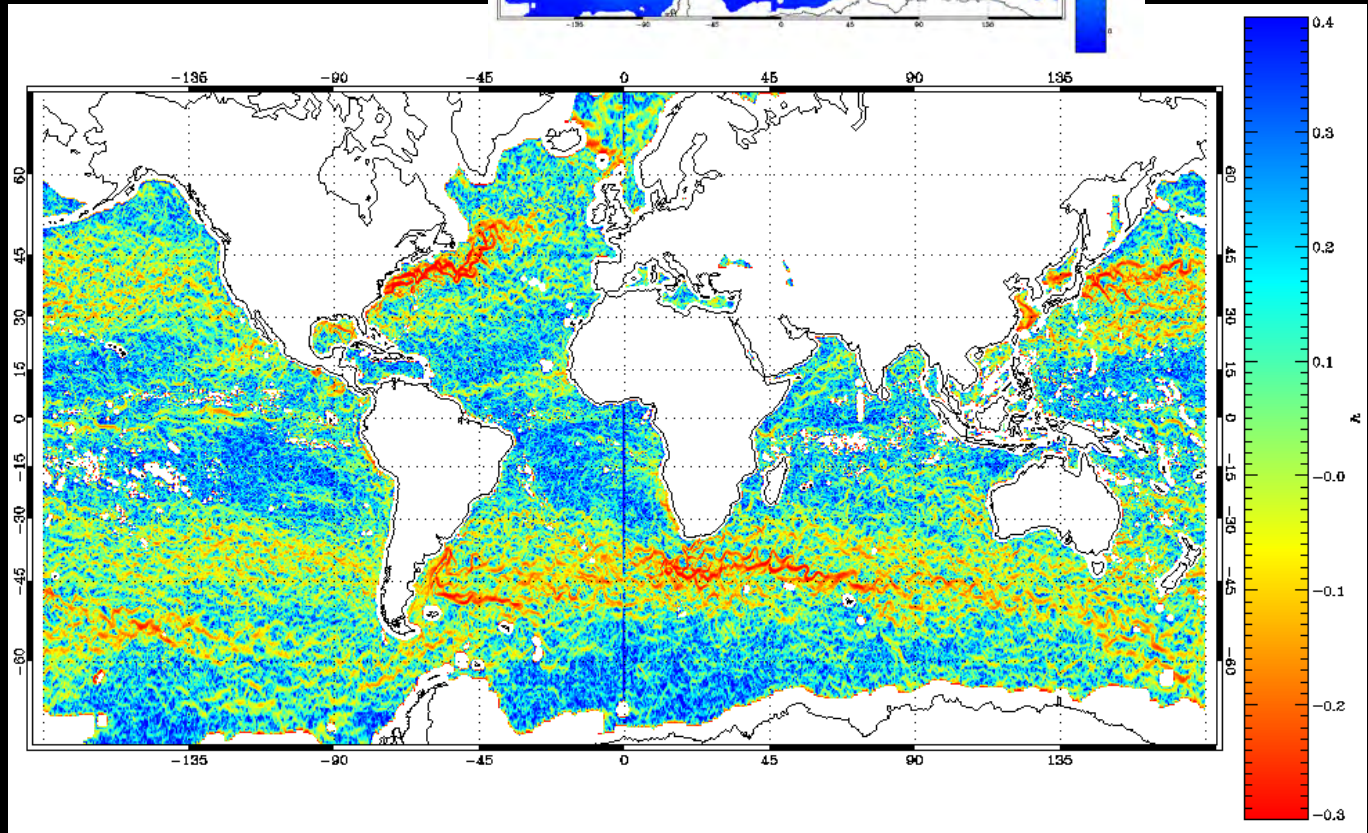

Meso-scale Air-Sea Interactions

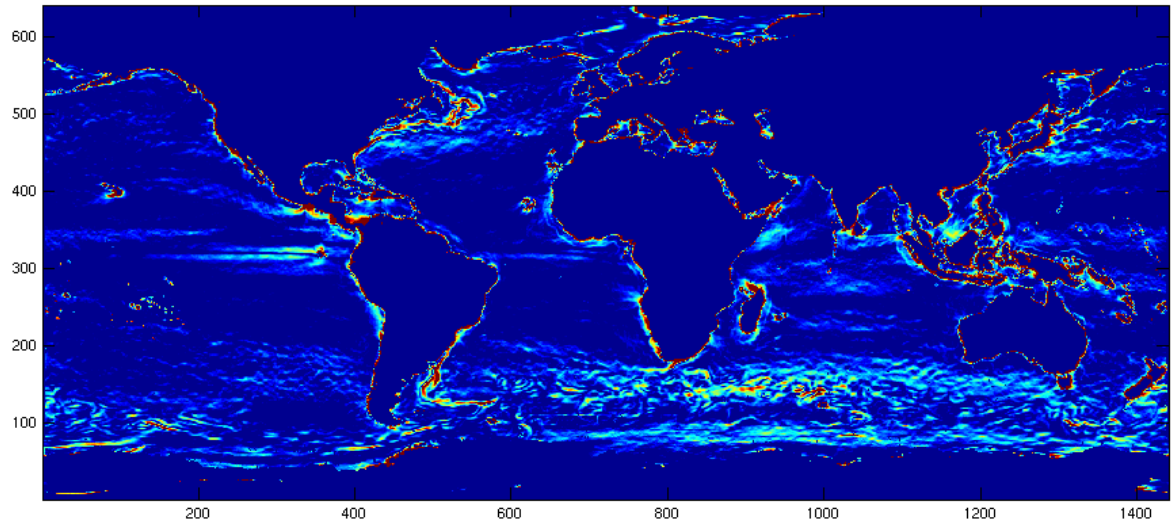

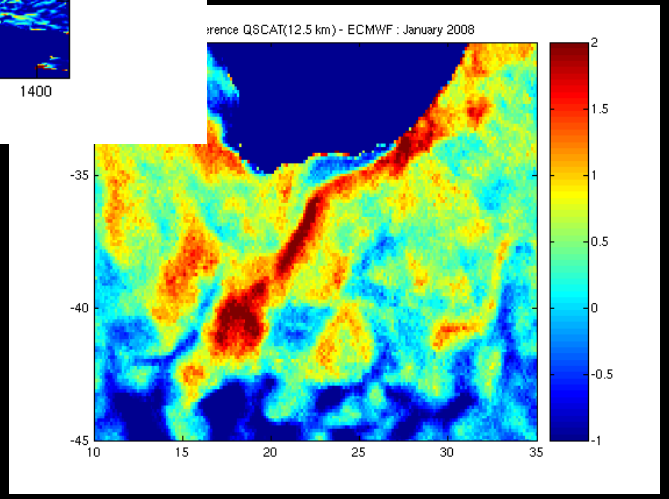

31Mar/07Apr (2010)
MODIS vs Altimetry-derived velocity field

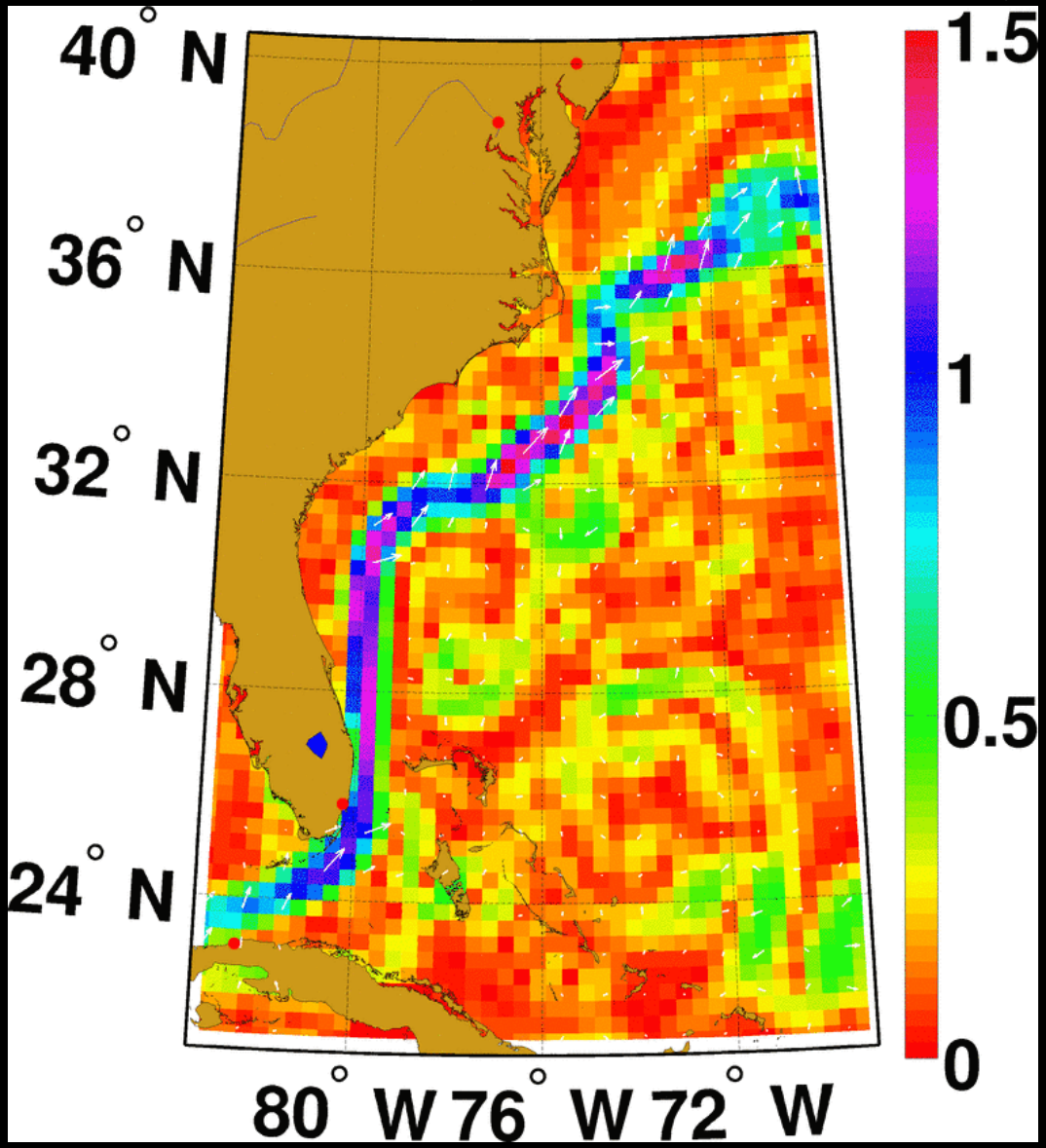


ERSAT
Ifremer

SST - Modis(L2P)

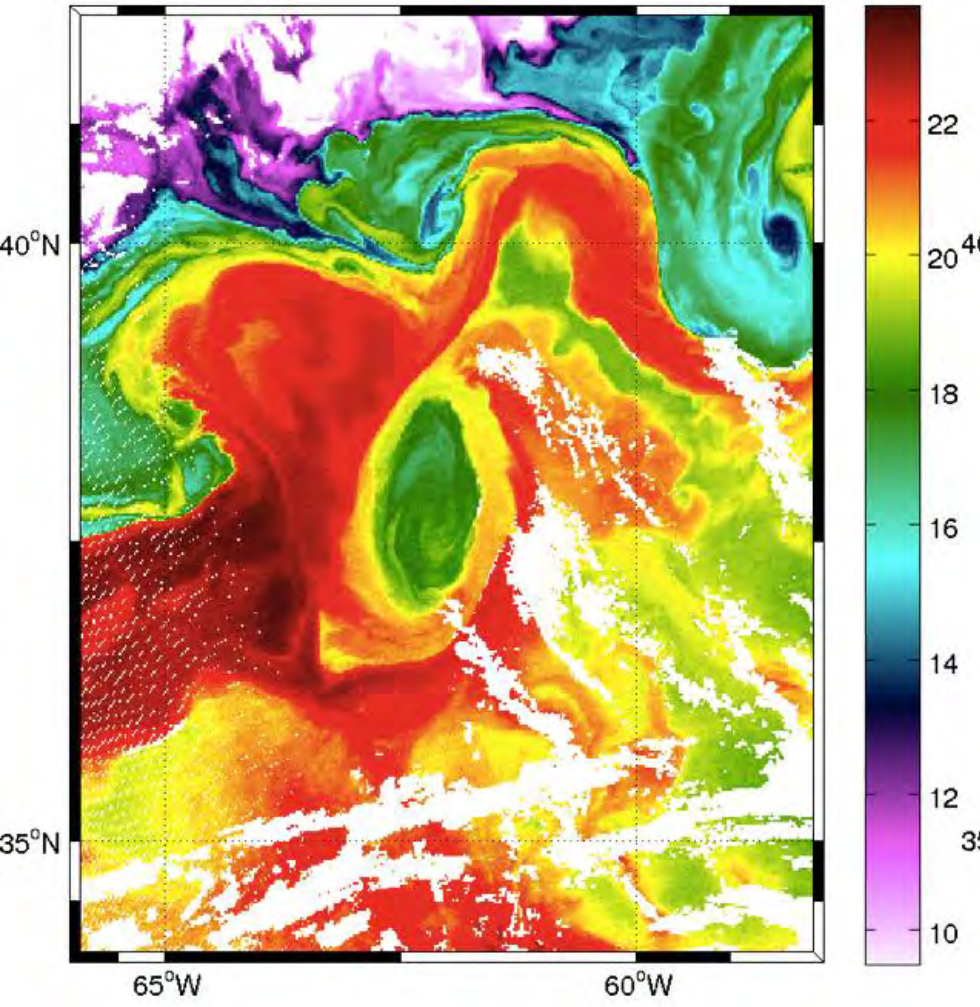

SST - AMSRE(L3)

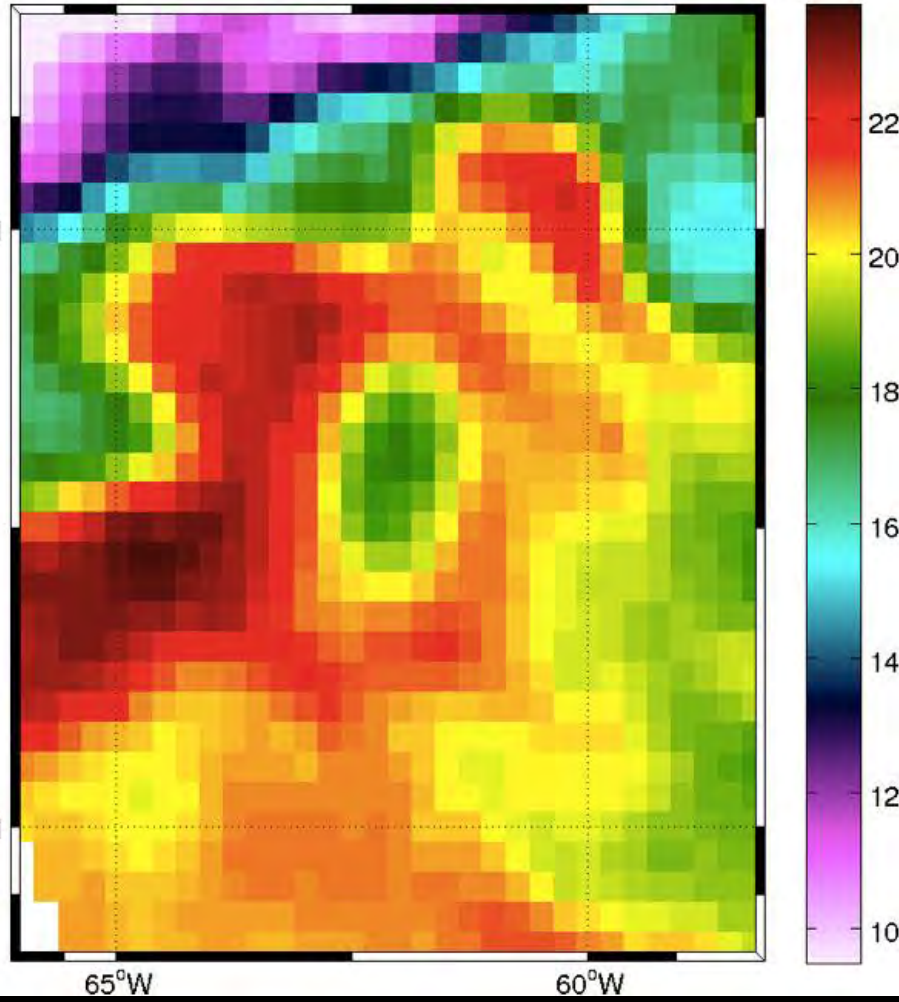

Characterizing the submesoscale - Spectral approach

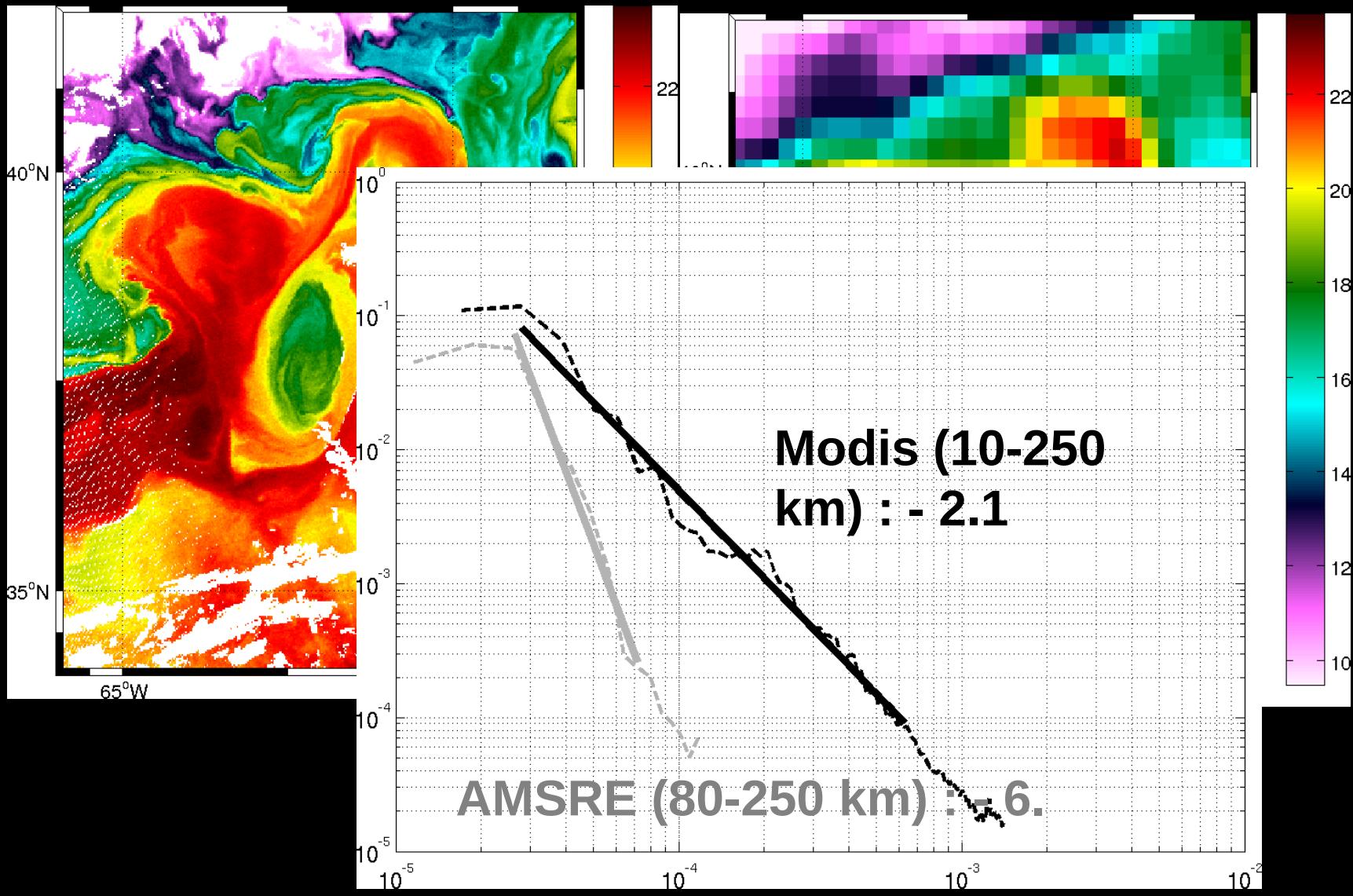

Characterizing the submesoscale - Spectral approach

SST wavenumber spectra in the 10-80 km band

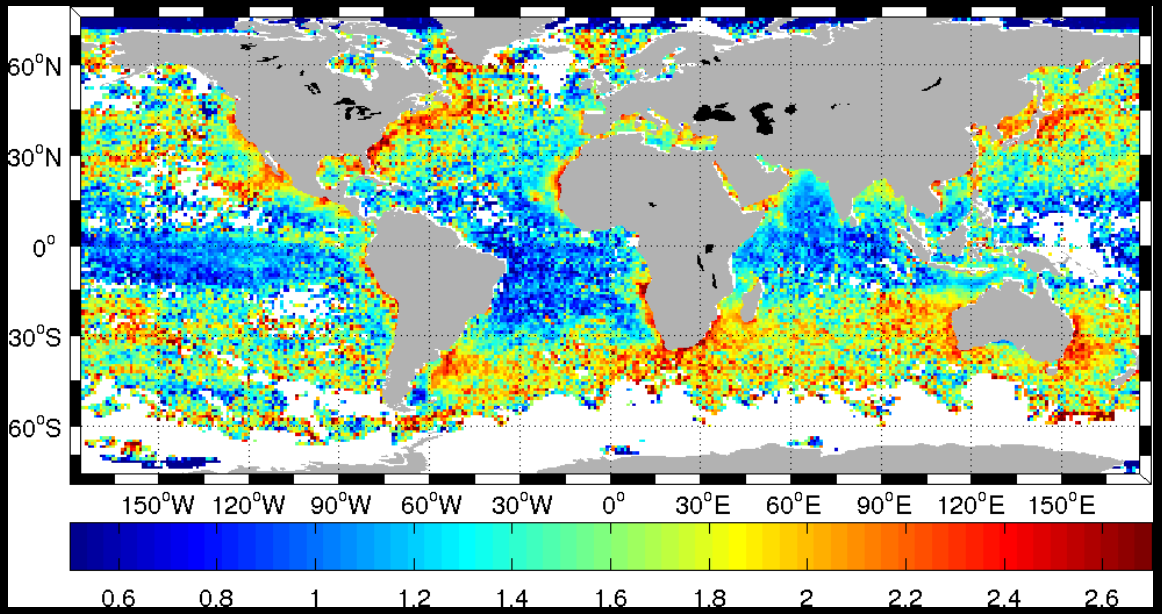

mid 2006-2007 wavenumber spectral slopes mean at 1° x1° resolution in the 10-80 km wavelength band calculated from MODIS SST data (~1 km resolution). 2D-Spectra computed over 1.28° x1.28° area with high coverage (>95%)

Eulerian Statistical Descriptors

Winding
angle statistics, statistical properties
of turbulent fields : e.g., Bernard et al. (2006)
Use of SLE analysis

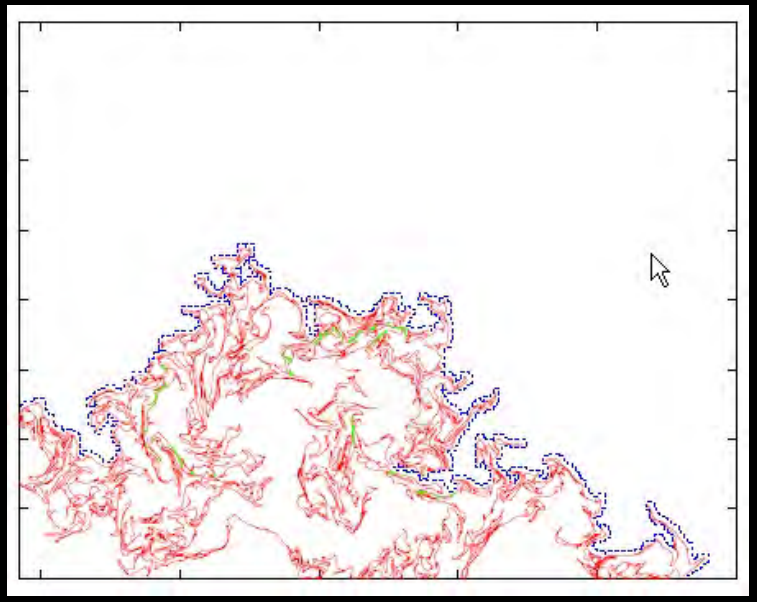

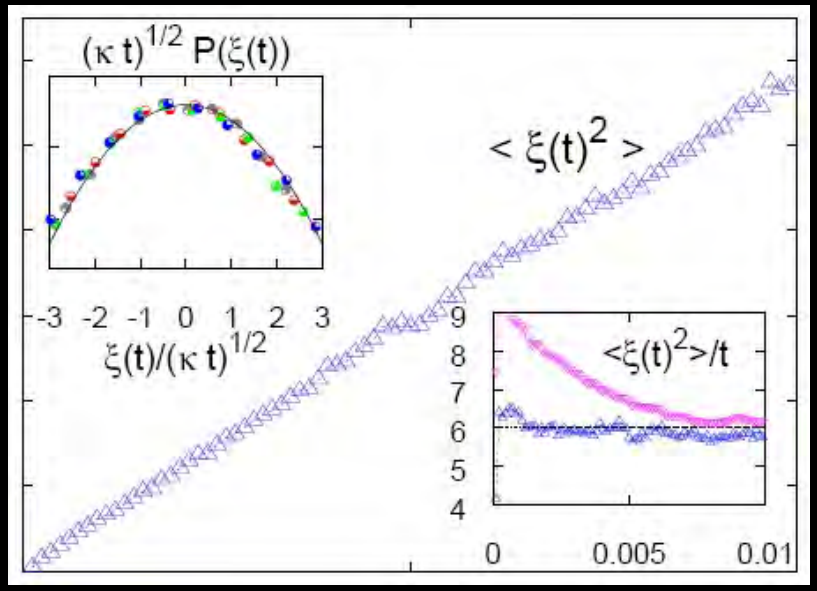

Characterizing the submesoscale - Level set analysis

Winding angle statistics

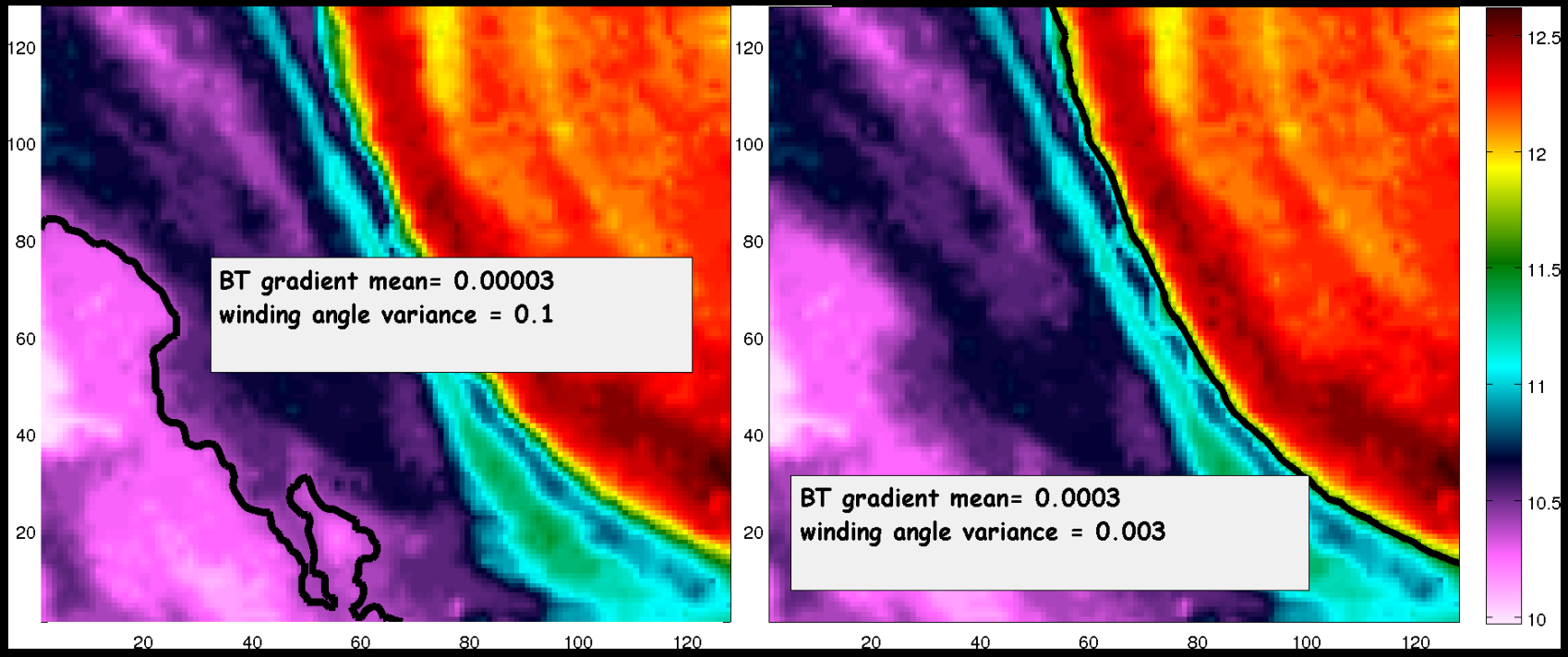

Winding angle histogram

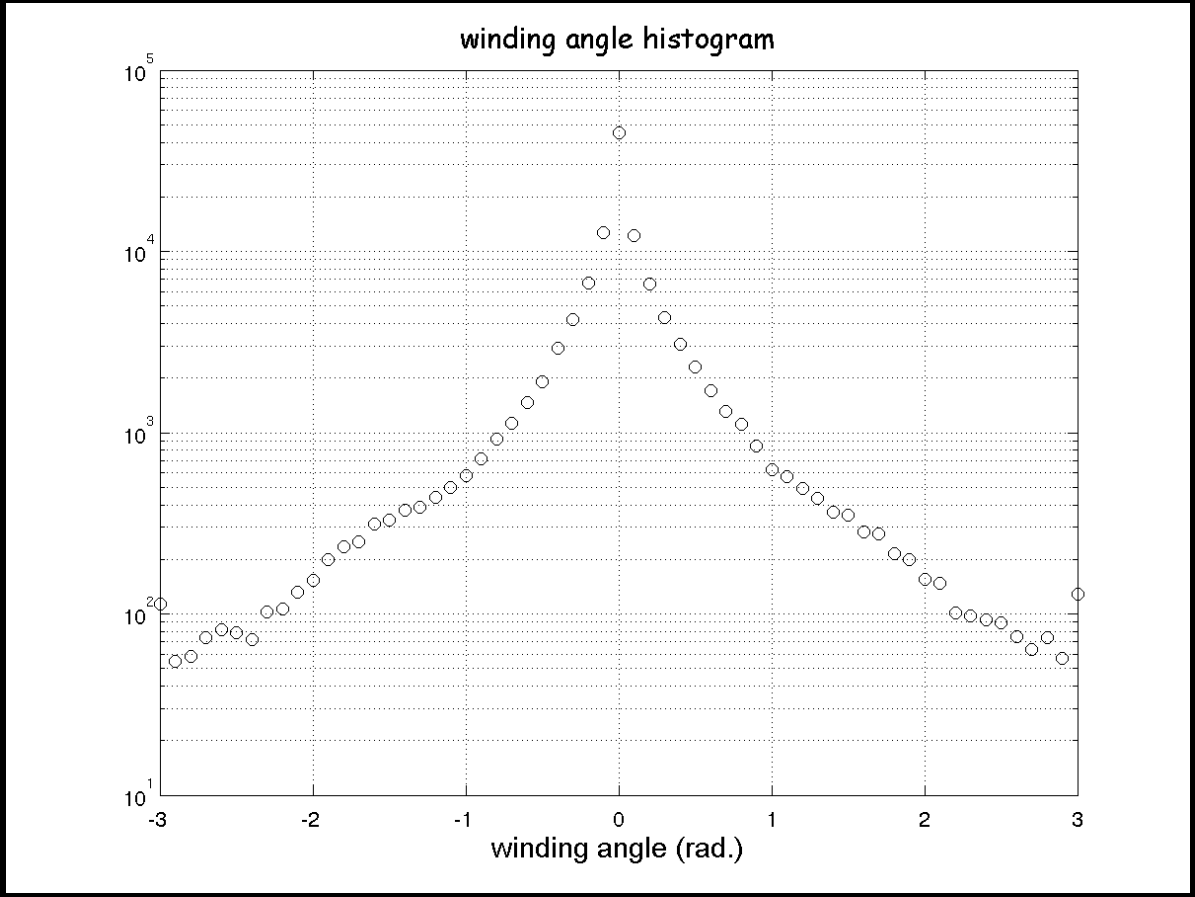

Characterizing the submesoscale - Level set analysis

BT from Metop - 21/12/2010

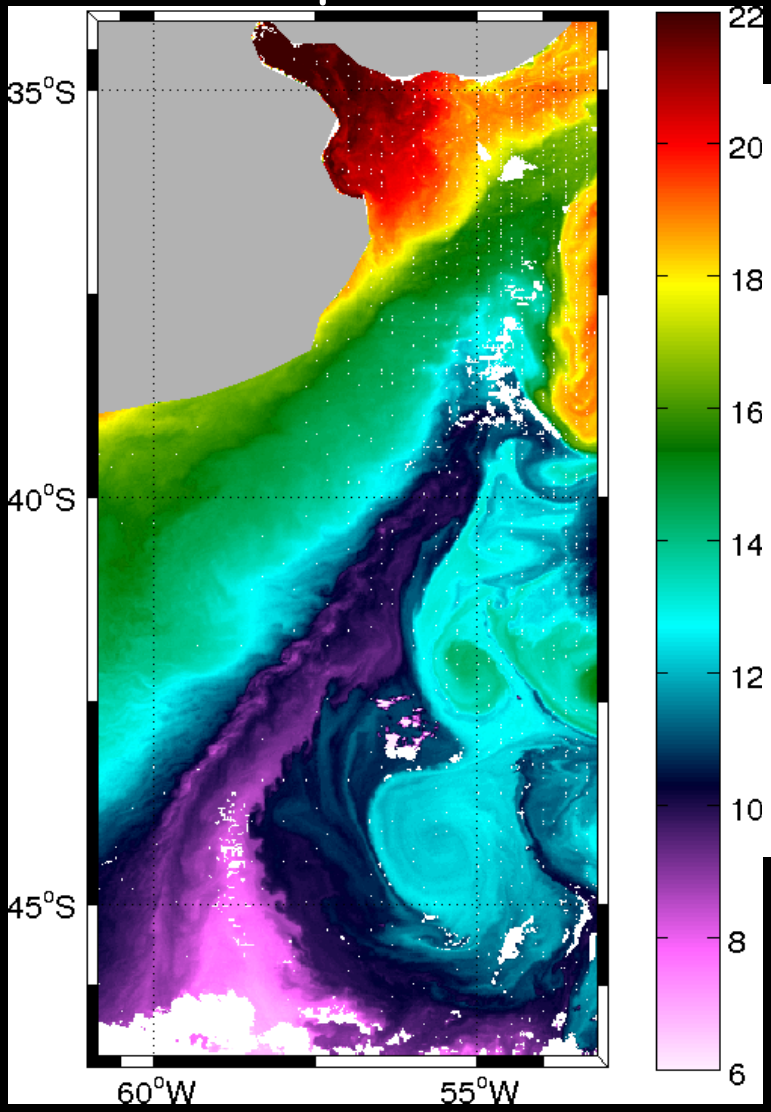

Winding angle variance vs gradient valu

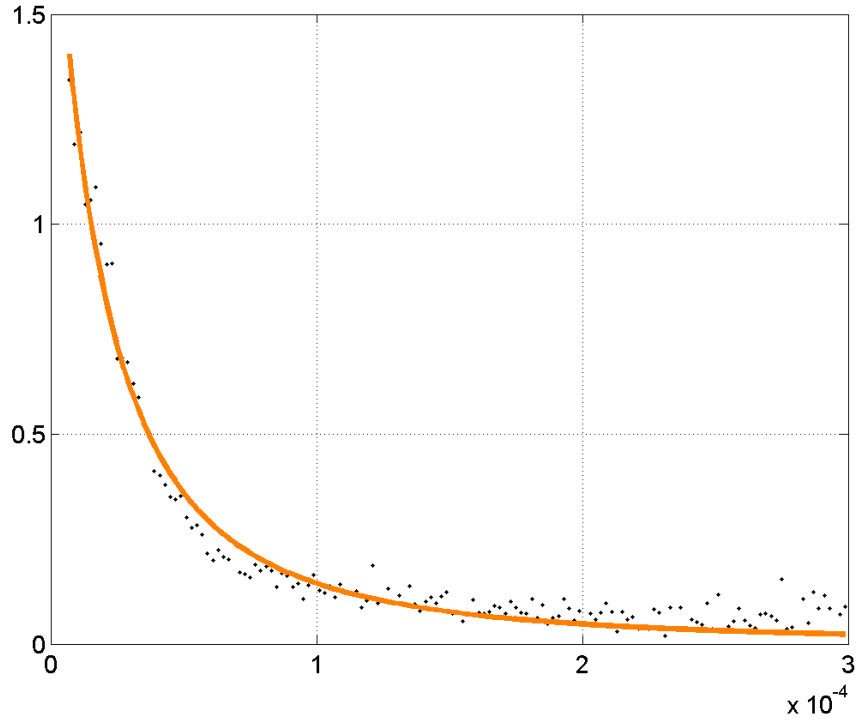

contour (winding angle) characterization

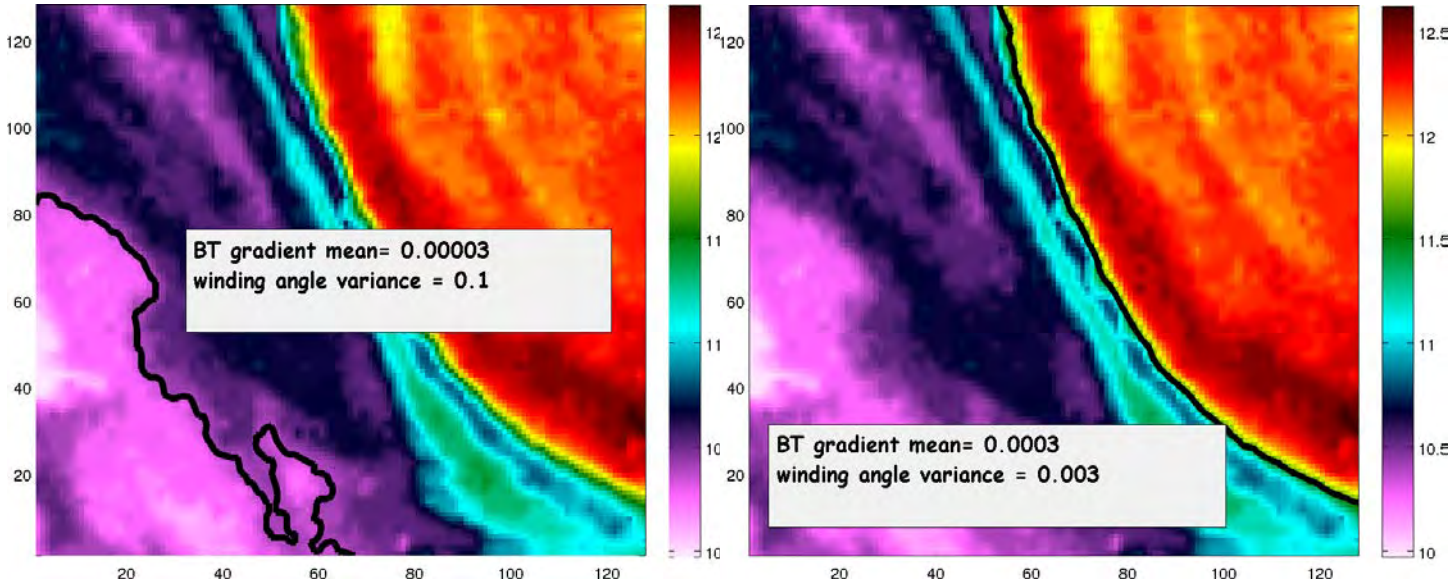

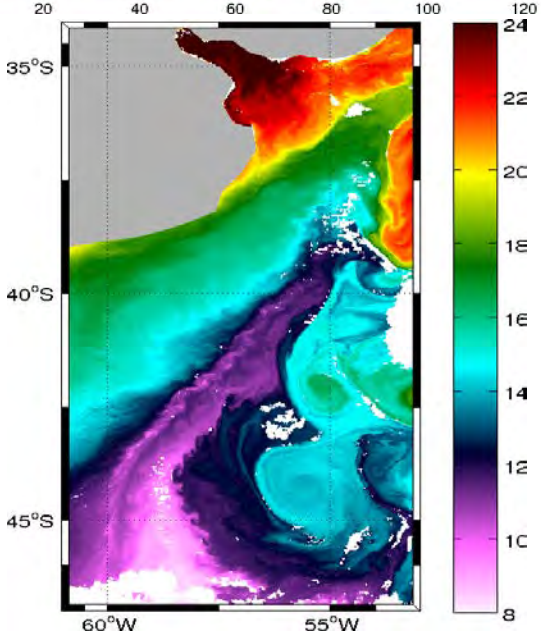

$$\frac{D}{Dt}\left(\kappa|\nabla^{\perp}\theta|\right) = \left(\nabla^{\perp}\theta \cdot \nabla\right) q$$

$$q = \left((\nabla v)\xi\right) \cdot \xi^{\perp}$$

$$\xi = \frac{\nabla^{\perp}\theta}{|\nabla^{\perp}\theta|}$$

Small scales / mesoscale

SST – Modis(L2P)

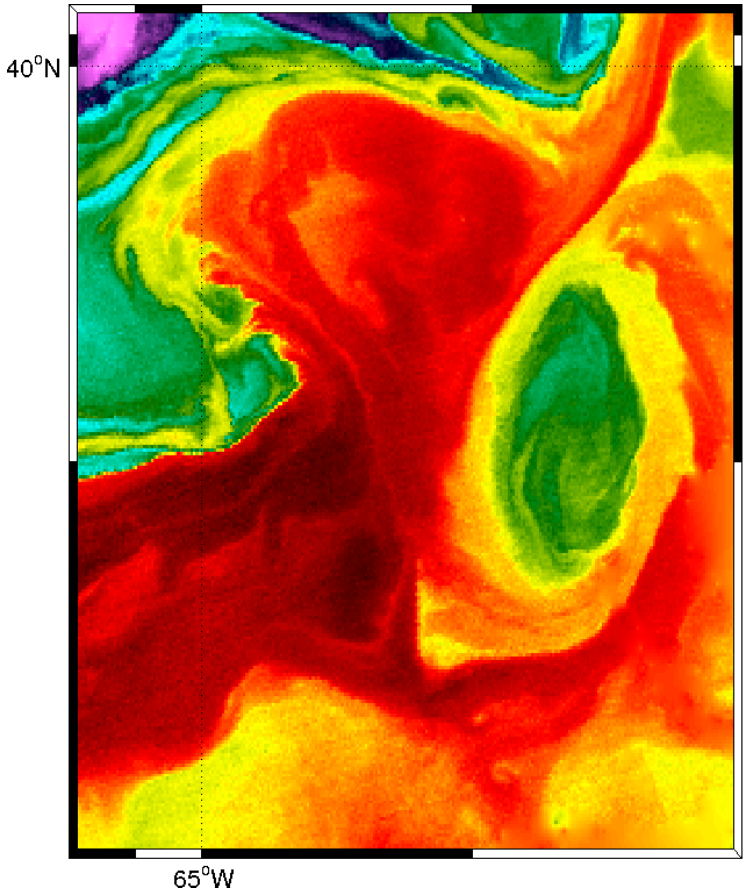

SST – AMSRE(L3)

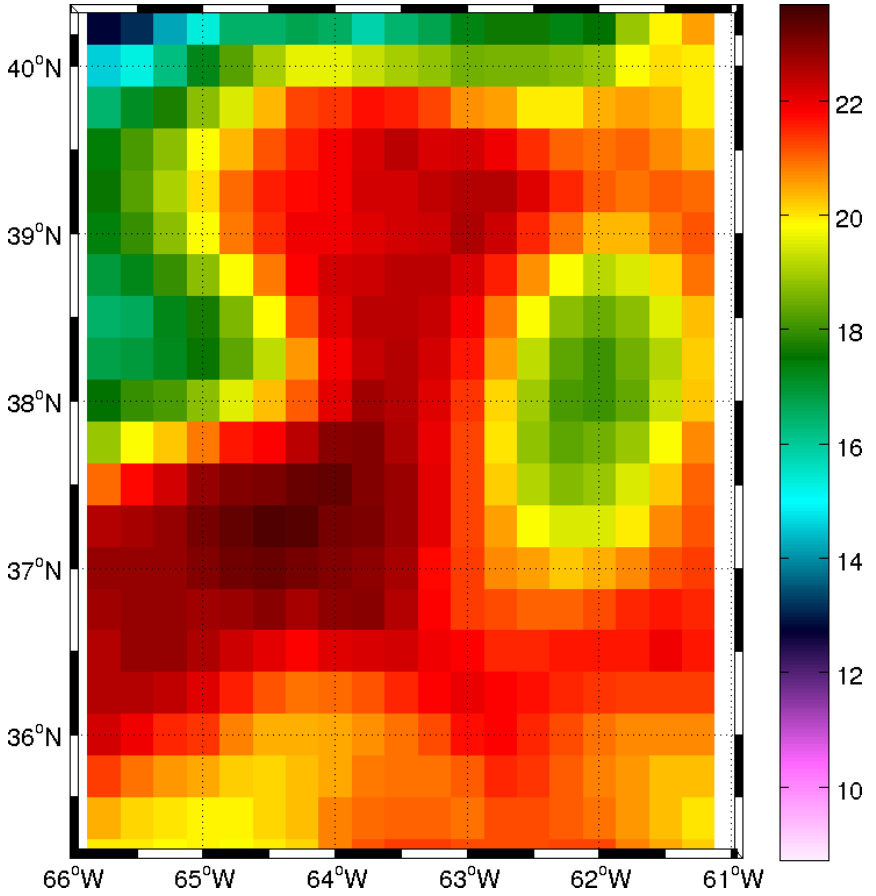

Small scales / mesoscale

SST – Modis(L2P)

SST – AMSRE(L3)

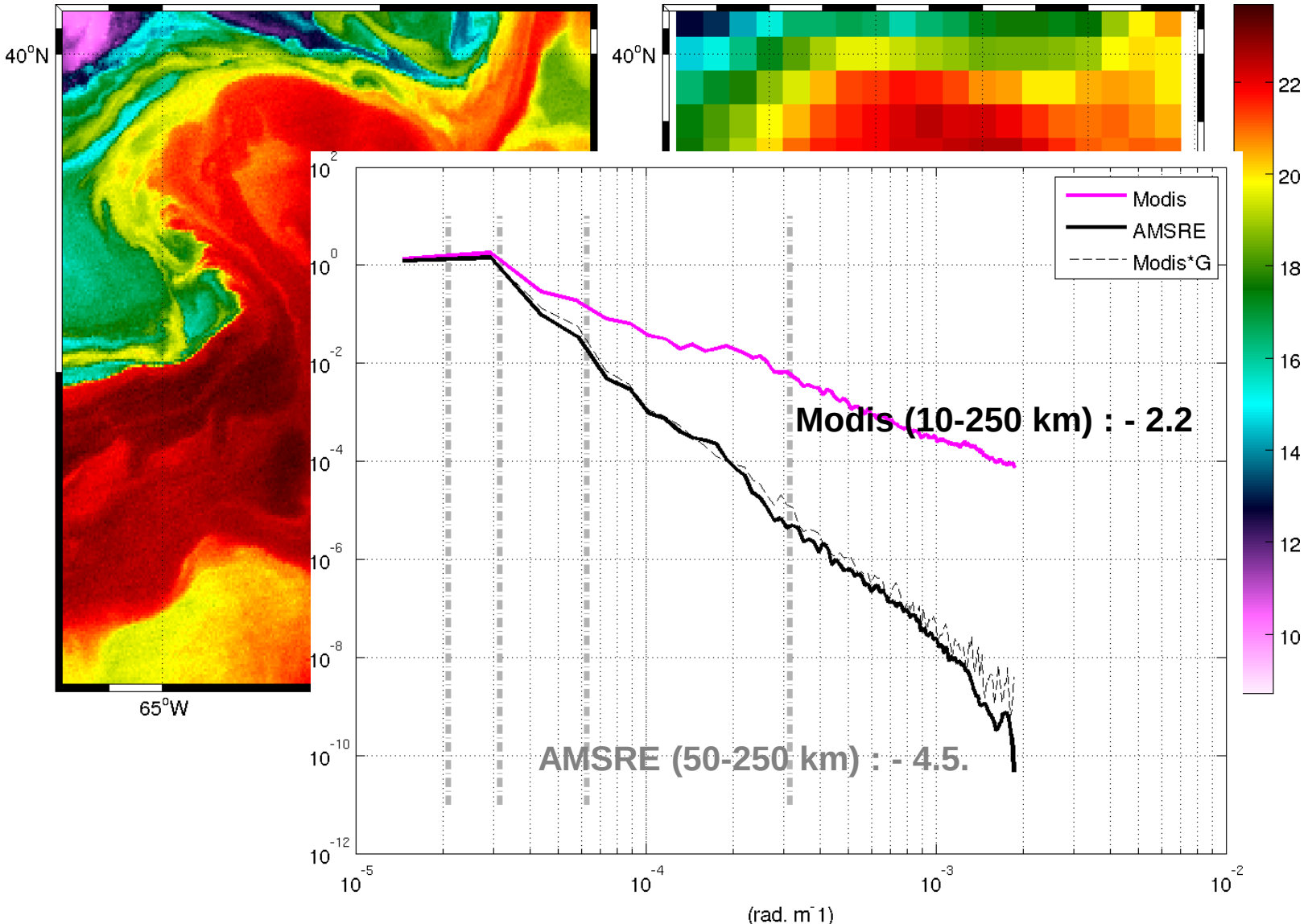

Small scales / mesoscale

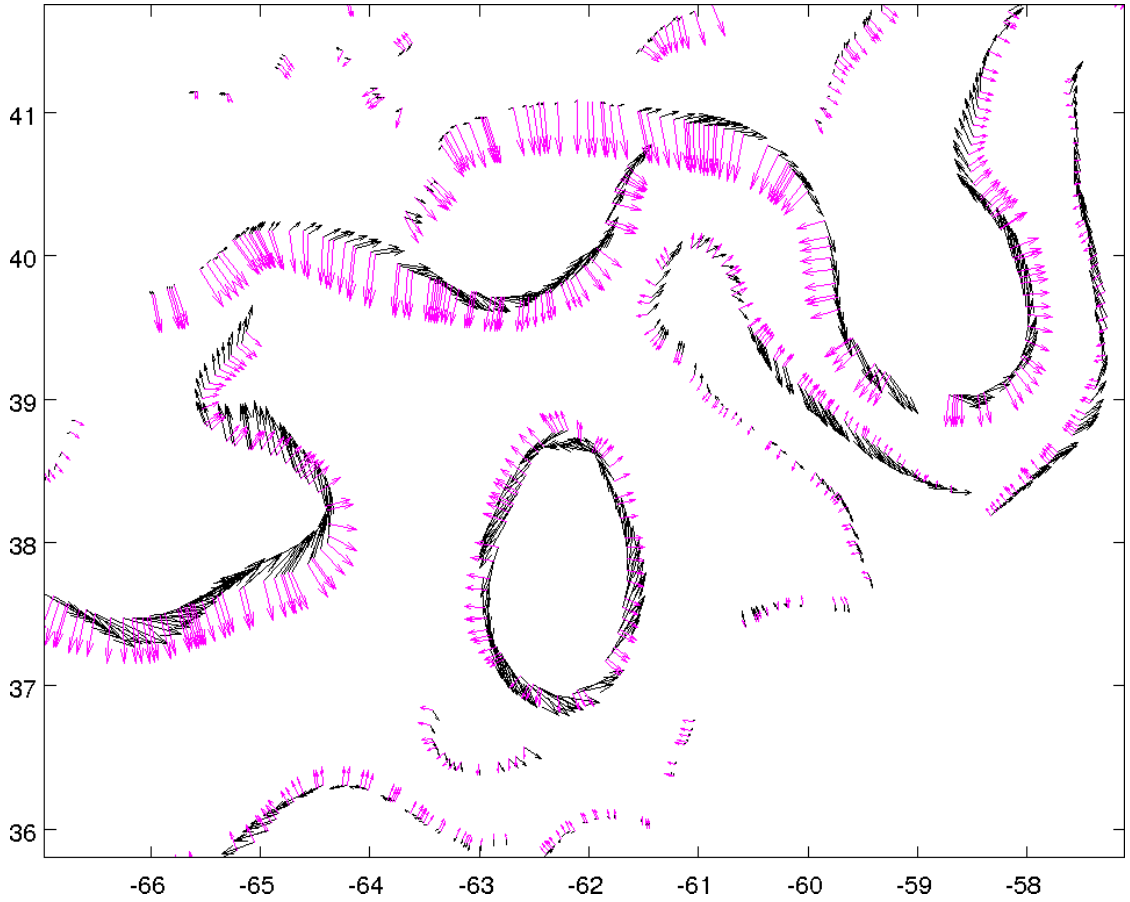

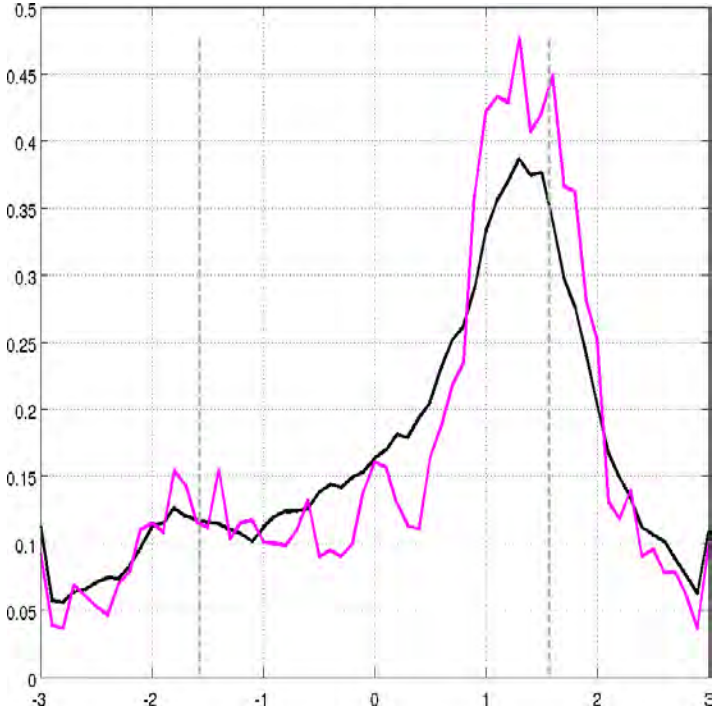

Lagrangian diagnostics: drifter analysis

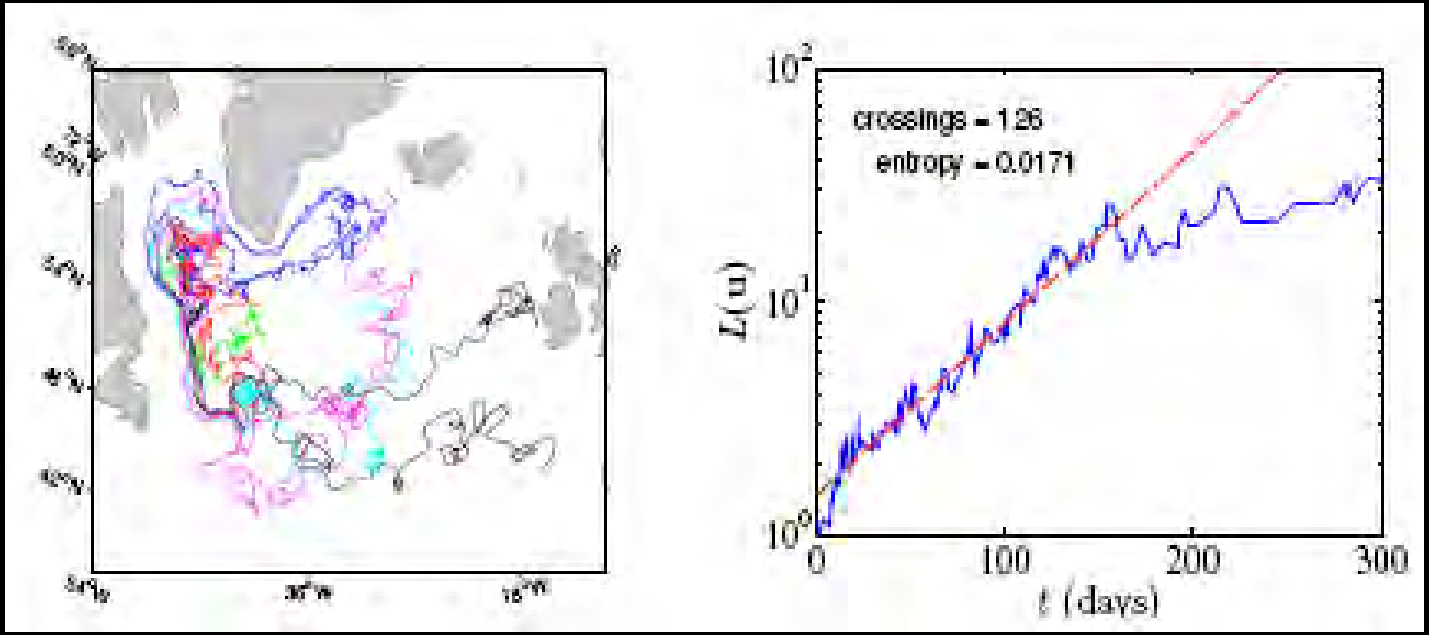

Analysis of drifters trajectories and the topological entropy from the degree of entanglement (Thiffeault, 2010)

$$d\theta(p) = -\gamma\left(\theta(p) - \theta_0(p)\right)dp + \sigma dW(p)$$

Stochastic Geometry-driven super-resolution

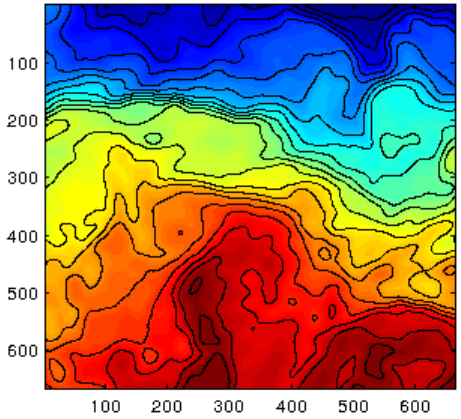

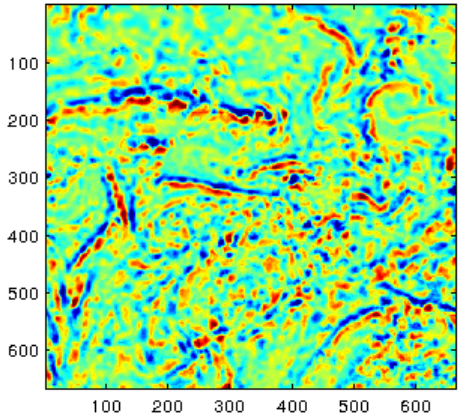

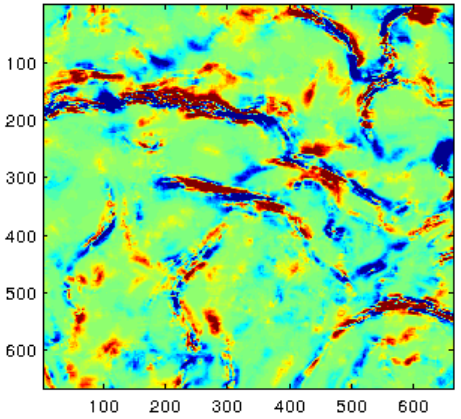

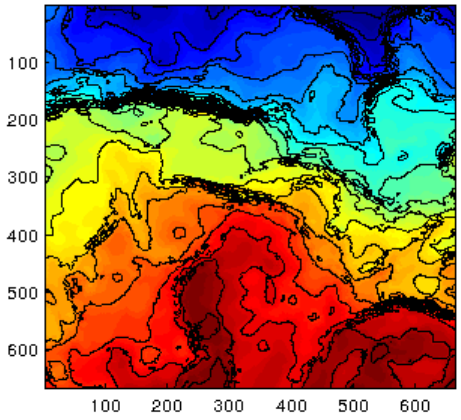

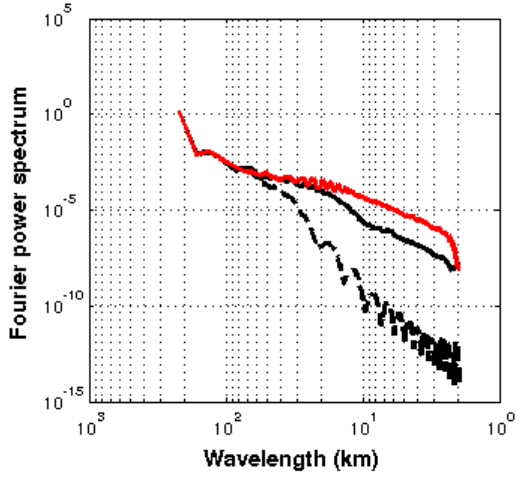

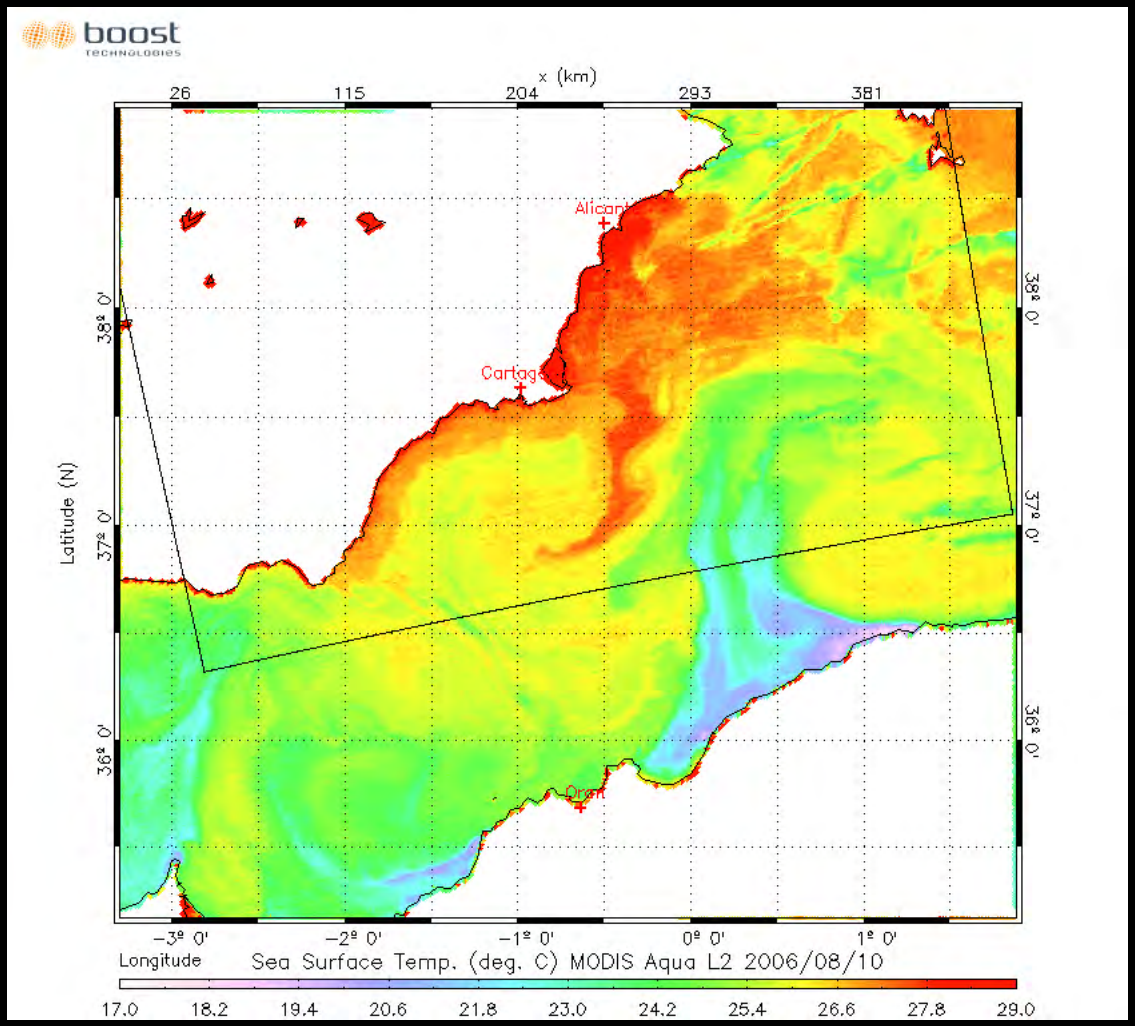

Numerous contemporaneous MODIS Brightness temperature and Ocean Colour surface signatures

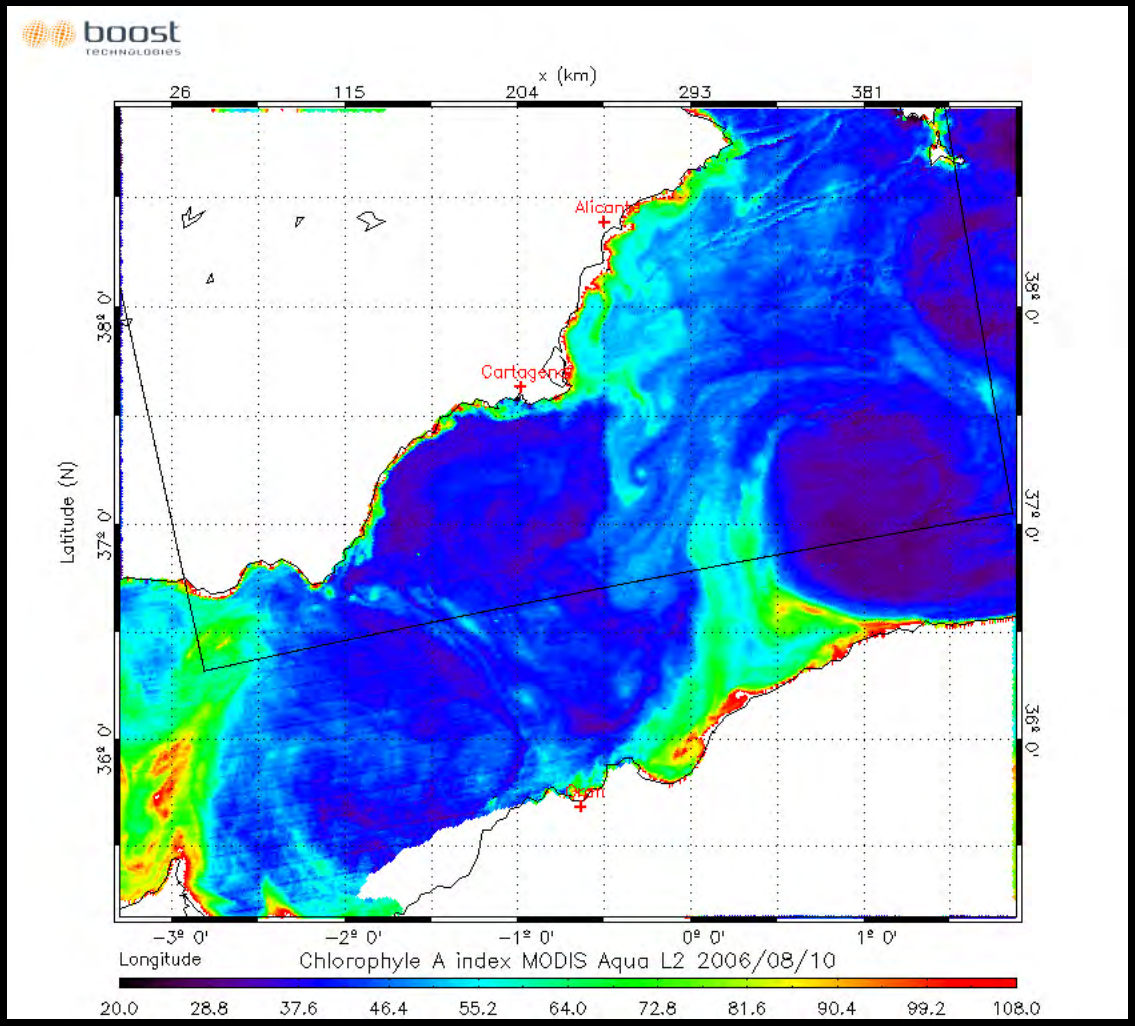

Numerous contemporaneous MODIS Brightness temperature and Ocean Colour surface signatures

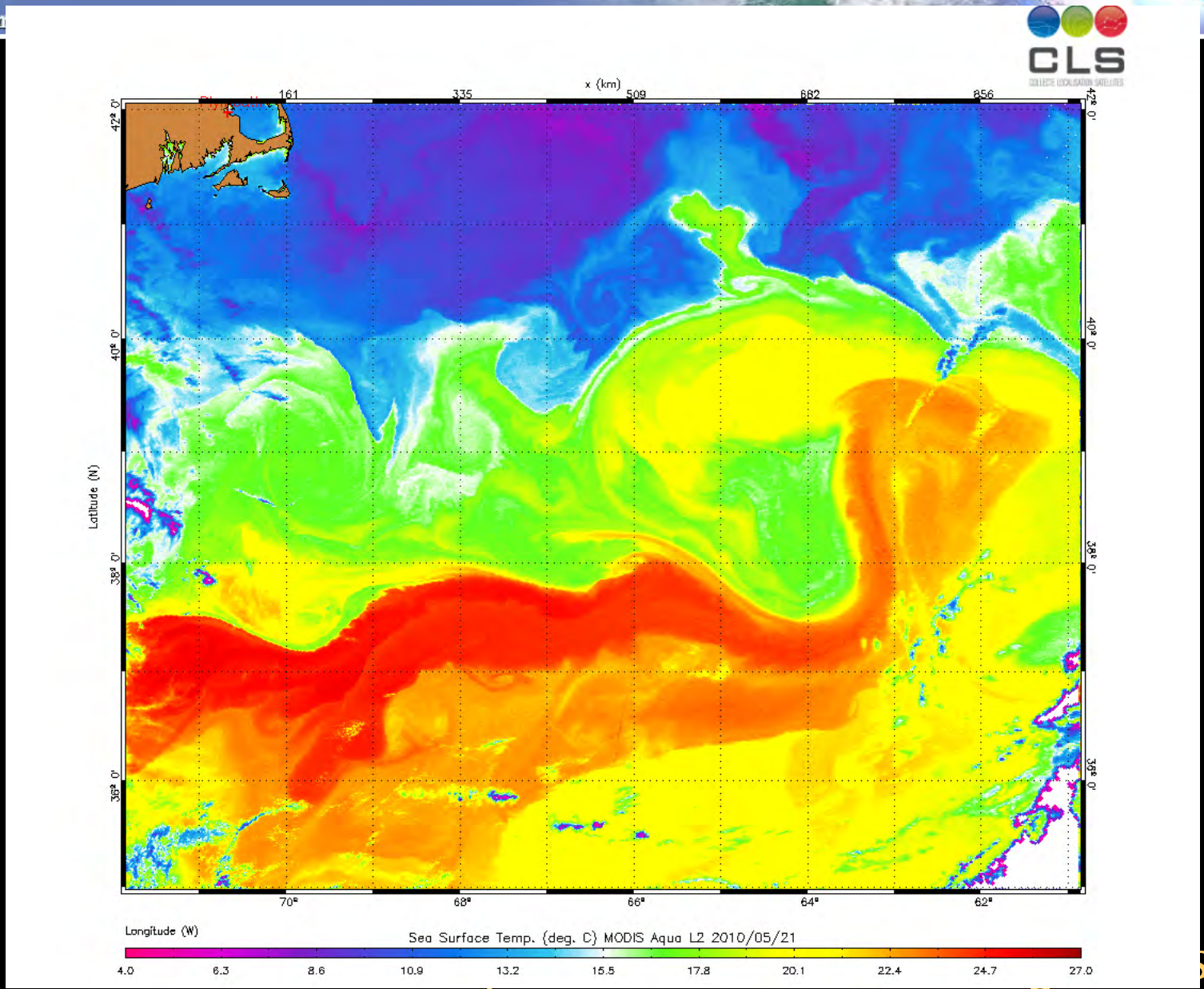

temperature and Ocean Colour surface signatures

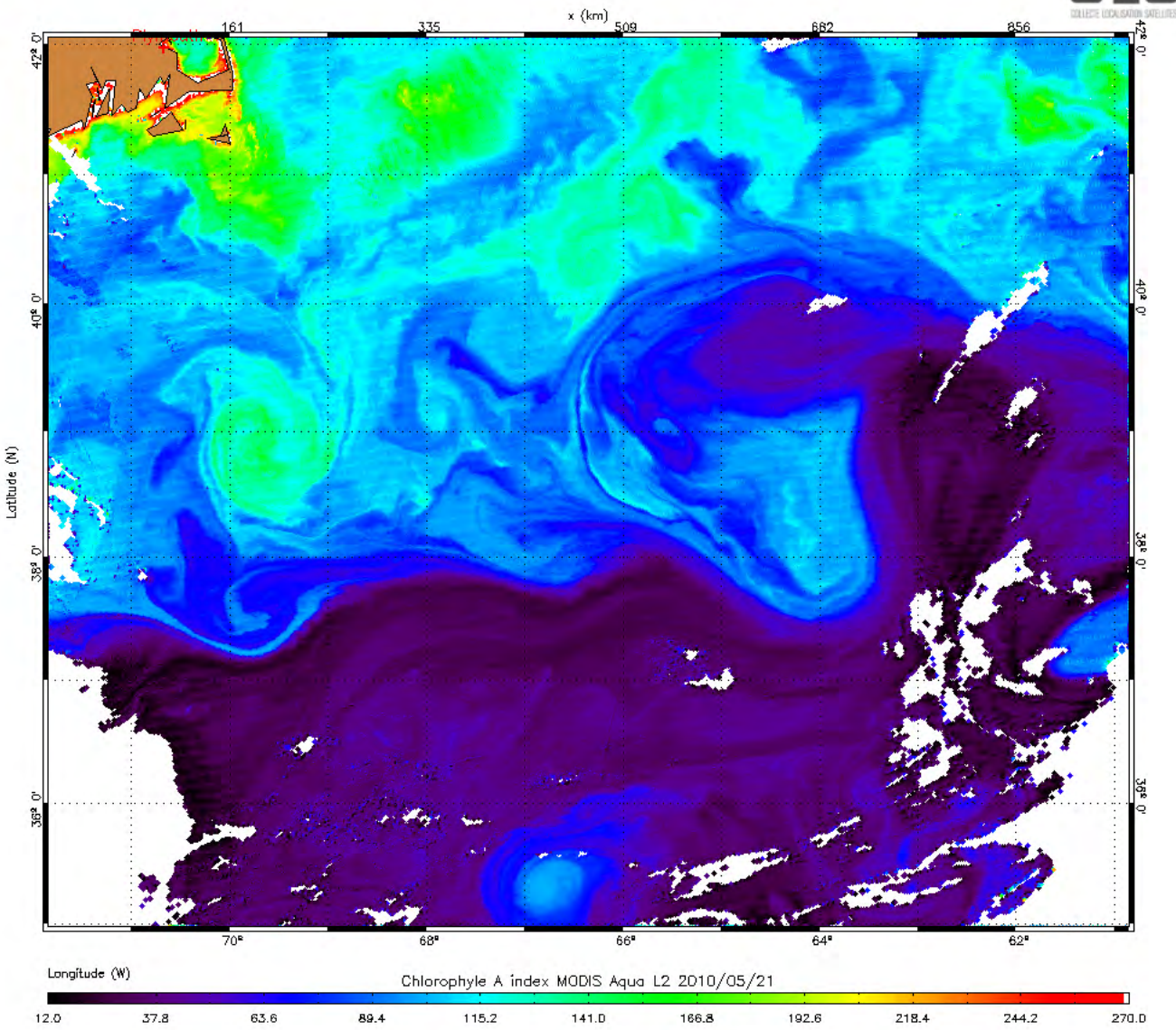

temperature and Ocean Colour surface signatures

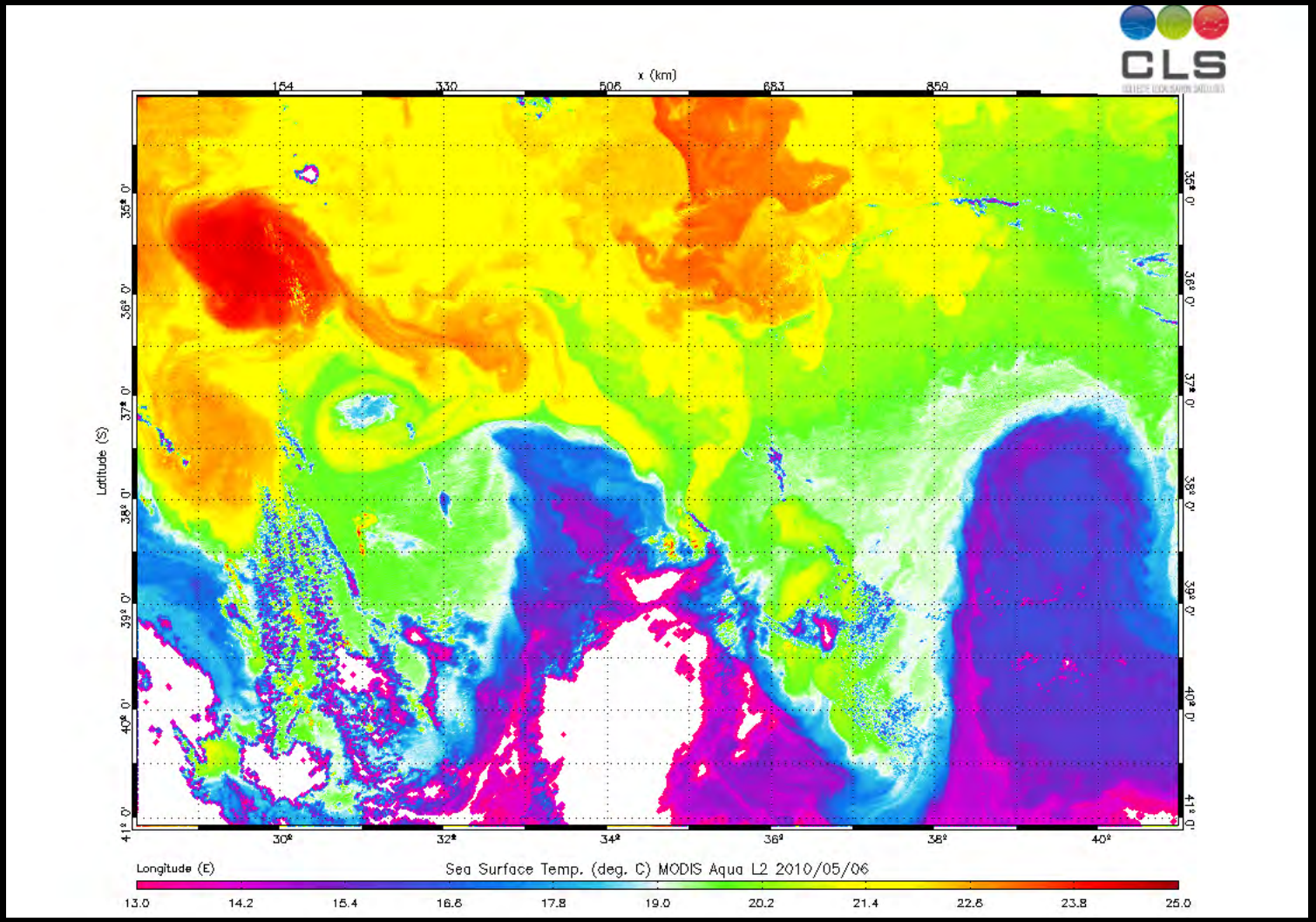

Numerous contemporaneous MODIS Brightness temperature and Ocean Colour surface signatures

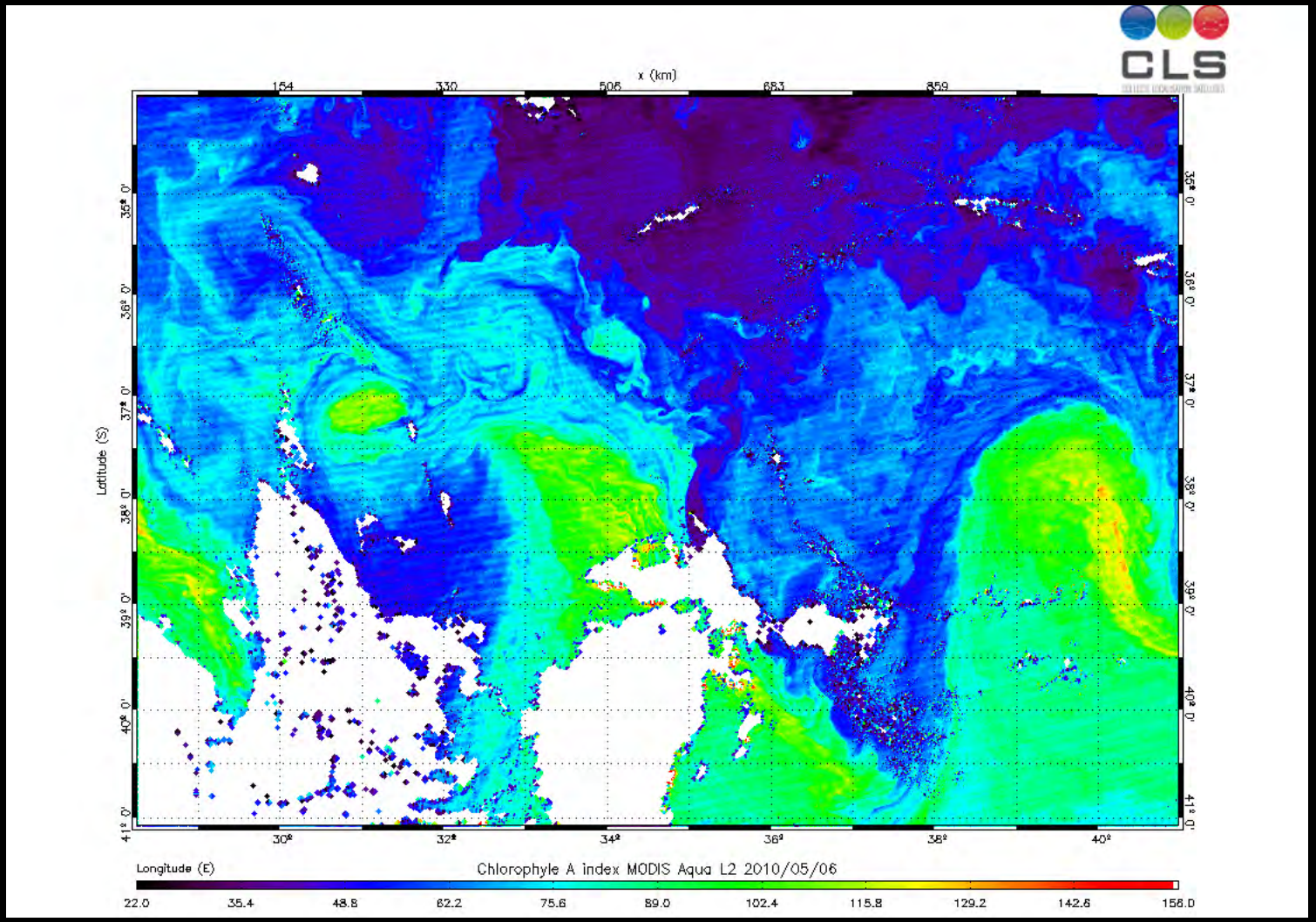

Numerous contemporaneous MODIS Brightness temperature and Ocean Colour surface signatures

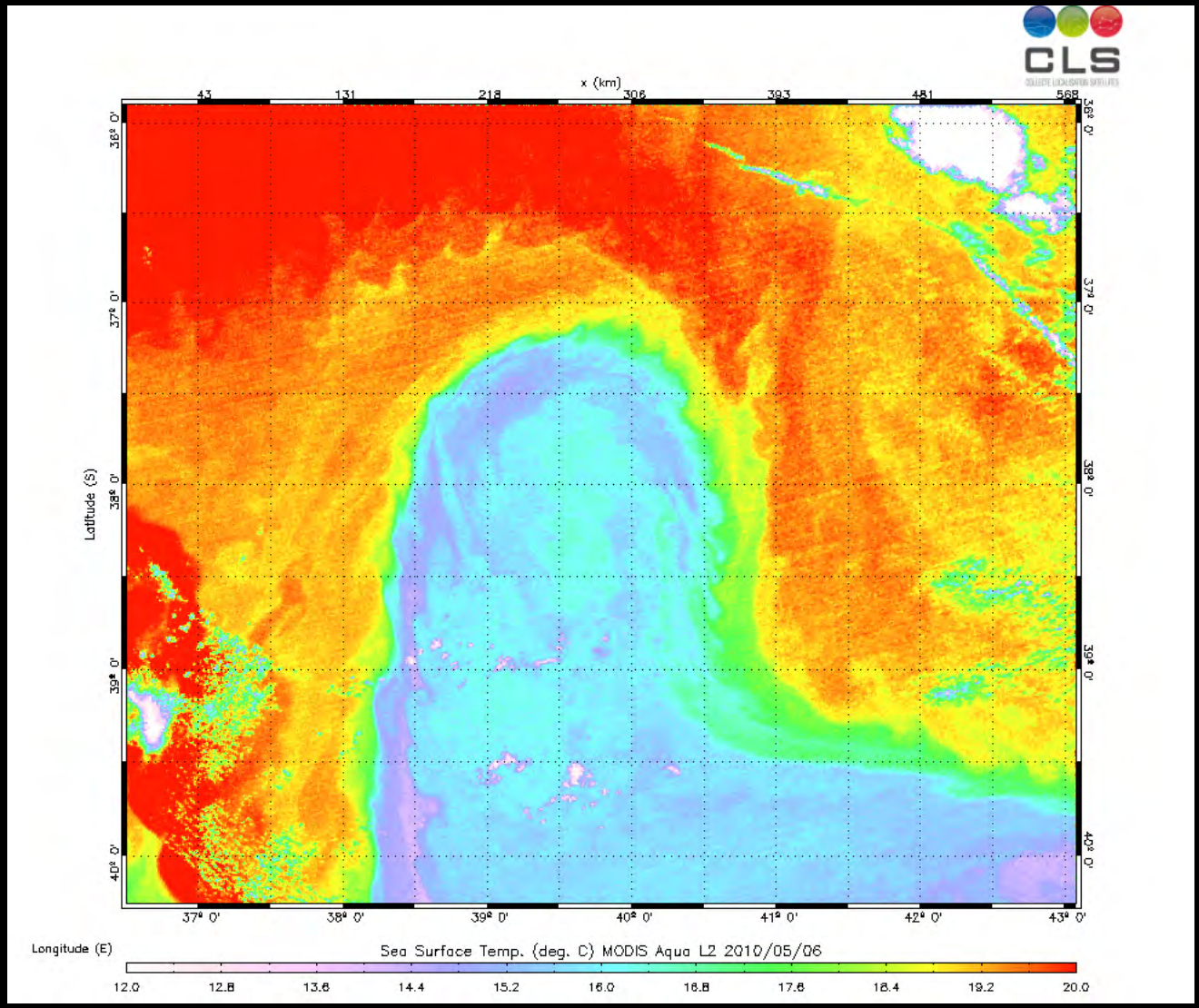
x (km)
43
131
218
306
393
481
568
Latitude (S)
36° 0'
37° 0'
38° 0'
39° 0'
40° 0'
37° 0'
38° 0'
39° 0'
40° 0'
41° 0'
42° 0'
43° 0'
Longitude (E)
Sea Surface Temp. (deg. C) MODIS Aqua L2 2010/05/06
12.0
12.8
13.6
14.4
15.2
16.0
16.8
17.6
18.4
19.2
20.0

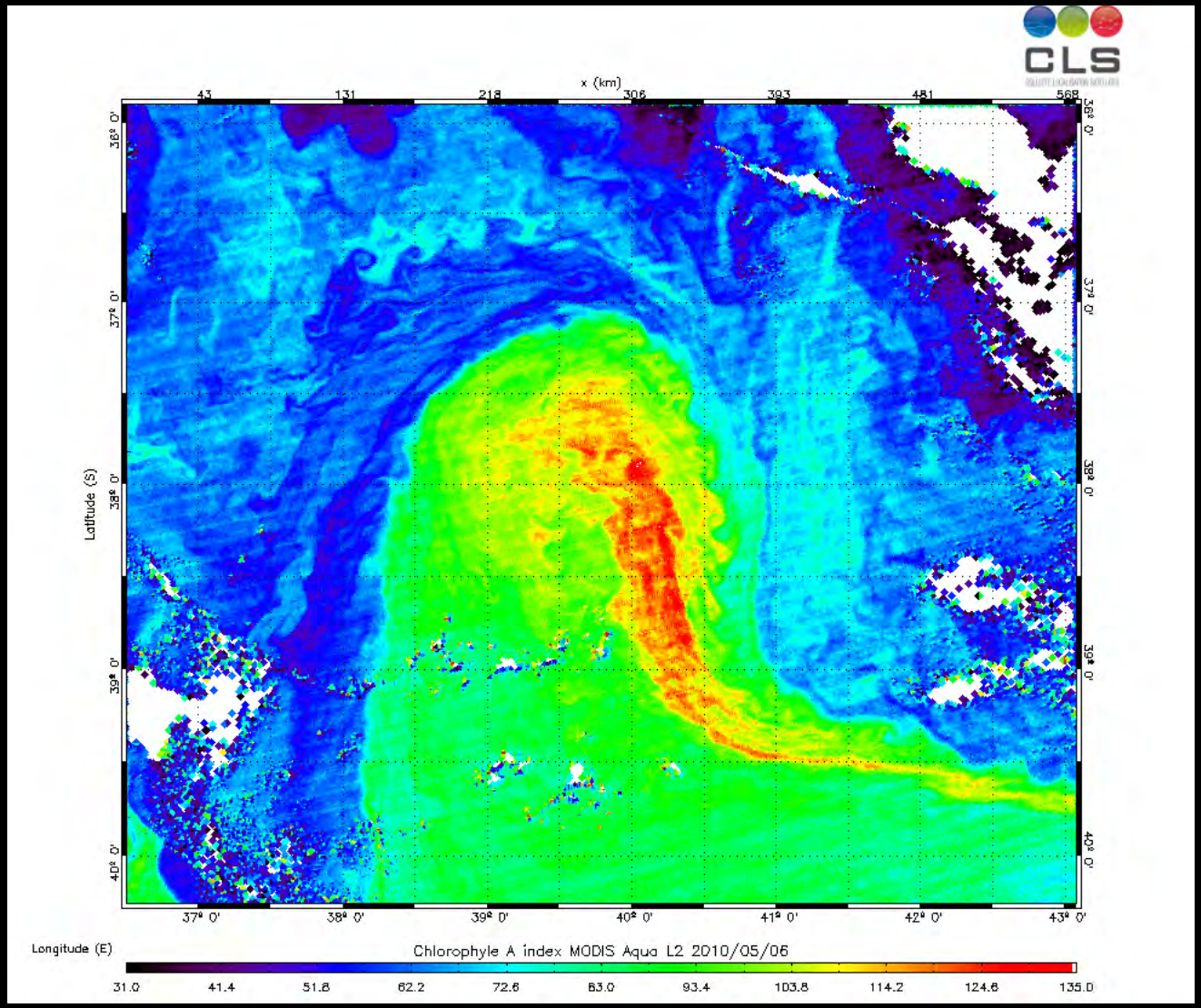
x (km)
43
131
218
306
393
481
568
Latitude (S)
36° 0'
37° 0'
38° 0'
39° 0'
40° 0'
37° 0'
38° 0'
39° 0'
40° 0'
41° 0'
42° 0'
43° 0'
Longitude (E)
Chlorophyle A index MODIS Aqua L2 2010/05/06
31.0
41.4
51.8
62.2
72.6
83.0
93.4
103.8
114.2
124.6
135.0

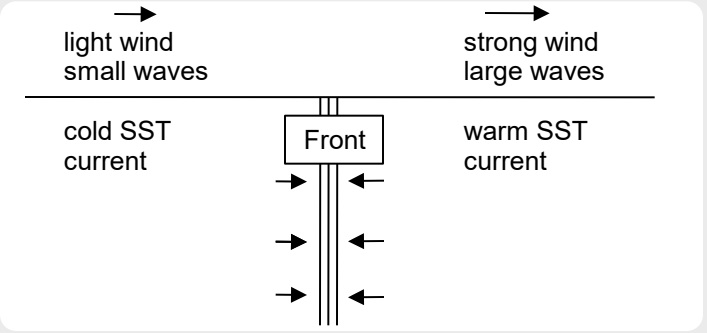

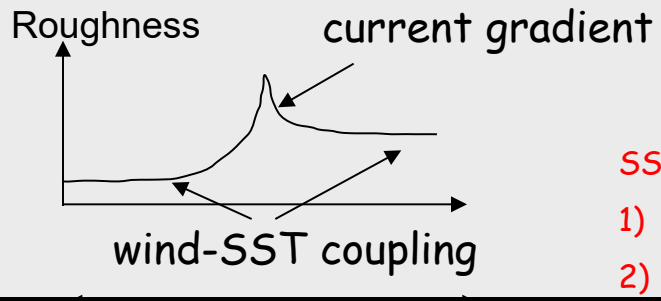

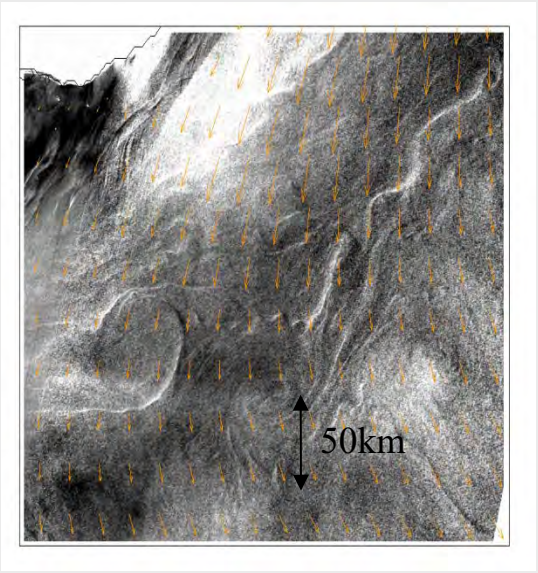

SST fronts and roughness gradients collocated

1) scales 10-50 km SST/wind coupling

2) scales 2-10 km wave/current coupling

Essentially related to the surface slope (mean square slope MSS) of short waves (roughly 1-10 cm)
Those waves are related to local wind and **current** (and surfactants)

Only 2 over 4 types of current deformations will sign on the roughness image.

$$\begin{bmatrix} \frac{\partial u}{\partial x} & \frac{\partial u}{\partial y} \\ \frac{\partial v}{\partial x} & \frac{\partial v}{\partial y} \end{bmatrix} = \frac{1}{2}\begin{bmatrix} D+S_t & -R+S_h \\ R+S_h & D-S_t \end{bmatrix}$$

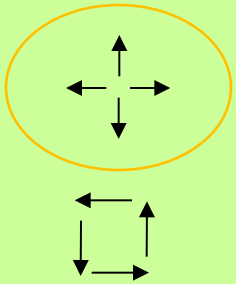

$$D = \frac{\partial u}{\partial x} + \frac{\partial v}{\partial y},\ S_t = \frac{\partial u}{\partial x} - \frac{\partial v}{\partial y},$$
$$R = \frac{\partial v}{\partial x} - \frac{\partial u}{\partial y},\ S_h = \frac{\partial v}{\partial x} + \frac{\partial u}{\partial y}.$$

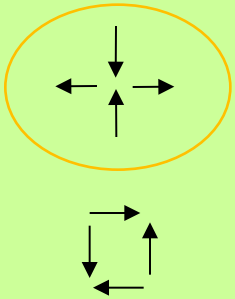

Which type of currents will sign?

- rotational currents
- **divergent currents**
- shear in the wind direction
- **strain in the wind direction**

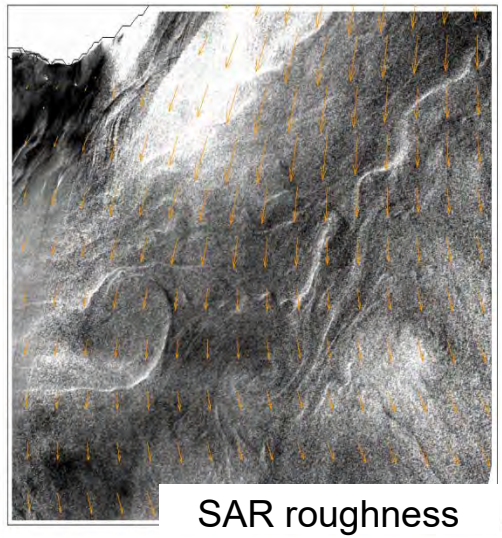

SAR roughness

- Divergent currents appear independently of the wind direction
- Non divergent currents appear with a 45°-sensitivity to the wind/current angle.

Sea Surface Roughness contrasts

Sea Surface Roughness

$$\frac{\partial N(\mathbf{k})}{\partial t} + \left(c_{gi} + u_i\right)\frac{\partial N(\mathbf{k})}{\partial x_i} - k_j \frac{\partial u_j}{\partial x_i}\frac{\partial N(\mathbf{k})}{\partial k_i} = Q(\mathbf{k})/\omega$$

$$Q(\mathbf{k}) = \beta_\nu(\mathbf{k})\omega E(\mathbf{k}) - D(\mathbf{k}) - Q^{nl}(\mathbf{k}) + Q^{wb}(\mathbf{k})$$

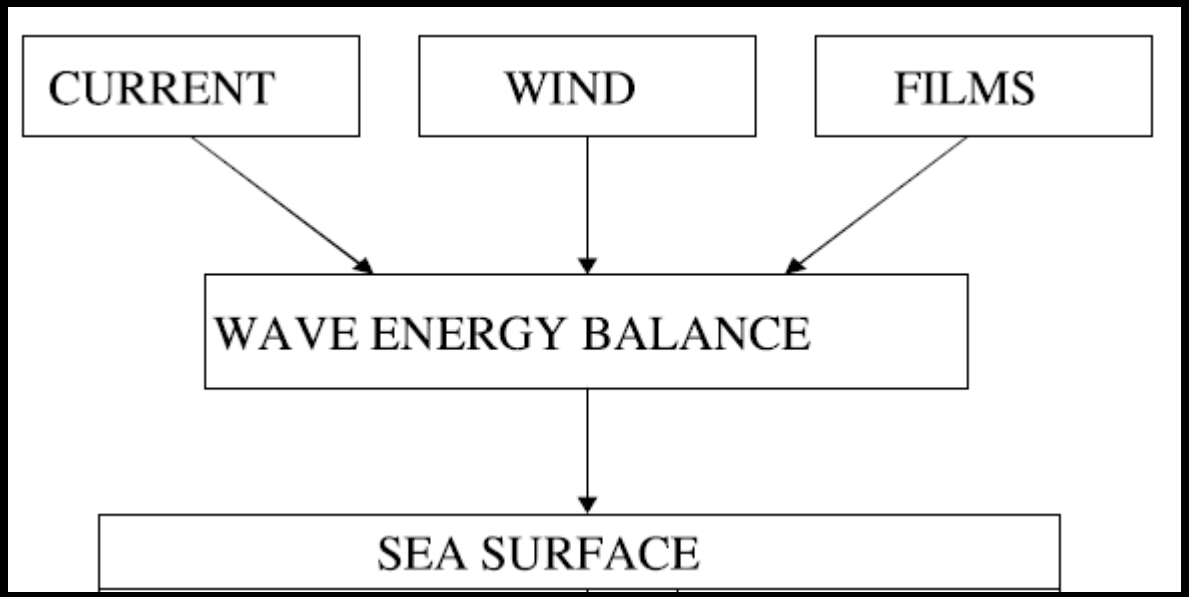

$$\partial\tilde{N}(\mathbf{k})/\partial t + c_{gi}\partial\tilde{N}(\mathbf{k})/\partial x_i = \omega^2 k^{-5}\left[\omega^{-1} m_k^{ij} u_{i,j} B_0 - \tilde{B}/\tau + \tilde{\beta} B_0 + \tilde{I}_{sw}\right]$$

$$m_k^{ij} = k_j \partial \ln \tilde{N}_0 / \partial k_i$$

Radar and Optical Imaging Model (RIM and OIM)

Kudryavtsev et al., 2005; Johannessen et al., 2005, Kudryavtsev et al., 2012

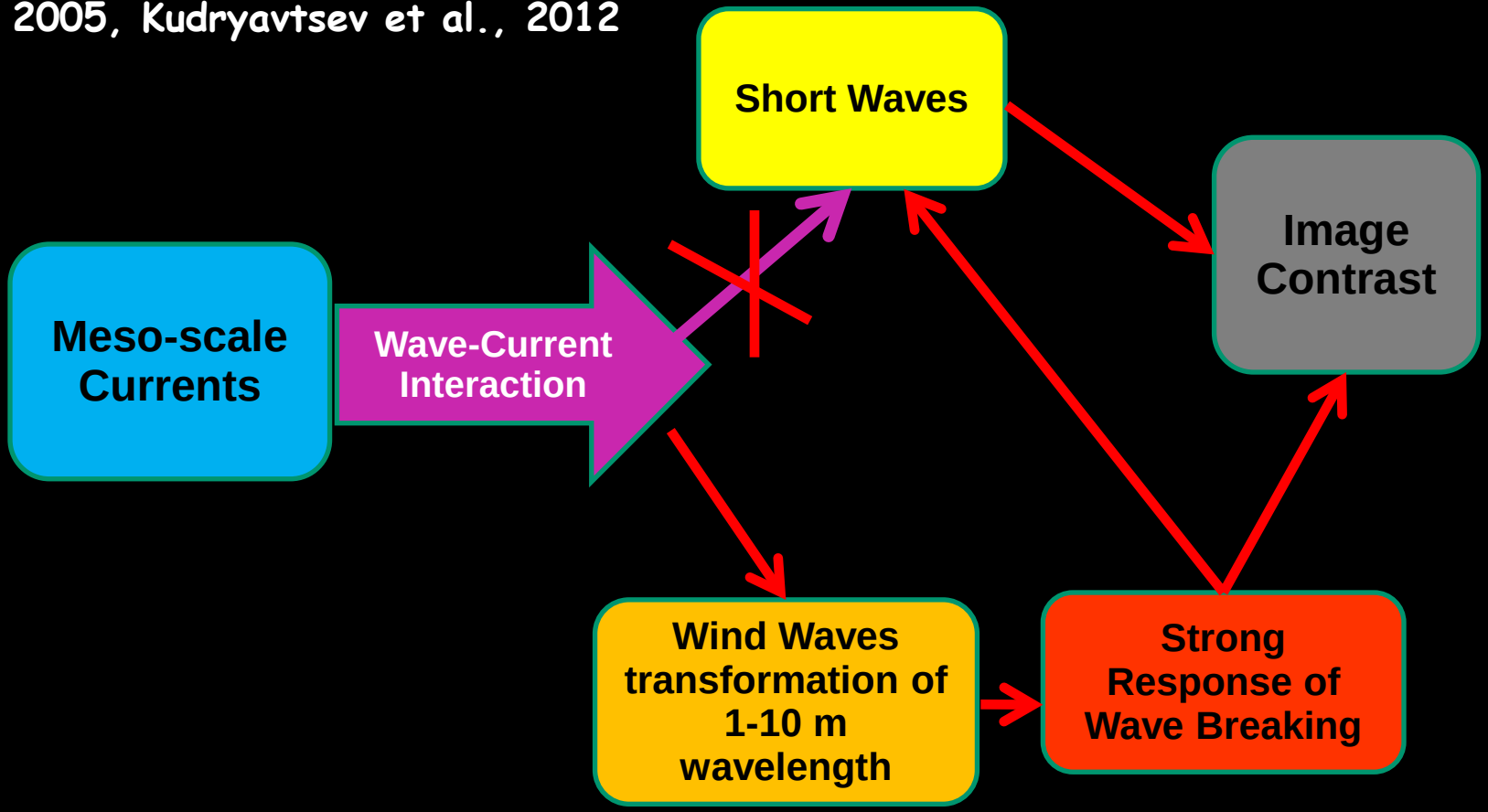

Application to high resolution data

- MODIS Brightness temperature and colour

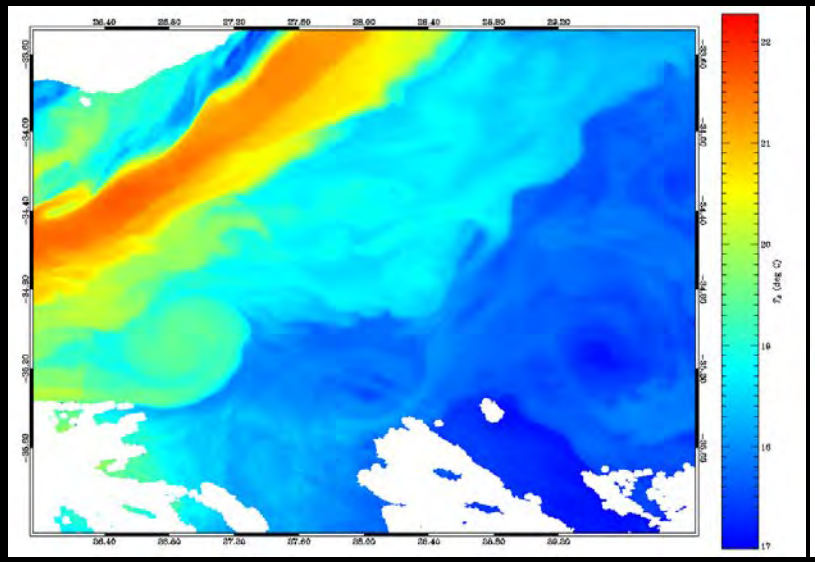

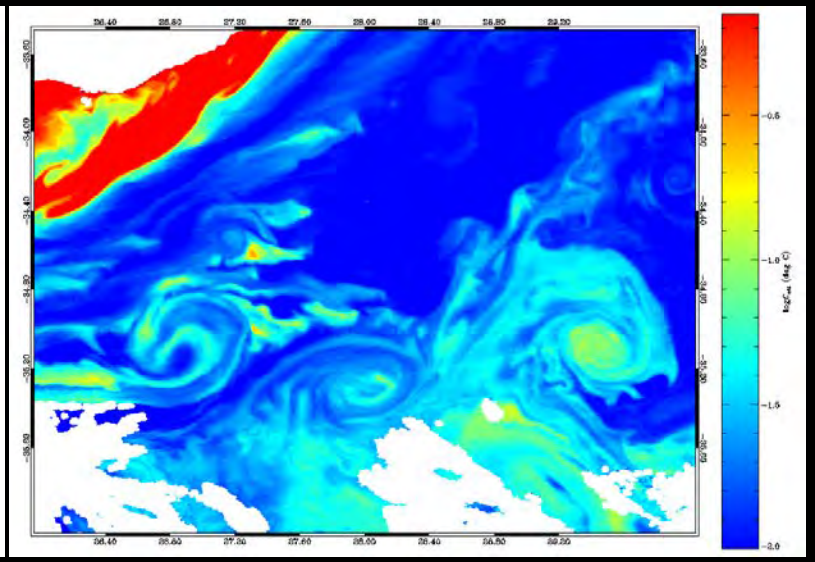

Application to high resolution data

- MODIS Brightness temperature SQG-derived vorticity $(\hat{\zeta}_{es} \propto k\hat{\rho}_s)$ and colour

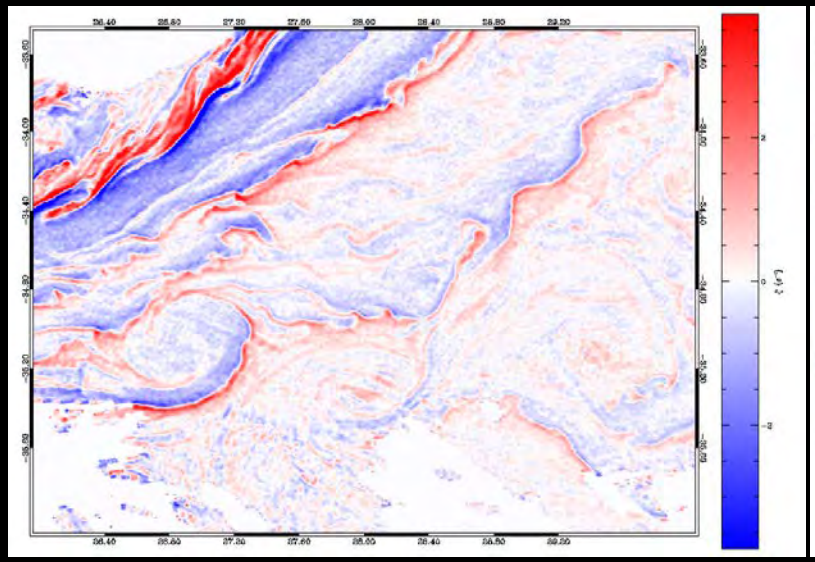

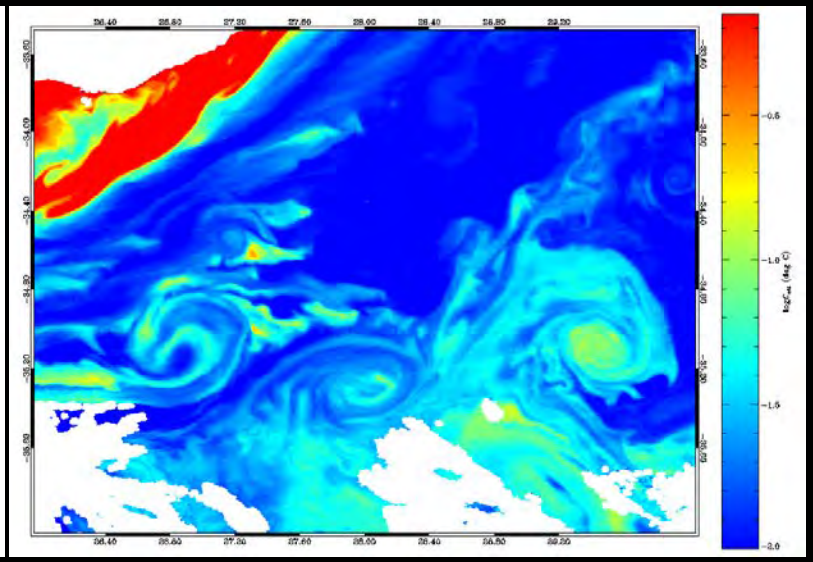

Application to high resolution data

- MODIS Brightness temperature SQG-derived vorticity $(\hat{\zeta}_{es} \propto k\hat{\rho}_s)$ and ENVISAT radar roughness variations

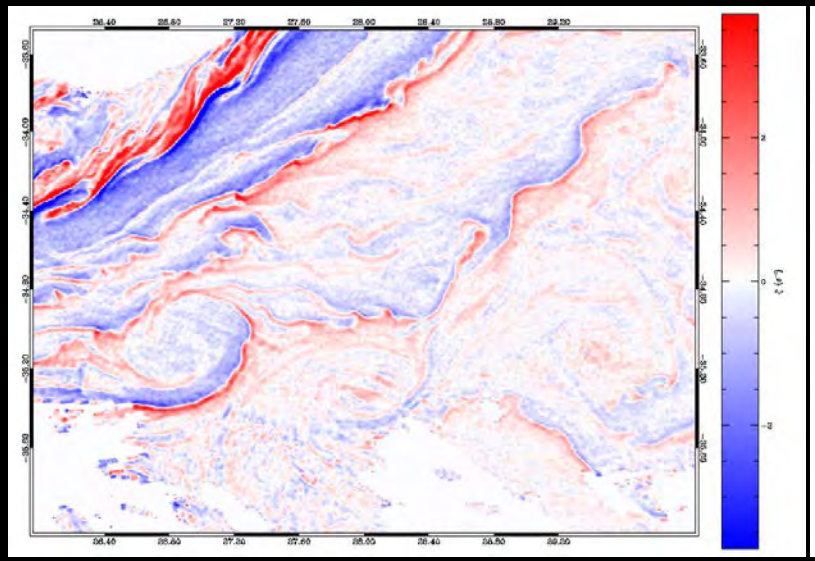

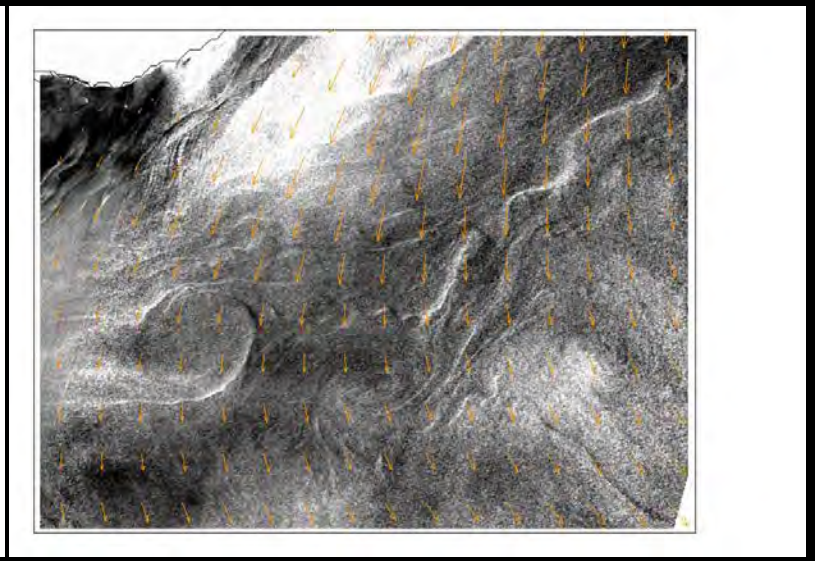

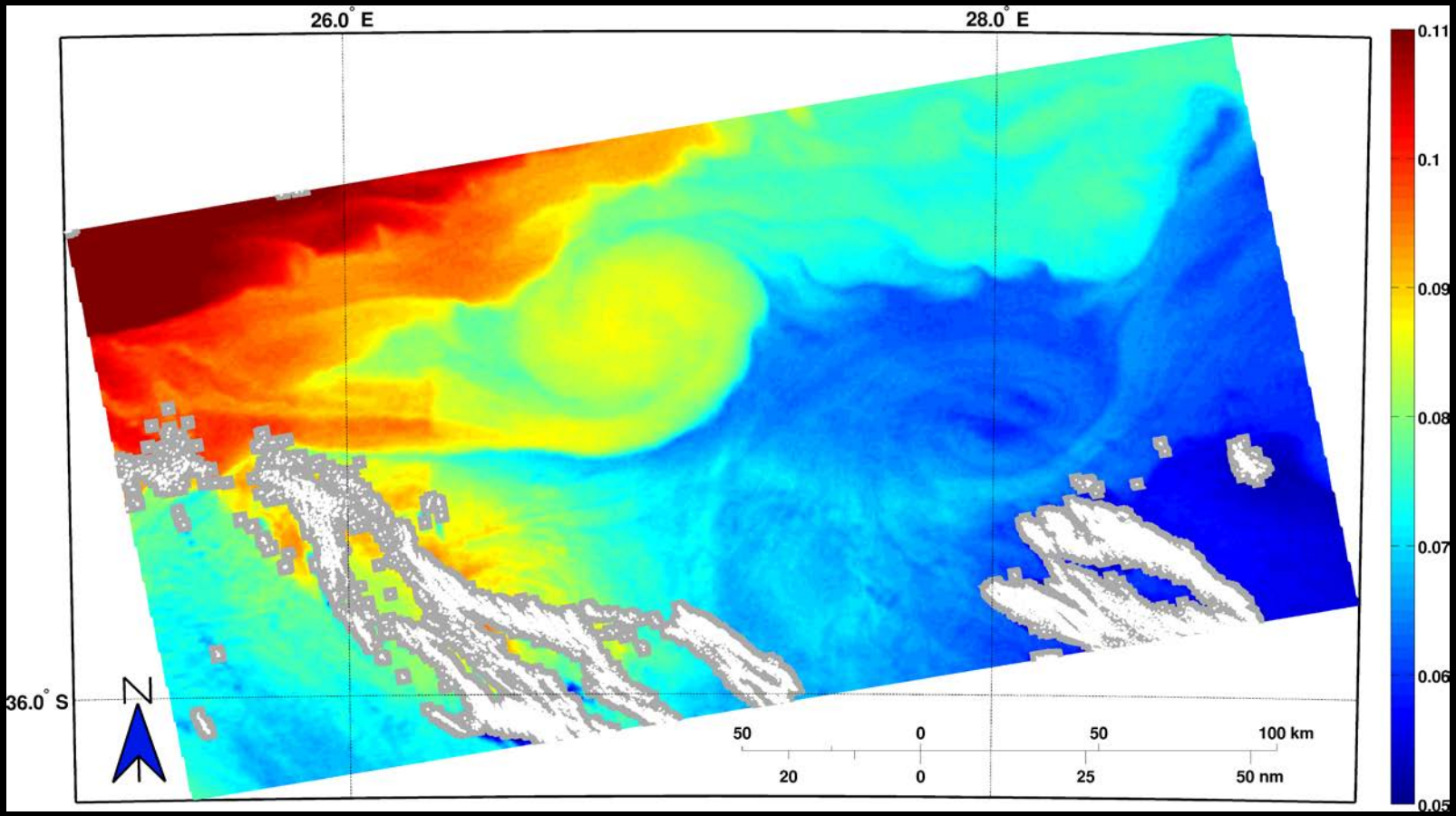
26.0° E
28.0° E
36.0° S
N
50
0
50
100 km
20
0
25
50 nm
0.11
0.1
0.09
0.08
0.07
0.06
0.05

Optical brigthness contrasts

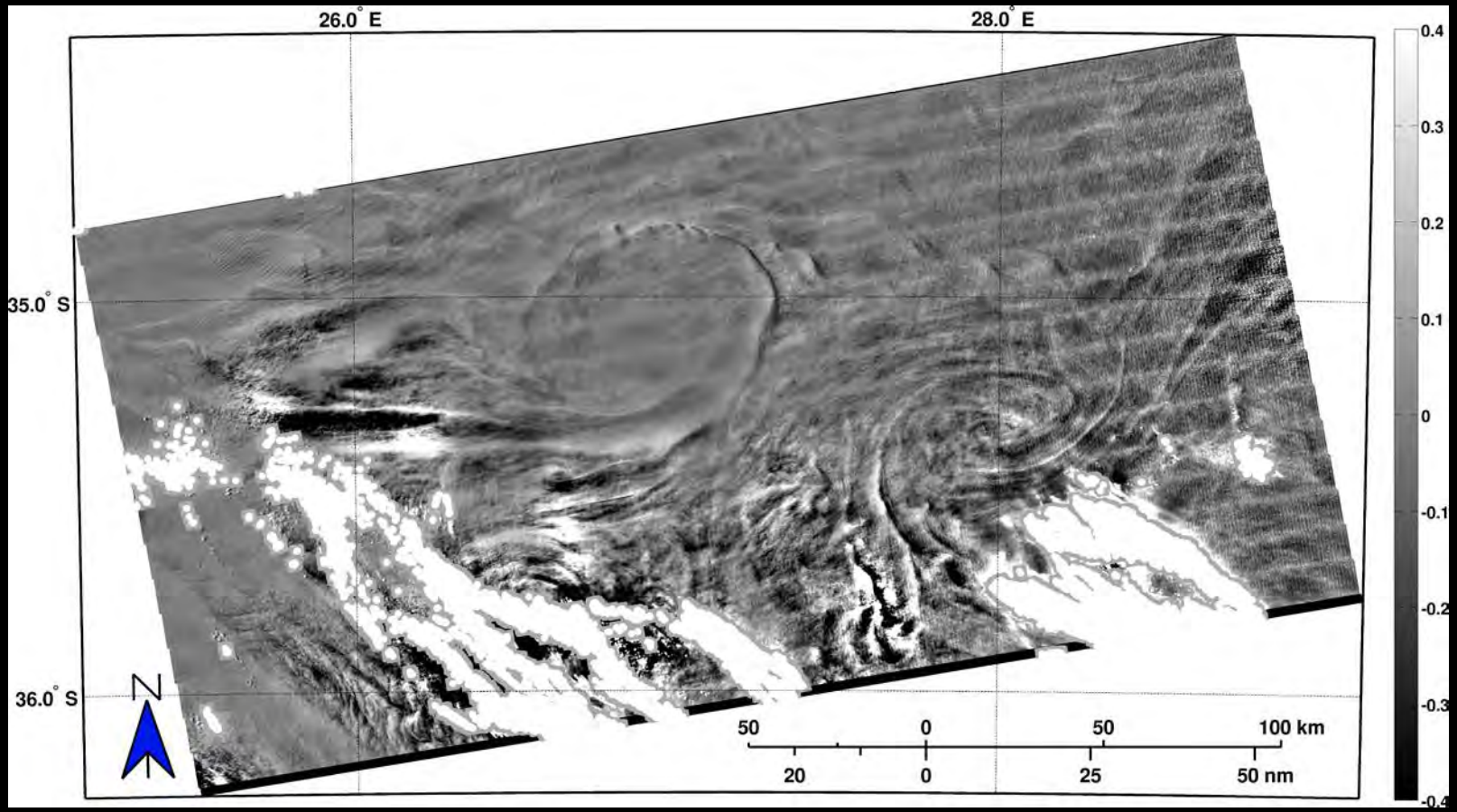

Radar roughness contrasts

MERIS Glitter analysis

MERIS Glitter analysis

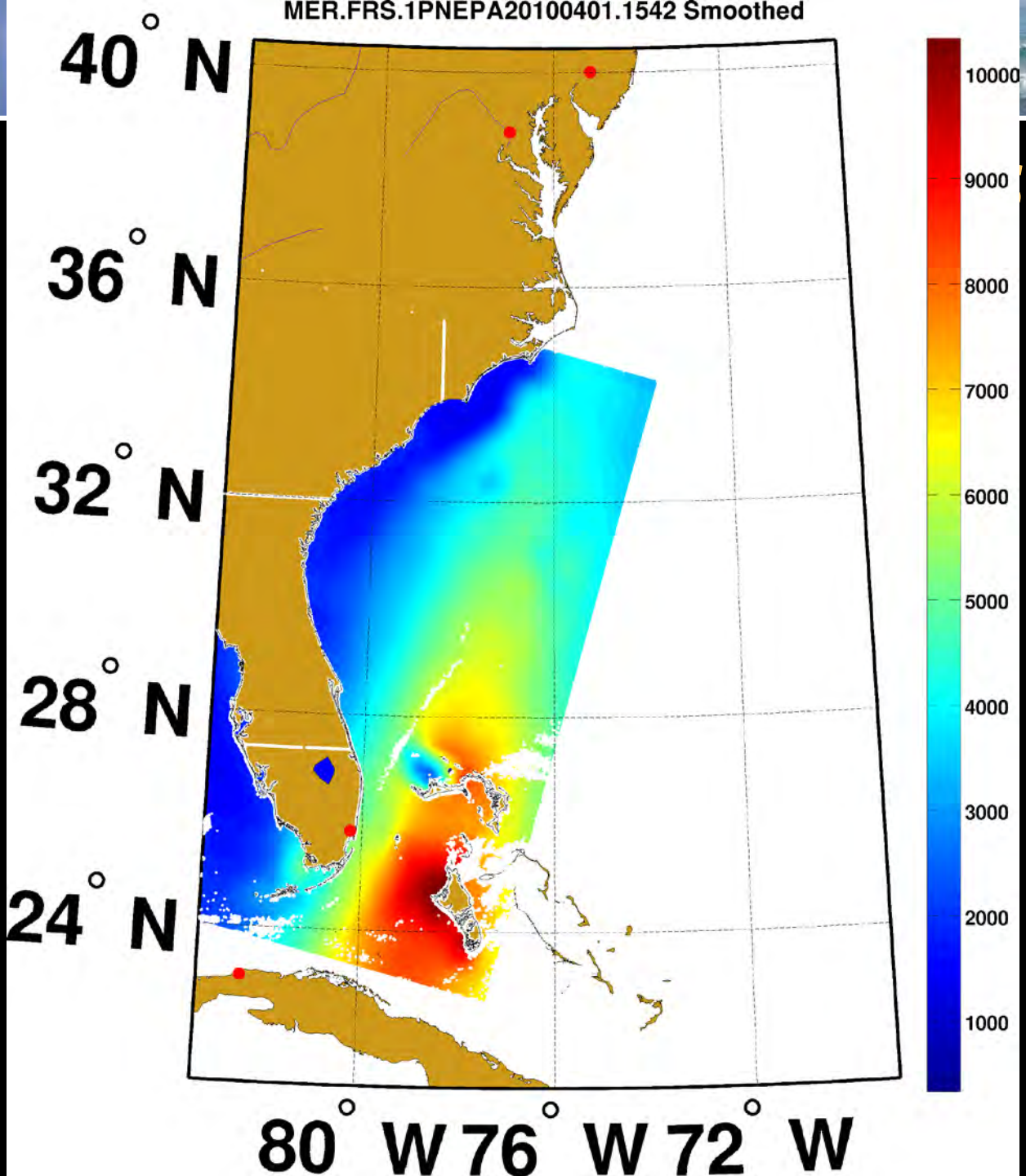

Glitter analysis

MERIS Glitter analysis

MODIS Glitter analysis

Meso- and submeso-scale details

Meso- and submeso-scale details

Meso- and submeso-scale details

Miso Turbulence (Mediterranean Sea)

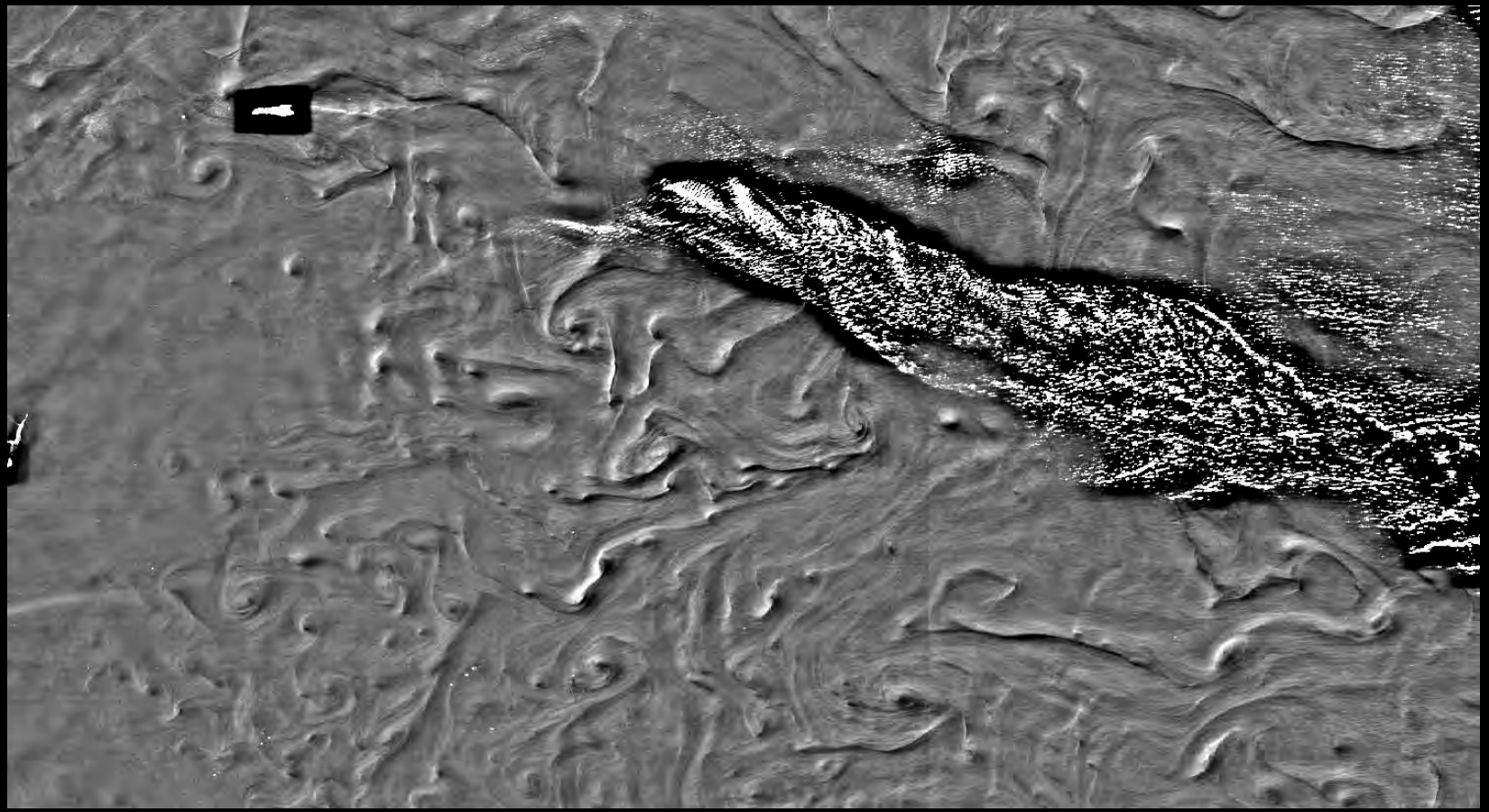

Miso Turbulence (Mediterranean Sea)